Czech Technical University in Prague
Faculty of Mechanical Engineering

DISSERTATION THESIS

2009   Ing. Pavel Moses

Czech Technical University in Prague
Faculty of Mechanical Engineering

DISSERTATION THESIS

Boundary Element Solver for Two-Dimensional Acoustic Scattering

Ing. Pavel Moses

Mathematical and Physical Engineering
Study Branch

Prof. RNDr. Pavel Burda, CSc.
Supervisor

2009   Praha

Acknowledgments

Abstract

The solution of problems of acoustic scattering in exterior domains requires accurate numerical approximation of Helmholtz equation in very large areas. In such cases Boundary Element Method is very strong tool allowing practical calculations by effectively reducing the dimension of the problem by one compared to Finite Element Method. The standard integral representations of the Helmholtz equation on which BEM is based are known to have non-unique solutions for certain data, and therefore several improved formulations have been proposed eliminating this drawback, namely the Burton-Miller method yielding unique solutions for arbitrary data. From the implementational point of view, collocation or Galerkin techniques may be used for discretization of the boundary integral. The purpose of this thesis is to introduce BEM solver for exterior problems and give comparison between the individual approaches. Several types of polynomial boundary elements are studied with appropriate theoretical background. An improved type of exponential elements aiming at better approximation of the practically important problems of plane wave scattering with high frequencies is also discussed and some issues of numerical evaluation of BEM equations in two dimensions are addressed. Numerical results obtained by the solver are presented and compared to analytical solutions to attest reliability of our approximation.

Anotace

Řešení problemů akustického rozptylu na vnějších doménách vyžaduje přesnou numerickou aproximaci Helmholtzovy rovnice na velmi rozsáhlé oblasti. V takovýchto případech se stává velmi silným nástrojem Boundary Element Method (metoda hraničních prvků), umožňující reálné výpočty díky tomu, že prakticky snižuje dimenzi problému o jednu ve srovnání s Finite Element Method (metoda konečných prvků). Standardní integrální reprezentace Helmholtzovy rovnice, na nichž je BEM postavena, nejsou pro jisté podmínky jednoznačně řešitelné, a proto bylo navrženo několik vylepšených formulací, které tento nedostatek eliminují. Jmenovitě se jedná o Burton-Millerovu metodu, která poskytuje jednoznačné řešení pro libovolná data. Mimo to, z hlediska implementace lze pro diskretizaci hraničního integrálu užít kolokační nebo Galerkinovu metodu. Cílem této práce je představit BEM řešič pro vnější problémy a srovnat jednotlivé zmíněné přístupy. V práci je analyzováno několik typů polynomiálních prvků s příslušným teoretickým pozadím. Rovněž je diskutován vylepšený typ exponenciálních prvků, vytvořený za účelem lepší aproximace prakticky významných případů rozptylu rovinné vlny při vysokých frekvencích, a jsou rozebrány některé praktické záležitosti implementace této metody ve dvou rozměrech. Představeny jsou také numerické výsledky spočítané naším řešičem, které jsou porovnány s analytickými řešeními pro kontrolu spolehlivosti aproximace.

Contents

List of Symbols

u^i ... incident wave

u^s ... scattered wave

u^t ... total wave

k ... wave number

ω ... frequency

ρ ... density

c ... speed of light

p ... pressure

v ... velocity

Ω ... domain

Γ ... boundary (surface) of Ω

ν ... normal

$\mathbf{r}$ ... distance from center of coordinate system

T^{int}, T^{ext} ... interior, exterior trace operators

$g(\mathbf{x}, \mathbf{y})$ ... fundamental solution

θ^e, θ^i ... exterior, interior angle of two lines

u ... solution of Helmholtz equation

u_h ... approximate solution of Helmholtz equation

u_Γ ... restriction of u to the boundary

σ ... potential density

V_k ... single-layer potential

W_k ... double-layer potential

L_k, M_k, N_k ... boundary operators

M_k' ... adjoint boundary operator

H^s ... Sobolev space

L^2 ... space of square integrable functions

$C^{0,\alpha}$ ... space of Hölder functions

φ ... shape function

ϕ ... basis function

S_h^0 ... space of constant basis functions

S_h^1 ... space of linear basis functions

S_h^2 ... space of quadratic basis functions

$\mathbf{K}_h$ ... stiffness matrix

J_n ... Bessel function of the first kind

Y_n ... Bessel function of the second kind

H_n ... Hankel function

iv

1

Introduction

Scattering of sound on obstacles submerged in the fluid is a problem of great practical importance. Research in this field has been propelled by the development of underwater detection devices, the sonars. Recently, analysis of noise in the vicinity of motorways, railroads and aeroports has become a major issue. From the physical point of view it represents finding solution of the wave equation (in some of its forms) which constitutes the model of propagation of sound, i.e. pressure perturbations, through given medium. Mathematically it is a problem of theoretical study of the physical model and its correctness as well as of devising methods capable of calculating solutions for models of real-life situations in sufficiently short time.

The present work focuses on development of a computer algorithm suitable for computations of approximate solutions of sound-scattering problems on unbounded exterior domains. The wave equation is considered in its time-harmonic form, the well-known Helmholtz equation, which is well-suited for many practical applications while simplifying the problem by eliminating its time component. For study of the Helmholtz equation see e.g. [33]. The solution of the Helmholtz equation for all but the simplest cases is only possible using numerical approximation techniques on computers. The Finite Element Method (FEM) has often been used for numerical discretization of the Helmholtz equation (cf. [36]), but the nature of the exterior problems on unbounded domains makes the FEM solutions too expensive in terms of time needed for the calculation, while certain difficulties in its practical application also arise. Therefore, the use of Boundary Element Method (BEM) has been suggested in combinations with boundary integral formulation of the Helmholtz equation. In fact, since the development of BEM in 1960's and early 70's by Shaw, Cruse, Rizzo, Brebbia and others, it has become a major tool for solution of sound-scattering problems. It is tailored for the use on exterior domains, since it allows to transfer the bulk of calculations to the boundary and thus virtually reduce the dimension of the problem by one. Application of BEM requires that the Helmholtz equation be transformed into integral representation form comprising boundary integrals with free-space Green's function as kernel. This approach had in fact been brought forward long past for calculation of analytical solutions but only in combination with BEM discretization can be used for complex problems with non-symmetric domains etc.

The standard boundary integral representation of the Helmholtz equation had been known to have non-unique solutions or no solutions at all under certain conditions and in 1968 the first modification was carried out by Schenck (see [32]) in order to resolve this drawback. Other reformulations followed and in early 1970's they were summarized and thoroughly analysed in [8], [9] by Burton and Miller. They suggested an improved formulation known as Burton-Miller method for which unique solution exists for arbitrary data.

Since Burton-Miller formulation is difficult to discretize and evaluate numerically due to hypersingular terms, standard formulation is still commonly implemented for engineering purposes. Its discretization may be carried out in different ways, using the collocation principle, Nyström or Galerkin method. Thus, application of BEM for solution of the Helmholtz equation is still subject to extensive ongoing research. A number of books have been published by Colton, Kress, McLean and others thoroughly analyzing properties of the various integral formulations, cf. [10], [13], [14], [24], providing proofs and theoretical background. The practical discretization of the integral equations using BEM is still far from a completely resolved issue. The problems of numerical treatment of singular (or hypersingular) integrals are studied, as well as the influence of the boundary shape (with or without corners), error estimates and convergence properties of the individual discretization techniques and number of other questions. Some important results concerning the collocation and Galerkin methods are summarized by Steinbach and Rjasanow in [34], while Nyström method is advertised in [14].

The goal of this work is development of BEM solver for two-dimensional exterior problems adopting the collocation and Galerkin principles and testing their properties and behaviour. The first part introduces fundamental theoretical background concerning the Helmholtz equation and its integral form. In the second part the solver is introduced and some numerical results given with focus on comparison of our solutions with the analytical ones to test reliability of the solver.

It should be mentioned, that results concerning the Helmholtz equation may be in large part used in other areas, e.g. electromagnetics or elasticity and contact problems, cf. [34], [25], [31].

2

Helmholtz Equation

2.1 Wave Equation

The motion of fluid of velocity $\mathbf{v}(\mathbf{x}, t)$, pressure $p(\mathbf{x}, t)$ and density $\rho(\mathbf{x}, t)$ is locally governed by two well-known equations, continuity equation

$$\frac{\partial \rho}{\partial t} + \mathrm{div}(\rho \mathbf{v}) = 0, \tag{2.1}$$

which is mathematical formulation of conservation of mass law, and equation of motion

$$\rho \frac{\partial \mathbf{v}}{\partial t} = -\nabla p, \tag{2.2}$$

expressing the Newton's law of momentum conservation. We assume small oscillations and therefore the equation of motion is considered in the linearized form known as Euler equation. Also, we may decompose pressure and density into the mean values p_0 and ρ_0 respectively and components p and ρ which denote the small perturbations from the constant state.

If the relation between pressure and density in the ideal compressible fluid is taken to be linear governed by the expression

$$p = c^2 \rho,$$

where c denotes speed of sound in given medium, then for the second derivative of p with respect to time holds

$$\frac{\partial^2 p}{\partial t^2} = c^2 \frac{\partial^2 \rho}{\partial t^2}.$$

Substitution of $p_0 + p$ and $\rho_0 + \rho$ into the continuity equation (2.1), differentiation with respect to time and neglection of the very small terms yields

$$\frac{\partial^2 \rho}{\partial t^2} = -\rho_0 \ \text{div} \left(\frac{\partial \mathbf{v}}{\partial t} \right). \tag{2.3}$$

Now, applying the conservation of momentum equation (2.2), the right-hand side can be re-written

$$-\rho_0 \ \text{div} \left(\frac{\partial \mathbf{v}}{\partial t} \right) = \text{div}(\nabla p),$$

and so finally all quantities other than p may be eliminated in (2.3), which gives

$$\frac{\partial^2 p}{\partial t^2} = c^2 \Delta p. \tag{2.4}$$

This is the wave equation for ideal fluid. Solution to the wave equation represents pressure perturbations throughout the medium, which give rise to sound, and therefore (2.4) is basic acoustic equation.

2.2 Reduced Wave Equation - Helmholtz Equation

Assuming the waves are time-harmonic with frequency ω, the temporal and spatial components of the unknown function can be separated,

$$p(\mathbf{x}, t) = u(\mathbf{x}) e^{-i\omega t}. \tag{2.5}$$

Here i denotes imaginary unit and the resultant function is therefore complex, but only its real part has physical meaning and is of interest. Substituting (2.5) into the wave equation (2.4) gives

$$\frac{\partial^2}{\partial t^2} (u(\mathbf{x}) e^{-i\omega t}) = c^2 \Delta u(\mathbf{x}) e^{-i\omega t}.$$

Since

$$\frac{\partial^2}{\partial t^2} (u(\mathbf{x}) e^{-i\omega t}) = i^2 \omega^2 u(\mathbf{x}) e^{-i\omega t},$$

it holds that

$$\frac{\omega^2}{c^2} u(\mathbf{x}) e^{-i\omega t} = -\Delta u(\mathbf{x}) e^{-i\omega t},$$

and dividing by $e^{-i\omega t}$ yields

$$-\frac{\omega^2}{c^2} u(\mathbf{x}) - \Delta u(\mathbf{x}) = 0,$$

which finally gives

$$\Delta u(\mathbf{x}) + k^2 u(\mathbf{x}) = 0. \tag{2.6}$$

The constant k defined as $k = \frac{\omega}{c}$ is called *wave number*; in general it is an arbitrary non-zero complex number. Since time component has been eliminated, the equation (2.6) is known as reduced wave equation, or rather as the Helmholtz equation. Thus, the Helmholtz equation describes the spatial component of time-harmonic acoustic wave and it is the equation subject to our investigation in this work.

2.3 Problem Setting for the Helmholtz Equation

The problem for the Helmholtz equation can either be defined on a bounded domain Ω (e.g. calculation of noise inside a car produced by its engine), in which case we speak of *interior problem*, or on an unbounded domain $R^n \setminus \overline{\Omega}$, being then known as an *exterior problem* (noise in the neighbourhood of a motorway, scattering of sonar impulses on a submarine etc.). The sound may be produced on the boundary, or by the boundary (e.g. vibrations of elastic frame of the car) and spreads throughout the domain, or comes in the form of incident impulse from afar and is modified (scattered) by the presence of an obstacle. In general, the total pressure (sound) field will be given as a superposition of the incident field $u(\mathbf{x})^i$ and the scattered (radiated) field $u(\mathbf{x})^s$,

$$u^t(\mathbf{x}) = u^i(\mathbf{x}) + u^s(\mathbf{x}).$$

Our primary interest lays in the sound-scattering problem, however, it is but a special case where the boundary condition for calculation of $u(\mathbf{x})^s$ is prescribed by the presence of non-zero incident field. Apparently, the other cases may be treated in the very similar way from the point of view of numerical approximation.

A plane wave traveling through the medium in given direction $\mathbf{d}$ is defined as

$$u(\mathbf{x}) = e^{ik(\mathbf{d}.\mathbf{x})}.$$

Plane wave itself represents a particular solution to the Helmholtz equation in R^n. It will play the role of incident field. Mode of scattering of the wave on the obstacle depends on the material properties of the body. Two basic cases from the point of view of the properties of the body are known as the *sound-hard* and the *sound-soft* obstacle. Sound-hard body reflects the wave completely, so that

$$\frac{\partial u^t}{\partial \nu}(\mathbf{x}) = 0 \ \text{ for } \ \mathbf{x} \in \Gamma,$$

where $\Gamma = \partial\Omega$ denotes the surface of the obstacle. Hence, we obtain Neumann boundary condition

$$\frac{\partial u^s}{\partial \nu}(\mathbf{x}) = -\frac{\partial u^i}{\partial \nu}(\mathbf{x}) \ \text{ for } \ \mathbf{x} \in \Gamma,$$

where ν is outward unit normal to the surface defined for almost all points $x \in \Gamma$. Outward will for our purposes always mean that it points away from the domain. On the other hand, on the sound-soft surface

$$u^t(\mathbf{x}) = 0 \ \text{ for } \ \mathbf{x} \in \Gamma,$$

which gives Dirichlet boundary condition

$$u^s(\mathbf{x}) = -u^i(\mathbf{x}) \ \text{ for } \ \mathbf{x} \in \Gamma.$$

General Robin boundary condition condition may also be defined

$$\frac{\partial u^t}{\partial \nu}(\mathbf{x}) + au^t(\mathbf{x}) = f(\mathbf{x}) \ \text{ for } \ \mathbf{x} \in \Gamma.$$

Considering the exterior problem, boundary is not only formed by the surface of the obstacle, but also by the 'infinity', so that suitable condition must also be prescribed for $|\mathbf{x}| \to \infty$. Naturally, it is required that no waves are reflected from the infinity, and also that amplitude of the wave decreases with the distance traveled, since it cannot have infinite energy. These assumptions are summarized in the condition known as Sommerfeld's

$$\frac{\partial u^s(\mathbf{x})}{\partial \mathbf{r}} - iku^s(\mathbf{x}) = o\left(\frac{1}{|\mathbf{r}|^2}\right) \ \text{ for } |\mathbf{x}| \to \infty \ \text{in } R^2, \tag{2.7}$$

or

$$\frac{\partial u^s(\mathbf{x})}{\partial \mathbf{r}} - iku^s(\mathbf{x}) = o\Big(\frac{1}{|\mathbf{r}|}\Big) \text{ for } |\mathbf{x}| \to \infty \text{ in } R^3, \tag{2.8}$$

where $\mathbf{r}$ is a position vector with respect to origin. The Sommerfeld's condition in fact ensures the uniqueness of solution, since it only allows particular solutions with appropriate direction, that means those which travel from the obstacle away (therefore it is also known as radiation condition). Waves of the opposite direction would also satisfy the Helmholtz equation, but are physically inadmissible and so are eliminated by the radiation condition. If function $u(\mathbf{x})$ satisfies (2.7),(2.8), it automatically satisfies also

$$u(\mathbf{x}) = \mathcal{O}(|\mathbf{r}|^{-(n-1)/2}),$$

so the Sommerfeld condition incorporates both physical requirements set above (cf. [16]). Therefore, we will be looking for function $u^s(\mathbf{x})$ which solves the problem

$$\Delta u^s(\mathbf{x}) + k^2 u^s(\mathbf{x}) = 0 \quad \text{in} \quad \Omega^\infty,$$

$$\frac{\partial u^s(\mathbf{x})}{\partial \nu} + au^s(\mathbf{x}) = f(\mathbf{x}) \quad \text{on} \quad \Gamma, \tag{2.9}$$

$$\frac{\partial u^s(\mathbf{x})}{\partial \mathbf{r}} - iku^s(\mathbf{x}) = o(|\mathbf{r}|^{-(n-1)/2}) \quad \text{for} \quad |\mathbf{x}| \to \infty,$$

where $\Omega^\infty = R^n \setminus \overline{\Omega}$ is the exterior domain. The sound-soft and sound-hard cases will only be considered.

2.4 Classification of Helmholtz Equation

The Helmholtz equation consists of Laplace operator and a lower order term, defining an operator

$$\mathcal{L} = -\Delta - k^2.$$

Definition 1 *Differential operator $\mathcal{A}$ is said to be strongly elliptic on Ω if*

$$\text{Re} \sum_{i=1}^n \sum_{j=1}^n (A_{ij}(x)\xi_j\eta)^*\xi_i\eta \geq c|\xi|^2|\eta|^2 \text{ for all } x \in \Omega, \ \xi \in R^n, \ \eta \in C^m.$$

Applying the definition, the Helmholtz equation may be shown to define a strongly elliptic operator. When the wave number k is real, which will be the case in our calculations, the operator $\mathcal{L}$ is self-adjoint.

3

Integral Representation of the Helmholtz Equation

3.1   Standard Representation Formulae

In the following text, the unknown scattered part of the wave will be denoted $u(\mathbf{x})$ instead of $u^s(\mathbf{x})$ for the sake of simplicity. For the derivations throughout this section, Ω will be assumed to be bounded, multiply or simply connected domain with Lipschitz boundary.

The interior problem will be examined first. After multiplying the Helmholtz equation with a test function v and integrating over the domain Ω, Green's theorem is applied to obtain

$$\int_\Omega (\Delta u(\mathbf{y}) + k^2 u(\mathbf{y})) v(\mathbf{y}) d\mathbf{y} = \tag{3.1}$$

$$= \int_\Gamma \frac{\partial u_\Gamma(\mathbf{y})}{\partial \nu} v_\Gamma(\mathbf{y}) ds_\mathbf{y} - \int_\Omega (\nabla u(\mathbf{y}), \nabla v(\mathbf{y})) d\mathbf{y} + \int_\Omega k^2 u(\mathbf{y}) v(\mathbf{y}) d\mathbf{y},$$

which is the Green's first formula. The subscript $._\Gamma$ represents restriction of a function to the boundary (defined by appropriate trace operators for interior problem T^{int} and $T^{\nu,int}$). Thus,

$$u_\Gamma(\mathbf{y}) = T^{int} u(\mathbf{y}) = u(\mathbf{y})\Big|_{\mathbf{y} \in \Gamma},$$

and

$$\frac{\partial u_\Gamma(\mathbf{y})}{\partial \nu} = T^{\nu,int} u(\mathbf{y}) = \frac{\partial u(\mathbf{y})}{\partial \nu}\Big|_{\mathbf{y} \in \Gamma}.$$

Similar expression to (3.1) may be obtained with u and v in interchanged positions. Rewriting (3.1) gives

$$\int_\Omega [(\nabla u(\mathbf{y}), \nabla v(\mathbf{y})) - k^2 u(\mathbf{y}) v(\mathbf{y})] d\mathbf{y} = \tag{3.2}$$

$$= \int_\Gamma \frac{\partial u_\Gamma(\mathbf{y})}{\partial \nu} v_\Gamma(\mathbf{y}) ds_\mathbf{y} - \int_\Omega (\Delta u(\mathbf{y}) + k^2 u(\mathbf{y})) v(\mathbf{y}) d\mathbf{y},$$

which is the first Green's formula for u, v after rearrangement, and similarly

$$\int_\Omega [(\nabla v(\mathbf{y}), \nabla u(\mathbf{y})) - k^2 v(\mathbf{y}) u(\mathbf{y})] d\mathbf{y} = \tag{3.3}$$

$$= \int_\Gamma \frac{\partial v_\Gamma(\mathbf{y})}{\partial \nu} u_\Gamma(\mathbf{y}) ds_\mathbf{y} - \int_\Omega (\Delta v(\mathbf{y}) + k^2 v(\mathbf{y})) u(\mathbf{y}) d\mathbf{y},$$

is the first Green's formula for v, u. Subtracting (3.2) - (3.3) and rearranging again the second Green's formula is obtained

$$\int_\Gamma \left(\frac{\partial u_\Gamma(\mathbf{y})}{\partial \nu} v_\Gamma(\mathbf{y}) - \frac{\partial v_\Gamma(\mathbf{y})}{\partial \nu} u_\Gamma(\mathbf{y}) \right) ds_\mathbf{y} = \tag{3.4}$$

$$= \int_\Omega [(\Delta u(\mathbf{y}) + k^2 u(\mathbf{y})) v(\mathbf{y}) - (\Delta v(\mathbf{y}) + k^2 v(\mathbf{y})) u(\mathbf{y})] d\mathbf{y}.$$

Now, a fundamental solution $g(\mathbf{x}, \mathbf{y})$ to the Helmholtz equation will be used as a test function instead of an arbitrary function v. The general form of fundamental solution for the Helmholtz operator in R^n is given by

$$g(\mathbf{x}, \mathbf{y}) = \frac{k^{n-2}}{2(2\pi)^{(n-1)/2}} (-y_0(n, k|\mathbf{y} - \mathbf{x}|) + aj_0(n, k|\mathbf{y} - \mathbf{x}|)), \tag{3.5}$$

where $a \in \mathcal{C}$ is an arbitrary constant and y_0, j_0 represent the spherical Bessel functions. For the derivation of (3.5) and definition of the Bessel functions cf. [24]. From here follows, that the fundamental solution in two dimensions is expressed as

$$g(\mathbf{x}, \mathbf{y}) = \frac{i}{4} H_0^{(1)}(k|\mathbf{y} - \mathbf{x}|),$$

and in three dimensions it takes form

$$g(\mathbf{x}, \mathbf{y}) = \frac{e^{ik|\mathbf{y} - \mathbf{x}|}}{4\pi|\mathbf{y} - \mathbf{x}|},$$

both of which satisfy

$$\Delta_{\mathbf{y}} g(\mathbf{x}, \mathbf{y}) + k^2 g(\mathbf{x}, \mathbf{y}) = \delta(|\mathbf{y} - \mathbf{x}|),$$

where δ is the Dirac function. Apparently, both fundamental solutions are singular. Denoting $|\mathbf{y} - \mathbf{x}| = r$ it is clear, that the singularity appears for $r = 0$, so the respective free space Green's functions only need to by examined for small r. Hankel function of the first kind, which forms the fundamental solution in two dimensions, is defined as

$$H_m^{(1)}(x) = J_m(x) + iY_m(x),$$

where $J_m(x)$ and $Y_m(x)$ are Bessel functions of the first and second kind respectively. For these the following asymptotic forms are valid in case $0 < x << \sqrt{m+1}$,

$$J_m(x) \rightarrow \frac{1}{\Gamma(m+1)} \left(\frac{x}{2}\right)^m,$$

$$Y_m(x) \rightarrow \frac{2}{\pi}(\ln(x/2) + \gamma) \approx \frac{2}{\pi}\ln(x) \quad \text{for} \quad m = 0,$$

in which Γ stands for gamma function (generalized factorial) and γ is the Euler-Mascheroni constant, cf [2]. Applying the asymptotics for Hankel function it turns out that for small r the real part of the fundamental solutions may be approximated by

$$g(\mathbf{x}, \mathbf{y}) \approx -\frac{1}{2\pi}\ln(r) \quad \text{in} \quad R^2,$$

and

$$g(\mathbf{x}, \mathbf{y}) \approx \frac{e^{ikr}}{4\pi r} \quad \text{in} \quad R^3,$$

The singularity of both fundamental solutions is of a weak type, which comes a result of application of the following definition.

Definition 2 *The kernel $K(\mathbf{x}, \mathbf{y})$ for points $\mathbf{x}, \mathbf{y} \in D$, where $D \in R^n$ is a bounded measurable set, is weakly singular if*

$$K(\mathbf{x}, \mathbf{y}) = \frac{A(\mathbf{x}, \mathbf{y})}{r^\alpha}, \quad 0 \le \alpha < n, \quad r = |\mathbf{y} - \mathbf{x}|,$$

where α is a constant, n denotes the dimension of the space and $A(\mathbf{x}, \mathbf{y})$ is a bounded measurable function on $D \times D$.

The singular behaviour of the integral kernels will call for special attention and treatment. Substituting the free space Green's function into (3.4) yields

$$\int_\Gamma \left(\frac{\partial u_\Gamma(\mathbf{y})}{\partial \nu} g(\mathbf{x}, \mathbf{y}) - \frac{\partial g(\mathbf{x}, \mathbf{y})}{\partial \nu} u_\Gamma(\mathbf{y}) \right) ds_{\mathbf{y}} = \tag{3.6}$$
$$= \int_\Omega [(\Delta u(\mathbf{y}) + k^2 u(\mathbf{y})) g(\mathbf{x}, \mathbf{y}) \quad - \quad (\Delta g(\mathbf{x}, \mathbf{y}) + k^2 g(\mathbf{x}, \mathbf{y})) u(\mathbf{y})] d\mathbf{y}.$$

Here and in all expressions, ν represents the outward unit normal to the boundary, i.e. it is directed into Ω^∞ since the interior problem is discussed (see Chapter 2). Let now only $\mathbf{y} \in \Gamma$ be considered in (3.6). Then, taking the other coordinate from exterior only, $\mathbf{x} \in \Omega^\infty$, gives

$$\int_\Gamma \left(\frac{\partial u_\Gamma(\mathbf{y})}{\partial \nu} g(\mathbf{x}, \mathbf{y}) - \frac{\partial g(\mathbf{x}, \mathbf{y})}{\partial \nu} u_\Gamma(\mathbf{y}) \right) ds_{\mathbf{y}} = 0, \tag{3.7}$$

as both u, g satisfy the Helmholtz equation in Ω. If $\mathbf{x} \in \Omega$ are considered, $g(\mathbf{x}, \mathbf{y})$ will be singular for the point $\mathbf{y} = \mathbf{x}$. To avoid this, let a ball $B_\epsilon(\mathbf{x})$ centered at the singular point be constructed. Now, the integral in (3.7) will be over $\Gamma + \Gamma_{B_\epsilon}$. The normal on Γ_{B_ϵ} is also outward, therefore it points inside B_ϵ, and so one has

$$\epsilon = (\mathbf{y} - \mathbf{x}), \quad \frac{\partial}{\partial \nu} = -\frac{\partial}{\partial \epsilon}, \quad ds_{\mathbf{y}} = \epsilon d\theta,$$

where ϵ and θ are polar coordinates. Differentiating the approximation of the two-dimensional fundamental solution in the normal direction gives

$$\frac{\partial}{\partial \nu} \left(-\frac{1}{2\pi} \ln |\mathbf{y} - \mathbf{x}| \right) = -\frac{\partial}{\partial \epsilon} \left(-\frac{1}{2\pi} \ln |\epsilon| \right) = \frac{1}{2\pi\epsilon}.$$

Substituting this result into (3.6) and letting $\epsilon \to 0$ the integral over Γ_{B_ϵ} will yield

$$\lim_{\epsilon \to 0} \int_{\Gamma_{B_\epsilon}} \left(\frac{\partial u_\Gamma(\mathbf{y})}{\partial \nu} g(\mathbf{x}, \mathbf{y}) - \frac{\partial g(\mathbf{x}, \mathbf{y})}{\partial \nu} u_\Gamma(\mathbf{y}) \right) ds_{\mathbf{y}} =$$
$$= \lim_{\epsilon \to 0} \left[-\int_0^{2\pi} \frac{\partial u_\Gamma(\mathbf{y})}{\partial \nu} \frac{1}{2\pi} \ln |\epsilon| \epsilon d\theta - \int_0^{2\pi} \frac{1}{2\pi\epsilon} u_\Gamma(\mathbf{y}) \epsilon d\theta \right] =$$
$$= \lim_{\epsilon \to 0} \left[-\epsilon \ln |\epsilon| \int_0^{2\pi} \frac{\partial u_\Gamma(\mathbf{y})}{\partial \nu} d\theta - \frac{1}{2\pi} \int_0^{2\pi} u_\Gamma(\mathbf{y}) d\theta \right] = -u(\mathbf{x}),$$

and again, since u, g satisfy the Helmholtz equation in Ω, it will result in
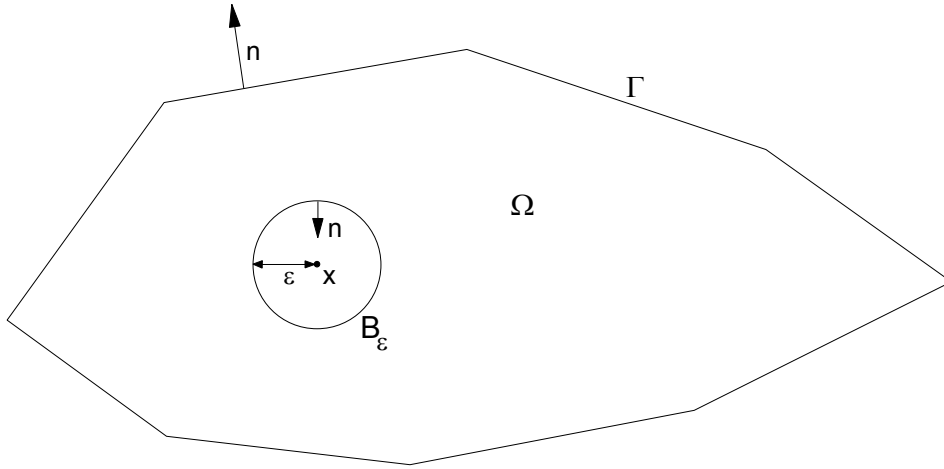
Figure 3.1: *Interior problem when $x \in \Omega$.*

$$\int_{\Gamma} \left(\frac{\partial u_{\Gamma}(\mathbf{y})}{\partial \nu} g(\mathbf{x}, \mathbf{y}) - \frac{\partial g(\mathbf{x}, \mathbf{y})}{\partial \nu} u_{\Gamma}(\mathbf{y}) \right) ds_{\mathbf{y}} = u(\mathbf{x}) \quad \text{for} \quad \mathbf{x} \in \Omega. \tag{3.8}$$

Finally, the most intricate case when $\mathbf{x} \in \Gamma$ will be dealt with. Again, the singularity needs to be treated, for which similar approach will be adopted as above. Apparently, there will be a jump in properties on the boundary, since a transition from (3.7) to (3.8) must occur. Replacing the singular point in (3.6) with a semicircle (hemisphere) C_{ϵ} of radius ϵ bent outwards into the exterior will produce

$$\int_{\Gamma_- + C_{\epsilon}} \left(\frac{\partial u_{\Gamma}(\mathbf{y})}{\partial \nu} g(\mathbf{x}, \mathbf{y}) - \frac{\partial g(\mathbf{x}, \mathbf{y})}{\partial \nu} u_{\Gamma}(\mathbf{y}) \right) ds_{\mathbf{y}} = u(\mathbf{x}) \quad \text{for} \quad \mathbf{x} \in \Omega,$$

since now the singular point will be inside the augmented domain Ω. Here Γ_- is the boundary minus the semicircle. Again, the radius of C_{ϵ} will be denoted by $\epsilon = (\mathbf{y} - \mathbf{x})$, and so

$$\frac{\partial}{\partial \nu} = \frac{\partial}{\partial \epsilon}, \quad ds_{\mathbf{y}} = \epsilon d\theta,$$

since the outward normal and the radius have the same direction. Taking the limit $\epsilon \to 0$ gives

$$\lim_{\epsilon \to 0} \int_{\Gamma_{C_\epsilon}} \left(\frac{\partial u_\Gamma(\mathbf{y})}{\partial \nu} g(\mathbf{x}, \mathbf{y}) - \frac{\partial g(\mathbf{x}, \mathbf{y})}{\partial \nu} u_\Gamma(\mathbf{y}) \right) ds_\mathbf{y} =$$

$$= \lim_{\epsilon \to 0} \left[-\int_0^{\theta^e} \frac{\partial u_\Gamma(\mathbf{y})}{\partial \nu} \frac{1}{2\pi} \ln|\epsilon| \epsilon d\theta + \int_0^{\theta^e} \frac{1}{2\pi\epsilon} u_\Gamma(\mathbf{y}) \epsilon d\theta \right] =$$

$$= \lim_{\epsilon \to 0} \left[-\frac{\epsilon \ln|\epsilon|}{2\pi} \int_0^{\theta^e} \frac{\partial u_\Gamma(\mathbf{y})}{\partial \nu} d\theta + \frac{1}{2\pi} \int_0^{\theta^e} u_\Gamma(\mathbf{y}) d\theta \right] = \frac{\theta^e}{2\pi} u(\mathbf{x}).$$

Here, θ^e is the external angle between tangents to the boundary at the points where the semicircle is connected to it, θ^i will be the inner angle of the same. Apparently, if the boundary is smooth at $\mathbf{x}$, $\theta^e = \pi$, as is also θ^i. If $\mathbf{x}$ is a corner of the boundary, $\theta^i = 2\pi - \theta^e$. Therefore,

$$\int_{\Gamma_- + C_\epsilon} \left(\frac{\partial u_\Gamma(\mathbf{y})}{\partial \nu} g(\mathbf{x}, \mathbf{y}) - \frac{\partial g(\mathbf{x}, \mathbf{y})}{\partial \nu} u_\Gamma(\mathbf{y}) \right) ds_\mathbf{y} =$$

$$= \int_\Gamma \left(\frac{\partial u_\Gamma(\mathbf{y})}{\partial \nu} g(\mathbf{x}, \mathbf{y}) - \frac{\partial g(\mathbf{x}, \mathbf{y})}{\partial \nu} u_\Gamma(\mathbf{y}) \right) ds_\mathbf{y} + \frac{\theta^e}{2\pi} u(\mathbf{x}) = u(\mathbf{x}),$$

from which follows

$$\int_\Gamma \left(\frac{\partial u_\Gamma(\mathbf{y})}{\partial \nu} g(\mathbf{x}, \mathbf{y}) - \frac{\partial g(\mathbf{x}, \mathbf{y})}{\partial \nu} u_\Gamma(\mathbf{y}) \right) ds_\mathbf{y} = u(\mathbf{x}) - \frac{\theta^e}{2\pi} u(\mathbf{x}) \quad \text{for} \quad \mathbf{x} \in \Gamma,$$

and using the interior angle

$$\int_\Gamma \left(\frac{\partial u_\Gamma(\mathbf{y})}{\partial \nu} g(\mathbf{x}, \mathbf{y}) - \frac{\partial g(\mathbf{x}, \mathbf{y})}{\partial \nu} u_\Gamma(\mathbf{y}) \right) ds_\mathbf{y} = \frac{\theta^i}{2\pi} u(\mathbf{x}) \quad \text{for} \quad \mathbf{x} \in \Gamma.$$

To derive expressions valid in R^3 the very same procedure would be applied, only using the appropriate fundamental solution. Assembling all the above results together leads to the widely used representation formula for the interior problem for the Helmholtz equation

$$\int_\Gamma u_\Gamma(\mathbf{y}) \frac{\partial g(\mathbf{x}, \mathbf{y})}{\partial \nu} ds_\mathbf{y} - \int_\Gamma \frac{\partial u_\Gamma(\mathbf{y})}{\partial \nu} g(\mathbf{x}, \mathbf{y}) ds_\mathbf{y} = \begin{cases} -u(\mathbf{x}) & \text{for } \mathbf{x} \in \Omega, \\[2mm] -\frac{\theta^i}{2\pi} u(\mathbf{x}) & \text{for } \mathbf{x} \in \Gamma, \\[2mm] 0 & \text{for } \mathbf{x} \in \Omega^\infty. \end{cases} \tag{3.9}$$

The jump on the boundary is due to the singular properties of the integral kernels as could be seen above.
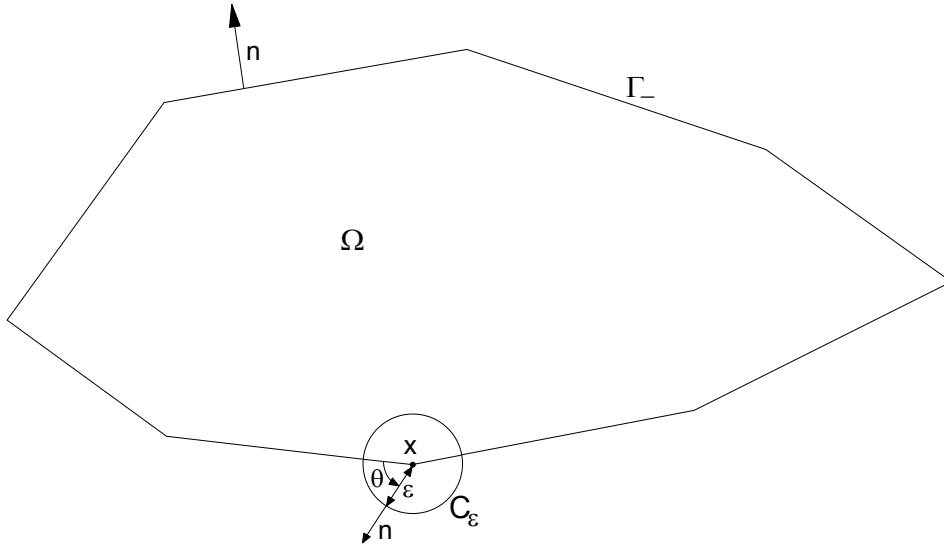
Figure 3.2: *Interior problem when $x \in \Gamma$.*

The procedure for derivation of integral representation for the exterior case is basically the same. The second Green's formula (3.4) is again the starting point, but trace operators T^{ext} and $T^{\nu,ext}$ will be used,

$$u_\Gamma(\mathbf{y}) = T^{ext}u(\mathbf{y}) = u(\mathbf{y})\Big|_{\mathbf{y}\in\Gamma}$$

and

$$\frac{\partial u_\Gamma(\mathbf{y})}{\partial \nu} = T^{\nu,ext}u(\mathbf{y}) = \frac{\partial u(\mathbf{y})}{\partial \nu}\Big|_{\mathbf{y}\in\Gamma}.$$

This time special care for the 'outer' boundary in the infinity must be taken. Enclosing Ω into a ball $B_\infty(\mathbf{x})$ the integration will now be over $\Gamma + \Gamma_{B_\infty}$. Taking $\mathbf{r} \to \infty$ and recalling that both $u(\mathbf{y})$ and $g(\mathbf{x}, \mathbf{y})$ satisfy the radiation condition (namely its second part $v(\mathbf{y}) = O(\mathbf{r}^{-(n-1)/2})$), one can see that

$$\int_{\Gamma_{B_\infty}} \left(\frac{\partial u_\Gamma(\mathbf{y})}{\partial \nu} v_\Gamma(\mathbf{y}) - \frac{\partial v_\Gamma(\mathbf{y})}{\partial \nu} u_\Gamma(\mathbf{y}) \right) ds_y = 0.$$

Since the integral over Γ_{B_∞} vanishes, the rest of the reasoning is the same as for the interior problem. The outward normal ν will now be directed into the domain Ω. Going through

the same procedure as in the previous case, the integral representation of exterior problem is obtained

$$\int_\Gamma u_\Gamma(\mathbf{y})\frac{\partial g(\mathbf{x},\mathbf{y})}{\partial \nu}ds_\mathbf{y} - \int_\Gamma \frac{\partial u_\Gamma(\mathbf{y})}{\partial \nu}g(\mathbf{x},\mathbf{y})ds_\mathbf{y} = \begin{cases} 0 & \text{for } \mathbf{x} \in \Omega, \\ \frac{\theta^i}{2\pi}u_\Gamma(\mathbf{x}) & \text{for } \mathbf{x} \in \Gamma, \\ u(\mathbf{x}) & \text{for } \mathbf{x} \in \Omega^\infty. \end{cases} \qquad (3.10)$$

This way of deriving the boundary integral form of the Helmholtz equation is generally known as direct approach and the expressions (3.9), (3.10) as the Helmholtz formulae. The indirect approach formulates the boundary integral representation as a problem for single and double layer potentials, coming to basically the same equations.

It should be noted that the equation (3.10) according to the convention accepted at the beginning of the chapter refers to the values of scattered field u^s. However, the boundary condition may often be defined in terms of the total field; in fact the homogeneous Dirichlet and Neumann boundary conditions set for total field define the two most important cases, the sound-soft and sound-hard problems (see above). Therefore, it is sometimes convenient to state the integral representation form of the Helmholtz equation for total field. Applying the Green's theorems to $u = u^i$ and realising that there are no singularities for the incident wave gives

$$\int_\Gamma u_\Gamma^i(\mathbf{y})\frac{\partial g(\mathbf{x},\mathbf{y})}{\partial \nu}ds_\mathbf{y} - \int_\Gamma \frac{\partial u_\Gamma^i(\mathbf{y})}{\partial \nu}g(\mathbf{x},\mathbf{y})ds_\mathbf{y} = \begin{cases} -u^i(\mathbf{x}) & \text{for } \mathbf{x} \in \Omega, \\ -\frac{\theta^i}{2\pi}u_\Gamma^i(\mathbf{x}) & \text{for } \mathbf{x} \in \Gamma, \\ 0 & \text{for } \mathbf{x} \in \Omega^\infty. \end{cases}$$

Adding the last two equations leads to the formula for total field

$$\int_\Gamma u_\Gamma^t(\mathbf{y})\frac{\partial g(\mathbf{x},\mathbf{y})}{\partial \nu}ds_\mathbf{y} - \int_\Gamma \frac{\partial u_\Gamma^t(\mathbf{y})}{\partial \nu}g(\mathbf{x},\mathbf{y})ds_\mathbf{y} = \begin{cases} -u^i(\mathbf{x}) & \text{for } \mathbf{x} \in \Omega, \\ \frac{\theta^i}{2\pi}u_\Gamma^t(\mathbf{x}) - u^i(\mathbf{x}) & \text{for } \mathbf{x} \in \Gamma, \\ u^t(\mathbf{x}) - u^i(\mathbf{x}) & \text{for } \mathbf{x} \in \Omega^\infty. \end{cases}$$

Nevertheless, in the following (3.10) will be considered the basic form of integral representation for exterior problem and u will still denote the scattered part of the acoustic field if not specified differently.

3.2   Differentiated Representation Formulae

Other representations are also possible, as for example the differentiated Helmholtz formulae. The one for exterior problem will be achieved by taking (3.10) and differentiating it with respect to normal $\nu_{\mathbf{x}}$. The differentiation is not straightforward for $\mathbf{x} \in \Gamma$, but in result it yields

$$\frac{\partial}{\partial \nu_{\mathbf{x}}} \int_{\Gamma} \left(u_{\Gamma}(\mathbf{y}) \frac{\partial g(\mathbf{x}, \mathbf{y})}{\partial \nu} - \frac{\partial u_{\Gamma}(\mathbf{y})}{\partial \nu} g(\mathbf{x}, \mathbf{y}) \right) ds_{\mathbf{y}} = \begin{cases} 0 & \text{for } \mathbf{x} \in \Omega, \\[2mm] \frac{\theta^i}{2\pi} \frac{\partial u_{\Gamma}(\mathbf{x})}{\partial \nu_{\mathbf{x}}} & \text{for } \mathbf{x} \in \Gamma, \\[2mm] \frac{\partial u(\mathbf{x})}{\partial \nu_{\mathbf{x}}} & \text{for } \mathbf{x} \in \Omega^{\infty}. \end{cases} \tag{3.11}$$

Re-writing the differentiated formula for the total field gives

$$\frac{\partial}{\partial \nu_{\mathbf{x}}} \int_{\Gamma} \left(u_{\Gamma}^t(\mathbf{y}) \frac{\partial g(\mathbf{x}, \mathbf{y})}{\partial \nu} - \frac{\partial u_{\Gamma}^t(\mathbf{y})}{\partial \nu} g(\mathbf{x}, \mathbf{y}) \right) ds_{\mathbf{y}} = \begin{cases} -\frac{\partial u^i(\mathbf{x})}{\partial \nu_{\mathbf{x}}} & \text{for } \mathbf{x} \in \Omega, \\[2mm] \frac{\theta^i}{2\pi} \frac{\partial u_{\Gamma}^t(\mathbf{x})}{\partial \nu_{\mathbf{x}}} - \frac{\partial u_{\Gamma}^i(\mathbf{x})}{\partial \nu_{\mathbf{x}}} & \text{for } \mathbf{x} \in \Gamma, \\[2mm] \frac{\partial u^t(\mathbf{x})}{\partial \nu_{\mathbf{x}}} - \frac{\partial u^i(\mathbf{x})}{\partial \nu_{\mathbf{x}}} & \text{for } \mathbf{x} \in \Omega^{\infty}. \end{cases}$$

The differentiated Helmholtz formulae may be used for discretization in the same way as the standard ones. However, their main purpose will be seen in Chapter 4 when discussing the advanced formulations devised to resolve certain existence and uniqueness issues connected with the integral representations, which are examined in the following section.

3.3   Existence and Uniqueness of Solution for Standard Formulae

The standard representation formulation of Helmholtz equation for exterior problems derived in the previous section has been used for practical calculations since BEM emerged as computational tool. However, it has also been known to have no solution or have a non-unique solution for some critical data. The existence and uniqueness in fact depends on two major factors, namely the shape of the boundary and the value of wavenumber. While the first factor is quite natural, the dependence on k is not as self-evident. Both issues require detailed analysis which has been carried out in a number of works and is not within a scope of this treatise, however, main results concerning the existence and uniqueness are summarized in this section. In the following chapter some variant formulations devised in order to resolve the weak points of standard formulation are presented, however, the

standard integral representation remains of practical value when applied with care and in fact, most of the engineering solutions are still based on it because of the computational difficulties associated with the advanced formulations.

3.3.1 Helmholtz Integral Operators

The existence and uniqueness of solution both to the interior and exterior problems will naturally depend on the properties of integral operators present in the boundary representations, which in turn will depend on the properties of the function u itself, free space Green's function forming the kernel of the integrals and smoothness of the boundary.

The integrals comprised in the representations (3.9), (3.10) are in fact the so-called single and double-layer potentials. In general, taking an integrable function σ (density function) defined on the boundary of a closed domain, the integral

$$V_k(\mathbf{x}) = \int_\Gamma \sigma(\mathbf{y}) g(\mathbf{x}, \mathbf{y}) ds_{\mathbf{y}}, \tag{3.12}$$

represents the single-layer potential, and the integral

$$W_k(\mathbf{x}) = \int_\Gamma \sigma(\mathbf{y}) \frac{\partial g(\mathbf{x}, \mathbf{y})}{\partial \nu_{\mathbf{y}}} ds_{\mathbf{y}}, \tag{3.13}$$

is the so-called double-layer potential. Taking $g(\mathbf{x}, \mathbf{y})$ to be the fundamental solution of the Helmholtz equation, (3.12), (3.13) will be called Helmholtz potentials. Both potentials satisfy the Helmholtz equation in the interior and exterior and the Sommerfeld condition holds for them. Properties of the acoustic potentials and solvability of boundary integral equations based on them have been subject to thorough studies by many scholars. The particular case of the boundary representation for the Helmholtz equation has been researched by G*ü*nter, Kellogg, Panich, Werner and Brakhage to name but a few. The following summary of the main results follows essentially the work of Burton, cf. [8], and Colton and Kress, cf. [14]. Here, the theory for second kind Fredholm equations is the basis for uniqueness proofs. A different approach has been adopted e.g. in McLean, cf. [24].

The existence and regularity of the Helmholtz potentials are basically proved using their proximity to the well-known potentials for Laplace equation. The main complication arises in case of the derivative of W_k. Its existence requires $\sigma \in C^{(2)}$, but this condition can be weakened to σ being H*ö*lder continuously differentiable. This result is not important at the time being, but is essential for analysis of the advanced formulations discussed in the next chapter.

Structure of the boundary also plays a crucial role. While in the derivation of the boundary representations Ω was assumed very general with Lipschitz boundary, some restrictions will have to be made for the following analysis. Theorems 1 - 4 give basic properties of the

operators formed by the acoustic potentials, all of them assuming $C^{(2)}$-continuous boundary. Burton in ([8]) shows, that in fact somewhat more general Kellogg regular boundary may be used. For definition of Kellogg regular surface see appendix and note, that there is a minor change needed, namely function F used in the definition having continuous second derivative. This kind of boundary will be reffered to as $\Gamma \in C_K^{(2)}$.

The basic properties of the Helmholtz potentials may be then summed up in the following theorems which are due to Colton and Kress, cf. [14].

Theorem 1 *Let $\Gamma \in C^{(2)}$ and let σ be continuous. Then the single-layer potential V_k is continuous in R^3 and*

$$||V_k||_{\infty,R^3} \leq C||\sigma||_{\infty,\Gamma}$$

for some constant C depending on Γ. On the boundary holds

$$V_k(\mathbf{x}) = \int_\Gamma \sigma(\mathbf{y})g(\mathbf{x},\mathbf{y})ds_\mathbf{y}, \quad \mathbf{x} \in \Gamma,$$

$$\frac{V_k(\mathbf{x}_\pm)}{\partial \nu} = \int_\Gamma \sigma(\mathbf{y})\frac{\partial g(\mathbf{x},\mathbf{y})}{\partial \nu_\mathbf{y}}ds_\mathbf{y} \mp \frac{1}{2}\sigma(\mathbf{x}), \quad \mathbf{x} \in \Gamma,$$

where

$$\frac{V_k(\mathbf{x}_\pm)}{\partial \nu} := \lim_{h \to +0} \nu(\mathbf{x}).\,\mathrm{grad}\,V_k(\mathbf{x} \pm h\nu(\mathbf{x}))$$

is to be understood in the sense of uniform convergence on Γ and where the integrals exist as improper integrals. The double-layer potential W_k can be continuously extended from Ω to $\bar{\Omega}$ and from $R^3 \setminus \bar{\Omega}$ to $R^3 \setminus \Omega$ with limiting values

$$W_k(\mathbf{x}_\pm) = \int_\Gamma \sigma(\mathbf{y})\frac{\partial g(\mathbf{x},\mathbf{y})}{\partial \nu_\mathbf{y}}ds_\mathbf{y} \pm \frac{1}{2}\sigma(\mathbf{x}), \quad \mathbf{x} \in \Gamma,$$

where

$$W_k(\mathbf{x}_\pm) := \lim_{h \to +0} W_k(\mathbf{x} \pm h\nu(\mathbf{x}))$$

and where the integral exists as an improper integral. Moreover,

$$||W_k||_{\infty,\bar{\Omega}} \leq C||\sigma||_{\infty,\Gamma}, \quad ||W_k||_{\infty,R^3\setminus\Omega} \leq C||\sigma||_{\infty,\Gamma}$$

for some constant C depending on Γ and

$$\lim_{h \to +0} \left[\frac{\partial W_k}{\partial \nu}(\mathbf{x} + h\nu(\mathbf{x})) - \frac{\partial W_k}{\partial \nu}(\mathbf{x} - h\nu(\mathbf{x})) \right] = 0, \quad \mathbf{x} \in \Gamma,$$

uniformly on Γ.

Thus, the single-layer potential is continuous at the boundary while the double-layer potential has a jump there. The opposite is true for the normal derivatives of the potentials.

More general version of the theorem utilizing Hölder continuous density function, which is needed for improved boundary integral formulations, is also given according to [14].

Theorem 2 *Let $\Gamma \in C^{(2)}$ and let $0 < \alpha < 1$. Then the single-layer potential V_k with density $\sigma \in C(\Gamma)$ is uniformly Hölder continuous in R^3 and*

$$||V_k||_{\alpha,R^3} \leq C_\alpha ||\sigma||_{\infty,\Gamma}.$$

The first derivatives of of the single-layer potential V_k with density $\sigma \in C^{0,\alpha}(\Gamma)$ can be uniformly Hölder continuously extended from Ω to $\bar{\Omega}$ and from $R^3 \setminus \bar{\Omega}$ to $R^3 \setminus \Omega$ with boundary values

$$\text{grad } V_k(\mathbf{x}_\pm) = \int_\Gamma \sigma(\mathbf{y})\text{grad}_\mathbf{x} \, g(\mathbf{x},\mathbf{y})ds_\mathbf{y} \mp \frac{1}{2}\sigma(\mathbf{x})\nu(\mathbf{x}), \quad \mathbf{x} \in \mathbf{\Gamma},$$

where

$$\text{grad } V_k(\mathbf{x}_\pm) := \lim_{h \to +0} \text{ grad } V_k(\mathbf{x} \pm h\nu(\mathbf{x}))$$

and it holds that

$$||\text{grad } V_k||_{\alpha,\bar{\Omega}} \leq C_\alpha ||\sigma||_{\alpha,\Gamma}, \quad ||\text{grad } V_k||_{\alpha,R^3\setminus\Omega} \leq C_\alpha ||\sigma||_{\alpha,\Gamma}.$$

The double-layer potential W_k with density $\sigma \in C^{0,\alpha}(\Gamma)$ can be uniformly Hölder continuously extended from Ω to $\bar{\Omega}$ and from $R^3 \setminus \bar{\Omega}$ to $R^3 \setminus \Omega$ such that

$$||W_k||_{\alpha,\bar{\Omega}} \leq C_\alpha ||\sigma||_{\alpha,\Gamma}, \quad ||W_k||_{\alpha,R^3\setminus\Omega} \leq C_\alpha ||\sigma||_{\alpha,\Gamma}.$$

The first derivatives of the double-layer potential W_k with density $\sigma \in C^{1,\alpha}(\Gamma)$ can be uniformly Hölder continuously extended from Ω to $\bar{\Omega}$ and from $R^3 \setminus \bar{\Omega}$ to $R^3 \setminus \Omega$ such that

$$||\text{grad } W_k||_{\alpha,\bar{\Omega}} \leq C_\alpha ||\sigma||_{1,\alpha,\Gamma}, \quad ||\text{grad } W_k||_{\alpha,R^3\setminus\Omega} \leq C_\alpha ||\sigma||_{1,\alpha,\Gamma}.$$

Everywhere, C_α denotes a constant depending on Γ and α.

Linear space $C^{0,\alpha}(D)$ is the *Hölder* space of all functions bounded and uniformly *Hölder* continuous with α on D. Similarly, $C^{1,\alpha}(D)$ is the space of uniformly *Hölder* continuously differentiable functions (such that grad $\sigma \in C^{0,\alpha}(D)$). Real or complex valued function $\sigma \in D$ is called uniformly *Hölder* continuous with exponent $0 < \alpha \leq$ if there exists a constant C such that

$$|\sigma(x) - \sigma(y)| \leq C|x - y|^{\alpha} \text{ for all } x, y \in D.$$

The proofs for Theorems 1,2 are to be found in [13].

3.3.2 Existence and Uniqueness for Exterior Problem

In the following we will deal with the direct values of the Helmholtz potentials and it will be more convenient to approach them as integral operators. The respective integral operators will be named L_k and M_k, so that

$$L_k\sigma = \int_\Gamma \sigma(\mathbf{y})g(\mathbf{x}, \mathbf{y})ds_{\mathbf{y}}, \tag{3.14}$$

and

$$M_k\sigma = \int_\Gamma \sigma(\mathbf{y})\frac{\partial g_\Gamma(\mathbf{x}, \mathbf{y})}{\partial \nu_{\mathbf{y}}}ds_{\mathbf{y}}. \tag{3.15}$$

The normal derivatives of both operators will also be needed,

$$M_k'\sigma = \int_\Gamma \sigma(\mathbf{y})g(\mathbf{x}, \mathbf{y})ds_{\mathbf{y}}, \tag{3.16}$$

(differentiation of V_k with respect to $\nu_{\mathbf{x}}$ yields an operator symmetric in $\mathbf{x}$ and $\mathbf{y}$ which is a transpose of M_k) and

$$N_k\sigma = \frac{\partial}{\partial \nu_{\mathbf{x}}} \int_\Gamma \sigma(\mathbf{y})\frac{\partial g_\Gamma(\mathbf{x}, \mathbf{y})}{\partial \nu_{\mathbf{y}}}ds_{\mathbf{y}}. \tag{3.17}$$

Using (3.14)-(3.17), the problem (3.10) will be written as

$$\{L_k u\}(\mathbf{x}) = \frac{1}{2}u(\mathbf{x}) - \{M_k u\}(\mathbf{x}) \text{ for } \mathbf{x} \in \Gamma,$$

while (3.11) will take form

$$\{L_k u\}(\mathbf{x}) = -\frac{1}{2} u(\mathbf{x}) + \{M_k u\}(\mathbf{x}) \text{ for } \mathbf{x} \in \Gamma.$$

The important properties of the operators L_k, M_k, M'_k, N_k are summed up in the following two theorems, which are again due to [14]. For *Hölder* space we have:

Theorem 3 *Let Γ be of class $C^{(2)}$. Then the operators L_k, M_k, M'_k are bounded operators from $C(\Gamma)$ into $C^{0,\alpha}(\Gamma)$, the operators L_k and M_k are also bounded from $C^{0,\alpha}(\Gamma)$ into $C^{1,\alpha}(\Gamma)$, and the operator N_k is bounded from $C^{1,\alpha}(\Gamma)$ into $C^{0,\alpha}(\Gamma)$.*

For classical Sobolev spaces then holds:

Theorem 4 *Let Γ be of class $C^{(2)}$ and let $H^1(\Gamma)$ be Sobolev space. Then the operator L_k is bounded from $L^2(\Gamma)$ into $H^1(\Gamma)$. Assume further that Γ belongs to $C^{2,\alpha}$. The the operators M_k and M'_k are bounded from $L^2(\Gamma)$ into $H^1(\Gamma)$ and the operator N_k is bounded from $H^1(\Gamma)$ into $L^2(\Gamma)$.*

The main result is, that under the assumptions of continuous density function σ and Kellogg regular boundary $C_K^{(2)}$, the integral operators L_k and M_k may be shown to be compact, and therefore Riesz-Fredholm theory for the equations of the second kind may be applied to them.

Very detailed study of the integral representation for the Helmholtz equation in its direct as well as indirect (potential) form in the framework of Fredholm theory had been undertaken by Burton in [8]. Both formulations lead to slightly different results, but in essence there is always the same outcome. The solution of the exterior problem is either non-unique or non-existent for certain values of k, which are closely related to the properties of the interior problem. Thus, the direct formulation fails to provide unique solution for $k \in K_N$, where K_N represents an infinite set of wavenumbers for which the interior Neumann problem has eigenvalue. The equivalent direct formulation based on the differentiated Helmholtz formulae has also been studied yielding similar conclusion. The exterior problem does not have unique solution in case $k \in K_D$, where K_D is a set of wavenumbers corresponding to interior Dirichlet eigenvalues.

Since both sets K_N and K_D are discrete, the standard representation formulae may still be used for solution, provided that the critical values are avoided. Vast amount of effort has been devoted to finding of formulation which would be free of this inherent deficiency. Results of this research are briefly summarized in the following chapter, nevertheless it may be concluded in advance that the standard formulation remains the basic and most often implemented one.

4

Improved Representation Formulations

It has been shown that both Dirichlet and Neumann exterior (and interior) problems have no solution or have multiple solutions fot certain values of wave number, and these critical values are grow denser with increasing frequency. A number of attempts have been made towards finding integral representation for the Helmholtz equation, which would overcome this major shortcoming.

4.1 Schenck Method (CHIEF)

First relatively successful modification avoiding the nonuniqueness problem was proposed by Schenck in [32] and has become known as CHIEF method. The idea is to combine the system of equations for the values at points on the boundary, for which solution always exists but is not necessarily unique, with system of equations for interior problem, for which solution is always unique, provided it exists. This results in an overdetermined system of equations for which the least squares method is used. Practical usefulness of this approach is hindered by the fact, that the choice of points at which the interior problem is solved is arbitrary. A wrong choice of nodes for interior problem will fail to give solution and the possibility of choosing a wrong point increases with growing wave number.

4.2 Werner-Brakhage Formulation

Another approach was suggested by Werner and Brakhage in [6], which allows to solve exterior Dirichlet problem for all wavenumbers. The authors used the fact that the solvability of the boundary problem is directly related to either the eigenvalues of interior Dirichlet problem or interior Neumann problem. Therefore, they suggested combining the boundary potentials into a mixed formulation. The idea has been carried further on by Panich, Kussmaul and others to formulate uniquely solvable integral representations for

Neumann and Robin problems. Unfortunately it was not too successfull and the boundary operator required some sort of regularization to obtain the desired result.

4.3 Burton-Miller Formulation

The existing re-formulations have been thoroughly analyzed in [8], [9] by Burton and Miller, who pointed out their disadvantages. In [9] they proposed a different approach to avoid the nonuniqueness problems. Instead of combining the single and double layer boundary potentials of the indirect approach, they offer a mixed formulation based on the standard and differentiated Helmholtz formulae of the direct approach. The idea is similar, to make advantage of the fact that both the standard and differentiated formulations fail to give unique solution for wavenumbers equal to eigenvalues of associated Dirichlet or Neumann problem respectively, but the mixed formulation loses this dependence.

A linear combination of (3.10) and (3.11) gives for the values on the boundary

$$
\begin{aligned}
\alpha \int_\Gamma u_\Gamma(\mathbf{y}) \frac{\partial g(\mathbf{x}, \mathbf{y})}{\partial \nu} ds_\mathbf{y} &+ \frac{\partial}{\partial \nu_\mathbf{x}} \int_\Gamma u_\Gamma(\mathbf{y}) \frac{\partial g(\mathbf{x}, \mathbf{y})}{\partial \nu} ds_\mathbf{y} - \\
-\alpha \int_\Gamma \frac{\partial u_\Gamma(\mathbf{y})}{\partial \nu} g(\mathbf{x}, \mathbf{y}) ds_\mathbf{y} &- \frac{\partial}{\partial \nu_\mathbf{x}} \int_\Gamma \frac{\partial u_\Gamma(\mathbf{y})}{\partial \nu} g(\mathbf{x}, \mathbf{y}) ds_\mathbf{y} = \\
&= \frac{\theta^i}{2\pi} \left(\alpha u_\Gamma(\mathbf{x}) + \frac{\partial u_\Gamma(\mathbf{x})}{\partial \nu_\mathbf{x}} \right) \quad \text{for} \quad \mathbf{x} \in \Gamma,
\end{aligned}
\tag{4.1}
$$

where α is a coupling parameter. One should notice, that the mixed equation (4.1) needs only be applied for calculation of the unknown values on the boundary. As soon as they are calculated, standard representation formula (3.10) may be used for the exterior values since there are no more uniqueness problems.

Here, the properties of the boundary curve again play role. It can be shown that all the operators in (4.1) are weakly singular with the exception of the last term on the left-hand side, which is a hypersingular operator, which poses a major problem for numerical approximation. Nevertheless, Burton-Miller formulation is a candidate for the formulation which should be adopted in solvers aiming at generality and robustness when solving the Helmholtz problem. However, practical use of this formulation is subject to ongoing research and it is far from being easily implemented in applications and the standard formulation is still the state-of-the-art today.

5

BEM for the Integral Helmholtz Equation

The boundary representation formulae devised in the previous chapters will be discretized using Boundary Element Method. The main advantage of solving the Helmholtz equation in the boundary integral form is that it effectively reduces the dimension of the problem by one. It also allows us to calculate the solution at an arbitrary point of the exterior (interior) explicitly without having to construct new mesh etc.

BEM comes in two basic variants, both of which will be introduced in this chapter and used for the calculations, the collocation method and Galerkin method. Collocation is the simplest approach possible and therefore it is favoured for practical solutions at least among engineers, usually based on constant approximation, again the simplest choice. However, it turns out to be unstable at some cases and Galerkin should therefore be given priority.

So far, the problem has been considered in general dimension, that is practically either in E_2 or E_3, and the only substantial difference in between the two was the form of free space Green's function. From now it will be restricted to two dimensions. Nevertheless, large part of the results can be extended to three dimensions in a straightforward way.

The concept of Boundary Element Method is based on approximation of the unknown function u which is being sought for as a linear combination of functions forming a base of certain space S_h, known as a trial space, so that the projection u_h,

$$u_h = \sum_{k=1}^{M} u_k \phi_k, \tag{5.1}$$

is close enough to the original function. The basis functions ϕ_k are in general polynomials of p-th degree on part of the boundary, extended by zero everywhere else. Usually, polynomials up to 2nd degree are used, which are also adopted here. However, basis functions of special type suited for solution of exterior problems with plane wave as the incident condition have been proposed in [1], [5], and these are also included and have been applied in calculations.

5.1 Boundary Discretization

Let $\Omega \in R^2$ be a domain with Kellogg regular boundary Γ (for definition see Appendix). In practice, the boundary will be piece-wise polynomial. Hence, it may be decomposed into set of segments Γ_i such, that

$$\Gamma = \bigcup_{m=1}^{S} \Gamma_m, \quad \Gamma_m \cap \Gamma_n = \oslash \ \text{ for } \ m \neq n,$$

each segment is defined by local parametrization. Choosing N nodes $\chi(\chi^x, \chi^y) \in \Gamma$ in such way, that all the segment joints belong into the set of nodes χ, the boundary may be divided into N elements $\mathbf{e}_i$ such that χ_i will be left-hand side end point of the element $\mathbf{e}_i$ and χ_{i+1} will be its right-hand side end point looking from the interior of Ω and

$$\Gamma = \bigcup_{i=1}^{N} \mathbf{e}_i.$$

In case the boundary is piece-wise linear, there will always exist discretization into line elements which will map the boundary exactly. For more complex boundaries either curved elements must be designed or they may be approximated by line elements, so that the problem will not be solved on Γ but on some Γ_h in fact.

What is commonly called an element throughout this work is a combination of a boundary segment $\mathbf{e}_i$ and a set of functions $\phi_k : \mathbf{e}_i \subset \text{supp } \phi_k$, which are known as basis functions, appearing in (5.1). Each type of element is defined via the reference element $\mathbf{e}^*$, for which local coordinate system is introduced. Since the boundary is one-dimensional in R^2, symbol ξ will be used for the local coordinate, and by definition $\xi = 0$ at the middle of the element and $\xi = -1$ at the starting point (corresponding to χ_i) and $\xi = 1$ at the end point (corresponding to χ_{i+1}). Line elements will be formed by straight lines connecting χ_i and χ_{i+1}. The actual coordinate of $\mathbf{e}_i$ is connected to ξ of the reference element through mapping $\mathcal{M}$. In case of line elements it is defined as

$$\mathbf{x} = \mathcal{M}(\xi) = \frac{1}{2}(\chi_i + \chi_{i+1}) + \frac{1}{2}\xi(\chi_{i+1} - \chi_i) \ \text{ for } \ \xi \in \langle -1, 1 \rangle \,.$$

The mesh suitable for calculations is supposed to be uniform with respect to element sizes (lengths), so that if h denotes the length of element,

$$h = \sqrt{(\chi_{i+1}^x - \chi_i^x)^2 + (\chi_{i+1}^y - \chi_i^y)^2},$$

the elements satisfy

$$\frac{h_{\max}}{h_{\min}} \leq c_{\mathrm{mesh}},$$

where $h_{\max}$ and $h_{\min}$ are lengths of largest and smallest elements respectively and c_{mesh} is a constant.

5.2 Space of Test Functions S_h

The basis functions appearing in (5.1) form a test space S_h. In the majority of implementations of BEM for the Helmholtz equation, piece-wise constant basis functions are used. They are simple to apply, enable easy treatment of discontinuous boundary conditions and Neumann boundary problems and produce satisfactory results. However, elements of higher order, namely first and second, are also of practical importance and will be introduced aside a new class of elements based on physical considerations combining polynomial with exponential function.

5.2.1 Piecewise Constant Basis Functions

The simplest choice of shape function is a function constant on the reference element, that is

$$\varphi(\xi) = 1 \quad \text{for} \quad \xi \in \langle -1, 1 \rangle\,.$$

The respective basis functions ϕ_k generating the test space will then be piece-wise constant on Γ,

$$\phi_k(\mathbf{x}) = \begin{cases} 1 & \text{for} \quad \mathbf{x} \in \mathbf{e}_k, \\ 0 & \text{for} \quad \mathbf{x} \notin \mathbf{e}_k, \end{cases}$$

where $k = 1, ..., N$; N still stands for the number of elements. For the trial space S_h^0 then holds

$$S_h^0(\Gamma) = \text{span} \ \{\phi_k\}_{k=1}^{N}\,, \quad \dim S_h^0(\Gamma) = N.$$

Each element has only one node coinciding with the mid-point of the element.

5.2.2 Piecewise Linear Basis Functions

Using the local coordinate system of the reference element, two linear shape functions

$$\varphi_1^{(1)}(\xi) = \frac{1}{2}(1 + \xi) \ \ \text{for} \ \ \xi \in \langle -1, 1 \rangle \,,$$

and

$$\varphi_2^{(1)}(\xi) = \frac{1}{2}(1 - \xi) \ \ \text{for} \ \ \xi \in \langle -1, 1 \rangle \,.$$

may be constructed. The global basis functions ϕ_k will then be piece-wise linear continuous with supports formed by two neighbouring elements $\mathbf{e}_k$ and $\mathbf{e}_{k+1}$, that is

$$\phi_k(\mathbf{x}) = \begin{cases} 1 & \text{for} \ \ \mathbf{x} = \chi_{k+1}, \\[2mm] 0 & \text{for} \ \ \mathbf{x} \notin \mathbf{e}_k \cup \mathbf{e}_{k+1}, \\[2mm] \varphi_1^{(1)}(\mathcal{M}(\xi)) & \text{for} \ \ \chi_k, \chi_{k+1}, \xi \in \langle -1, 1 \rangle \,, \\[2mm] \varphi_2^{(1)}(\mathcal{M}(\xi)) & \text{for} \ \ \chi_{k+1}, \chi_{k+2}, \xi \in \langle -1, 1 \rangle \,, \end{cases}$$

for $k = 1, ..., N$. These basis functions generate the trial space S_h^1, so that

$$S_h^1(\Gamma) = \text{span} \ \{\phi_k\}_{k=1}^N \,, \quad \dim S_h^1(\Gamma) = N.$$

Each linear element has two nodes coinciding with its end-points, which are shared by its neighbours.

5.2.3 Piecewise Linear Discontinuous Basis Functions

For some problems (discontinuous boundary condition, Neumann problem) a trial space of functions discontinuous across the element joints will be needed or advantageous. For linear polynomials, the shape functions on individual elements will be the same as was the case of continuous basis functions, i.e.

$$\varphi_1^{(1)}(\xi) = \frac{1}{2}(1 + \xi) \ \ \text{for} \ \ \xi \in \langle -1, 1 \rangle \,,$$

and

$$\varphi_2^{(1)}(\xi) = \frac{1}{2}(1 - \xi) \ \text{ for } \ \xi \in \langle -1, 1 \rangle \,.$$

The global basis functions ϕ_k will however be piece-wise linear discontinuous with supports formed by the individual elements $\mathbf{e}_k$ only, and there will be two types of them,

$$\phi_k^{(1)}(\mathbf{x}) = \begin{cases} 1 & \text{for } \ \mathbf{x} = \chi_{k+1}, \\ 0 & \text{for } \ \mathbf{x} \notin \mathbf{e}_k, \\ \varphi_1^{(1)}(\mathcal{M}(\xi)) & \text{for } \ \chi_k, \chi_{k+1}, \xi \in \langle -1, 1 \rangle \,, \end{cases}$$

and

$$\phi_k^{(2)}(\mathbf{x}) = \begin{cases} 1 & \text{for } \ \mathbf{x} = \chi_k, \\ 0 & \text{for } \ \mathbf{x} \notin \mathbf{e}_k, \\ \varphi_2^{(1)}(\mathcal{M}(\xi)) & \text{for } \ \chi_k, \chi_{k+1}, \xi \in \langle -1, 1 \rangle \,, \end{cases}$$

for $k = 1, ..., N$. Apparently, there will be $2N$ basis functions and for the trial space $S_h^{1,d}$ it holds

$$S_h^{1,d}(\Gamma) = \text{span} \ \left\{ \phi_k^{(1)}, \phi_k^{(2)} \right\}_{k=1}^N, \quad \dim S_h^{1,d}(\Gamma) = 2N.$$

As in previous case, each element has two nodes equal to its end-points, but because of the discontinuity the nodes only belong to the respective element. Naturally, use of discontinous linear elements will result in systems with rectangular matrices.

5.2.4 Piecewise Quadratic Basis Functions

Using the same local coordinate system as above, quadratic shape functions may be introduced on the reference element,

$$\varphi_1^{(2)}(\xi) = \frac{1}{2}\xi(\xi - 1) \ \text{ for } \ \xi \in \langle -1, 1 \rangle \,,$$

$$\varphi_2^{(2)}(\xi) = \frac{1}{2}\xi(\xi + 1) \ \text{ for } \ \xi \in \langle -1, 1 \rangle \,,$$

$$\varphi_3^{(2)}(\xi) = (1 - \xi)(1 + \xi) \quad \text{for} \ \ \xi \in \langle -1, 1 \rangle .$$

Thus, quadratic element will have three nodes, two at the end points and one in the middle. Adding the mid-points of the elements to the set of points χ_i we obtain $2N$ nodes. There will be the same number of global basis functions ϕ_k, which will be of two types.

$$\phi_k^{(1)}(\mathbf{x}) = \begin{cases} 1 & \text{for} \ \ \mathbf{x} = \chi_{k+1}, \\[2mm] 0 & \text{for} \ \ \mathbf{x} \notin \mathbf{e}_k \cup \mathbf{e}_{k+1}, \\[2mm] \varphi_1^{(2)}(\mathcal{M}(\xi)) & \text{for} \ \ \chi_k, \chi_{k+1}, \xi \in \langle -1, 1 \rangle , \\[2mm] \varphi_2^{(2)}(\mathcal{M}(\xi)) & \text{for} \ \ \chi_{k+1}, \chi_{k+2}, \xi \in \langle -1, 1 \rangle , \end{cases}$$

and

$$\phi_k^{(2)}(\mathbf{x}) = \begin{cases} \varphi_3^{(2)}(\mathcal{M}(\xi)) & \text{for} \ \ \chi_k, \chi_{k+1}, \xi \in \langle -1, 1 \rangle , \\[2mm] 0 & \text{for} \ \ \mathbf{x} \notin \mathbf{e}_k. \end{cases}$$

For the trial space S_h^2 then follows

$$S_h^2(\Gamma) = \text{span} \ \left\{ \phi_k^{(1)}, \phi_k^{(2)} \right\}_{k=1}^{N}, \quad \dim S_h^2(\Gamma) = 2N.$$

5.2.5 Approximating Properties of Polynomial Trial Spaces

Obviously, for any of the trial spaces it holds $S_h(\Gamma) \subset L_2(\Gamma)$. For each function $u \in L_2(\Gamma)$ there exists an approximation $u_h \in S_h(\Gamma)$ defined by an L_2-projection of u. The best approximation will arise from projection minimizing the difference $u - Pu$, hence

$$u_h = Pu = \sum_{k=1}^{N} c_k \phi_k(x), \quad \phi_k \in S_h(\Gamma),$$

with P satisfying

$$Pu = \arg \min_{u_h \in S_h(\Gamma)} ||u - u_h||_{L_2(\Gamma)}.$$

Since the solutions are assumed to be sufficiently regular functions $u \in H^s(\Gamma)$, the theorem of Steinbach and Rjasanow may be applied, cf. [34], giving the estimates for approximation by constant, linear and discontinuous linear test spaces.

Theorem 5 *Let $u \in H^s_{pw}(\Gamma)$ for $s \in [0,1]$. Then for piece-wise constant approximation holds*

$$\inf_{u_h \in S^0_h(\Gamma)} ||u - u_h||_{H^\sigma(\Gamma)} \leq ch^{s-\sigma}|u|_{H^s_{pw}(\Gamma)}, \quad \forall \ \sigma \in [-1,0].$$

Let $u \in H^s_{pw}(\Gamma)$ for $s \in [1,2]$. Then for piece-wise linear approximation holds

$$\inf_{u_h \in S^1_h(\Gamma)} ||u - u_h||_{H^\sigma(\Gamma)} \leq ch^{s-\sigma}|u|_{H^s_{pw}(\Gamma)}, \quad \forall \ \sigma \in [-2,1].$$

Let $u \in H^s_{pw}(\Gamma)$ for $s \in [0,2]$. Then for piece-wise linear discontinuous approximation holds

$$\inf_{u_h \in S^{1,d}_h(\Gamma)} ||u - u_h||_{H^\sigma(\Gamma)} \leq ch^{s-\sigma}|u|_{H^s_{pw}(\Gamma)}, \quad \forall \ \sigma \in [-2,0].$$

(Here, the subscript $._{pw}$ is an abbreviation for piece-wise.)

For the approximation properties of the quadratic elements we shall prove the following theorem.

Theorem 6 *Let $u \in H^s(\Gamma)$ for $s \in [\sigma,3]$ and $\sigma = 0,1$. Then for quadratic approximation holds*

$$\inf_{u_h \in S^2_h(\Gamma)} ||u - u_h||_{H^\sigma(\Gamma)} \leq ch^{s-\sigma}|u|_{H^s(\Gamma)}.$$

Proof: First, we give the theorem proved by Brenner and Scott in [7] as a lemma, which applies to d-dimensional domains.

Lemma 1 *Let $(\mathcal{K}, \mathcal{P}, \mathcal{N})$ be a finite element satisfying*

(i) *$\mathcal{K}$ is star-shaped with respect to some ball,*

(ii) *$\mathcal{P}_{m-1} \subseteq \mathcal{P} \subseteq W^m_\infty(\mathcal{K})$ and*

(iii) *$\mathcal{N} \subseteq (C^l(\bar{\mathcal{K}}))'$.*

Suppose $1 \leq q \leq \infty$ and either $m - l - d/q > 0$ when $q > 1$ or $m - l - d \geq 0$ when $q = 1$. Then for $0 \leq s \leq m$ and $v \in W^m_q(\mathcal{K})$ we have

$$|v - Iv|_{W^s_q(\mathcal{K})} \leq c_{m,d,\sigma(\hat{\mathcal{K}})}(\text{diam } \mathcal{K})^{m-s}|v|_{W^m_q(\mathcal{K})},$$

where $\hat{\mathcal{K}} = \{1/\text{diam } \mathcal{K}\} x : x \in \mathcal{K}$.

Using this lemma for the case $d = 1, l = 0, q = 2$ we have

$$||w - I_h w||_{H^s(\mathbf{e}_k)} \leq ch_k^{m-s}|w|_{H^m(\mathbf{e}_k)} \quad \text{for} \quad w \in H^m,$$

where I_h is the interpolation operator and $0 \leq s \leq m$. From here

$$||w - I_h w||_{H^s(\mathbf{e}_k)}^2 \leq ch_k^{2(m-s)}|w|_{H^m(\mathbf{e}_k)}^2, \tag{5.2}$$

and hence for given discretization into N elements

$$||w - I_h w||_{H^s(\Gamma)}^2 = \sum_{k=1}^{N} ||w - I_h w||_{H^s(\mathbf{e}_k)}^2 \leq$$

$$\leq c \sum_{k=1}^{N} h_k^{2(m-s)}|w|_{H^m(\mathbf{e}_k)}^2 \leq ch^{2(m-s)}|w|_{H^m(\Gamma)}^2.$$

From here follows the estimate

$$||w - I_h w||_{H^s(\Gamma)} \leq ch^{m-s}|w|_{H^m(\Gamma)}, \tag{5.3}$$

where $0 \leq s \leq m$, for $w \in H^m(\Gamma)$. For quadratic elements $m = 3$.

Let us for given $u \in L_2(\Gamma)$ define an L_2-projection $Q_h u \in S_h^2(\Gamma)$ as given by the variational problem

$$\langle Q_h u, v_h \rangle_{L_2(\Gamma)} = \langle u, v_h \rangle_{L_2(\Gamma)} \quad \forall v_h \in S_h^2(\Gamma).$$

Since it is satisfied for arbitrary v_h, we may choose $v_h = Q_h u$. Then we obtain

$$||Q_h(u)||_{L_2(\Gamma)}^2 = \langle Q_h u, Q_h u \rangle_{L_2(\Gamma)} = \langle u, Q_h u \rangle_{L_2(\Gamma)} \leq ||u||_{L_2(\Gamma)}.||Q_h u||_{L_2(\Gamma)}.$$

From here follows

$$||Q_h(u)||_{L_2(\Gamma)} \leq ||u||_{L_2(\Gamma)},$$

that is, we have stability. Moreover, orthogonality follows

$$\langle u - Q_h u, v_h \rangle_{L_2(\Gamma)} = 0 \quad \forall v_h \in S_h^2(\Gamma).$$

Using the orthogonality and the Schwarz inequality we obtain

$$||u - Q_h u||^2_{L_2(\Gamma)} = \langle u - Q_h u, u - Q_h u \rangle_{L_2(\Gamma)} =$$
$$\langle u - Q_h u, u \rangle_{L_2(\Gamma)} - \langle u - Q_h u, Q_h u \rangle_{L_2(\Gamma)} \leq ||u - Q_h u||_{L_2(\Gamma)}.||u||_{L_2(\Gamma)}.$$

From here

$$||u - Q_h u||_{L_2(\Gamma)} \leq ||u||_{L_2(\Gamma)} \quad \forall u \in L_2(\Gamma). \tag{5.4}$$

Besides, from the orthogonality also follows

$$
\begin{aligned}
||u - Q_h u||^2_{L_2(\Gamma)} &= \langle u - Q_h u, u - Q_h u \rangle_{L_2(\Gamma)} = \\
&= \langle u - Q_h u, u - I_h u + I_h u - Q_h u \rangle_{L_2(\Gamma)} = \\
&= \langle u - Q_h u, u - I_h u \rangle_{L_2(\Gamma)} + \langle u - Q_h u, I_h u - Q_h u \rangle_{L_2(\Gamma)} = \\
&= \langle u - Q_h u, u - I_h u \rangle_{L_2(\Gamma)} \leq ||u - Q_h u||_{L_2(\Gamma)}.||u - I_h u||_{L_2(\Gamma)}.
\end{aligned}
$$

and therefore

$$||u - Q_h u||_{L_2(\Gamma)} \leq ||u - I_h u||_{L_2(\Gamma)}.$$

Combining this result with 5.3 yields

$$||u - Q_h u||_{L_2(\Gamma)} \leq ch^3 ||u||_{H^3(\Gamma)}, \tag{5.5}$$

and also

$$||u - Q_h u||^2_{L_2(\Gamma)} \leq c \sum_{k=1}^{N} h_k^6 ||u||^2_{H^3(\mathbf{e}_k)}, \tag{5.6}$$

where N stands for the number of elements into which boundary is discretized.

Using 5.4 and 5.5 we obtain

$$||u - Q_h u||_{L_2(\Gamma)} \leq ch ||u||_{H^1(\Gamma)} \leq ch^2 ||u||_{H^2(\Gamma)}.$$

Further, let $Q_h : H^1(\Gamma) \to S_h^2(\Gamma)$ be an H^1-projection defined as the unique solution of

$$\langle Q_h u, v_h \rangle_{H^1} = \langle u, v_h \rangle_{H^1} \quad \forall v_h \in S_h^2.$$

By the same reasoning as in the case of L_2-projection we obtain the stability

$$||Q_h u||_{H^1} \leq ||u||_{H^1} \quad \forall u \in H^1(\Gamma),$$

and from here

$$||u - Q_h u||_{H^1} \leq ||u||_{H^1},$$

and also

$$||u - Q_h u||^2_{H^1(\Gamma)} \leq ||u - I_h u||^2_{H^1(\Gamma)} \leq c \sum_{k=1}^{N} h_k^4 |u|_{H^3(\mathbf{e}_k)},$$

by application of (5.2).

The proposition of the theorem for $\sigma = 0$ and $s = 3$ follows by substituting into (5.5). For $\sigma = 0$ and $s = 0$ the theorem follows from (5.4). The case of $\sigma = 0$ and $s \in (0, 3)$ is a result of interpolation of the two previous cases. Result for $\sigma = 1$ is obtained from (5.6) by setting $s = 3$.

5.2.6 Exponential Basis Functions

The polynomial basis functions introduced above give rise to what could be called standard boundary elements for general purposes. However, physical considerations have led to the proposal of special basis functions designed for the practically very important case of scattering of a plane wave. To capture waves of higher wave numbers properly, a dense discretization is needed since the length of the elements must be proportional to the wavelength, which leads to great increase in computational costs. Abboud and Nedelec in [1] and De La Bourdonnaye in [5] have suggested to resolve this issue by application of exponential basis functions in the form

$$\phi = p(\mathbf{x}) e^{-ik\mathbf{dx}}$$

where k is the wave number and $\mathbf{d}$ represents the direction of the incident wave, $p(\mathbf{x})$ is general polynomial. The idea is based on utilization of the known physical solutions and the basis functions are modelled to be close to these. Application of such basis functions should lead to a drastic decrease of the number of elements needed for the discretization. However, this approach is limited to the case of convex scatterer. A star of directions is used in several related methods (see the review [5]), but then the complexity order of the overall computation appears not to improve. A remedy for this may be choosing a small

number of directions adaptively, similarly as suggested in [23] in the case of FEM. This is an area of future research.

For practical purposes the polynomial part of the basis function will be defined by constant, linear or quadratic polynomial, so that the following trial spaces will be defined. $S_h^{0,p}$ will be given as

$$S_h^{0,p}(\Gamma) = \text{span } \{\phi_k\}_{k=1}^N, \quad \dim S_h^{0,p}(\Gamma) = N,$$

where the basis functions ϕ_k are given as

$$\phi_k(\mathbf{x}) = \begin{cases} e^{-ik\mathbf{dx}} & \text{for } \mathbf{x} \in \mathbf{e}_k, \\ \\ 0 & \text{for } \mathbf{x} \notin \mathbf{e}_k, \end{cases}$$

where $k = 1, ..., N$. For the trial space $S_h^{1,p}$ it holds

$$S_h^{1,p}(\Gamma) = \text{span } \{\phi_k\}_{k=1}^N, \quad \dim S_h^{1,p}(\Gamma) = N,$$

while the basis functions are given as

$$\phi_k(\mathbf{x}) = \begin{cases} 1 & \text{for } \mathbf{x} = \chi_{k+1}, \\ \\ 0 & \text{for } \mathbf{x} \notin \mathbf{e}_k \cup \mathbf{e}_{k+1}, \\ \\ \varphi_1^{(1)}(\mathcal{M}(\xi))e^{-ik\mathbf{dx}}/e^{-ik\mathbf{d}\chi_{k+1}} & \text{for } \chi_k, \chi_{k+1}, \xi \in \langle -1, 1 \rangle, \\ \\ \varphi_2^{(1)}(\mathcal{M}(\xi))e^{-ik\mathbf{dx}}/e^{-ik\mathbf{d}\chi_{k+1}} & \text{for } \chi_{k+1}, \chi_{k+2}, \xi \in \langle -1, 1 \rangle, \end{cases}$$

for $k = 1, ..., N$. Finally, for the space of test functions $S_h^{2,p}$ there is

$$S_h^2(\Gamma) = \text{span } \left\{\phi_k^{(1)}, \phi_k^{(2)}\right\}_{k=1}^N, \quad \dim S_h^2(\Gamma) = 2N,$$

and the basis functions are defined as

$$\phi_k^{(1)}(\mathbf{x}) = \begin{cases} 1 & \text{for } \mathbf{x} = \chi_{k+1}, \\ \\ 0 & \text{for } \mathbf{x} \notin \mathbf{e}_k \cup \mathbf{e}_{k+1}, \\ \\ \varphi_1^{(2)}(\mathcal{M}(\xi))e^{-ik\mathbf{dx}}/e^{-ik\mathbf{d}\chi_{k+1}} & \text{for } \chi_k, \chi_{k+1}, \xi \in \langle -1, 1 \rangle, \\ \\ \varphi_2^{(2)}(\mathcal{M}(\xi))e^{-ik\mathbf{dx}}/e^{-ik\mathbf{d}\chi_{k+1}} & \text{for } \chi_{k+1}, \chi_{k+2}, \xi \in \langle -1, 1 \rangle, \end{cases}$$

and

$$\phi_k^{(2)}(\mathbf{x}) = \begin{cases} \varphi_3^{(2)}(\mathcal{M}(\xi))e^{-ik\mathbf{dx}}/e^{-ik\mathbf{d}\chi_m} & \text{for} \quad \chi_k, \chi_{k+1}, \xi \in \langle -1, 1 \rangle, \\ \\ 0 & \text{for} \quad \mathbf{x} \notin \mathbf{e}_k, \end{cases}$$

where χ_m denotes the mid-point of the element. In our calculations only the first type of exponential elements has been used. The results are promising, but theoretical analysis giving necessary error estimates is lacking and is also a subject of further research.

5.3 Collocation Method

Collocation is the simplest implementation of Boundary Element Method. The values of the unknown function are calculated in pre-defined points known as collocation points. In practice, the unknown function in the boundary integral representation is substituted by its projection onto given space of test functions S_h and the collocation points coincide with the nodes of elements into which the boundary is discretized.

The Dirichlet problem will be taken as a sample problem. We are to find function $w(\mathbf{y})$ satisfying the integral Helmholtz equation

$$\int_\Gamma u_\Gamma(\mathbf{y}) \frac{\partial g(\mathbf{x}, \mathbf{y})}{\partial \nu} ds_\mathbf{y} - \int_\Gamma w(\mathbf{y}) g(\mathbf{x}, \mathbf{y}) ds_\mathbf{y} = \frac{\theta^i}{2\pi} u_\Gamma(\mathbf{x}) \text{ for } \mathbf{x} \in \Gamma, \tag{5.7}$$

with the Dirichlet boundary condition

$$u_\Gamma(\mathbf{y}) = \psi(\mathbf{y}) \text{ on } \Gamma.$$

The unknown function in fact represents the Neumann data,

$$w(\mathbf{y}) = \frac{\partial u_\Gamma(\mathbf{y})}{\partial \nu} \text{ for } \mathbf{y} \in \Gamma.$$

Approximating w by w_h, where

$$w_h(\mathbf{y}) = \sum_{k=1}^M c_k \phi_k(\mathbf{y}) \text{ for } \phi_k \in S_h,$$

discretizing the boundary into N elements and substituting into (5.7), one obtains

$$\sum_{i=1}^N \int_{\mathbf{e}_i} \psi(\mathbf{y}) \frac{\partial g(\mathbf{x}, \mathbf{y})}{\partial \nu} ds_\mathbf{y} - \sum_{k=1}^M \sum_{i=1}^N \int_{\mathbf{e}_i} c_k \phi_k(\mathbf{y}) g(\mathbf{x}, \mathbf{y}) ds_\mathbf{y} = \frac{\theta^i}{2\pi} \psi(\mathbf{x}) \text{ on } \Gamma. \tag{5.8}$$

The actual form of the system given by (5.8) will depend on choice of S_h.

5.3.1 Collocation with Constant Basis Functions

Taking the basis functions from the space of constant functions, $\phi_k \in S_h^0$, and substituting into (5.8) gives

$$\sum_{k=1}^{N} c_k \int_{\mathbf{e}_k} g(\mathbf{x}_i, \mathbf{y}) ds_{\mathbf{y}} = -\frac{\theta^i}{2\pi} \psi(\mathbf{x}_i) + \int_{\Gamma} \psi(\mathbf{y}) \frac{\partial g(\mathbf{x}_i, \mathbf{y})}{\partial \nu} ds_{\mathbf{y}},$$

where $\mathbf{x}_i$ for $i = 1, ..., N$ are the midpoints of the elements. (Since the supports of the basis functions coincide with the individual elements, only one sum is needed.) This represents a system of N linear equations for the vector of coefficients $\mathbf{c} = (c_1, c_2, ...c_N)^T$,

$$\mathbf{K}_h \mathbf{c} = \mathbf{f},$$

where the elements of the stiffness matrix are defined by

$$\mathbf{K}_h(i, j) = \int_{\mathbf{e}_j} g(\mathbf{x}_i, \mathbf{y}) ds_{\mathbf{y}},$$

and for the right-hand side there is

$$f_i = -\frac{\theta^i}{2\pi} \psi(\mathbf{x}_i) + \int_{\Gamma} \psi(\mathbf{y}) \frac{\partial g(\mathbf{x}_i, \mathbf{y})}{\partial \nu} ds_{\mathbf{y}}.$$

The system matrix is apparently full and in general, e.g. for irregular shape domains, not symmetric.

5.3.2 Collocation with Linear Basis Functions

Taking $\phi_k \in S_h^1$ and substituting into (5.8) leads to the discretized equation

$$\sum_{k=1}^{N} \sum_{j=1}^{N} c_k \int_{\mathbf{e}_j} \phi_k(\mathbf{y}) g(\mathbf{x}_i, \mathbf{y}) ds_{\mathbf{y}} = -\frac{\theta^i}{2\pi} \psi(\mathbf{x}_i) + \int_{\Gamma} \psi(\mathbf{y}) \frac{\partial g(\mathbf{x}_i, \mathbf{y})}{\partial \nu} ds_{\mathbf{y}},$$

for $i = 1, ..., N$. The points $\mathbf{x}_i$ are nodes of linear elements, that is they are the joints of the elements. This again represents system of N equations for coefficients c_k. The system matrix is dense and since each basis function ϕ_k has two neighbouring elements as its support, for its entries will hold

$$\mathbf{K}_h(i, j) = \int_{\mathbf{e}_j} \varphi_1^{(1)}(\mathcal{M}(\xi)) g(\mathbf{x}_i, \mathbf{y}) ds_{\mathbf{y}} + \int_{\mathbf{e}_{j+1}} \varphi_2^{(1)}(\mathcal{M}(\xi)) g(\mathbf{x}_i, \mathbf{y}) ds_{\mathbf{y}}.$$

The discontinuous basis functions $\phi_k \in S_h^{1,d}$ give rise to formula similar to the case of constant approximation

$$\sum_{k=1}^{2N} c_k \int_{\mathbf{e}_k} \phi_k(\mathbf{y}) g(\mathbf{x}_i, \mathbf{y}) ds_{\mathbf{y}} = -\frac{\theta^i}{2\pi} \psi(\mathbf{x}_i) + \int_{\Gamma} \psi(\mathbf{y}) \frac{\partial g(\mathbf{x}_i, \mathbf{y})}{\partial \nu} ds_{\mathbf{y}},$$

$i = 1, ..., N$, since each basis function only has one element as its support. Stiffness matrix will then have entries

$$\mathbf{K}_h(i,j) = \int_{\mathbf{e}_j} \varphi_1^{(1)}(\mathcal{M}(\xi)) g(\mathbf{x}_i, \mathbf{y}) ds_{\mathbf{y}},$$

for j odd, and

$$\mathbf{K}_h(i,j) = \int_{\mathbf{e}_{j+1}} \varphi_2^{(1)}(\mathcal{M}(\xi)) g(\mathbf{x}_i, \mathbf{y}) ds_{\mathbf{y}},$$

for j even. The right-hand side is independent of choice of trial space and is the same as for constant approximation.

5.3.3 Collocation with Quadratic Basis Functions

For basis function $\phi_k \in S_h^2$ the substitution into (5.8) yields

$$\sum_{k=1}^{2N} \sum_{j=1}^{N} c_k \int_{\mathbf{e}_j} \phi_k(\mathbf{y}) g(\mathbf{x}_i, \mathbf{y}) ds_{\mathbf{y}} = -\frac{\theta^i}{2\pi} \psi(\mathbf{x}_i) + \int_{\Gamma} \psi(\mathbf{y}) \frac{\partial g(\mathbf{x}_i, \mathbf{y})}{\partial \nu} ds_{\mathbf{y}},$$

for $i = 1, ..., 2N$. This represents a system of $2N$ equations for coefficients of basis functions at nodes $\mathbf{x}_i$, which are at element joints and midpoints. The stiffness matrix terms are defined as

$$\mathbf{K}_h(i,j) = \int_{\mathbf{e}_j} \varphi_1^{(2)}(\mathcal{M}(\xi)) g(\mathbf{x}_i, \mathbf{y}) ds_{\mathbf{y}} + \int_{\mathbf{e}_{j+1}} \varphi_2^{(2)}(\mathcal{M}(\xi)) g(\mathbf{x}_i, \mathbf{y}) ds_{\mathbf{y}},$$

for j odd, and

$$\mathbf{K}_h(i,j) = \int_{\mathbf{e}_j} \varphi_3^{(2)}(\mathcal{M}(\xi)) g(\mathbf{x}_i, \mathbf{y}) ds_{\mathbf{y}},$$

for j even. The right-hand side again stays the same.

It must be stressed out, that while collocation is widely used in engineering applications since it is easy to implement, general analysis of the method is not available yet. Stability of the scheme has so far only been proved for some special cases but not for general domains. For details see [4], [34].

5.4 Galerkin Method

Galerkin method for Boundary Elements is the variational approach similar to Finite Element techniques. Multiplying the representation formula (5.7) by a test function $v \in H^{-1/2}(\Gamma)$ and integrating along the boundary results in

$$\int_\Gamma \int_\Gamma w(\mathbf{y}) g(\mathbf{x}, \mathbf{y}) v(\mathbf{x}) ds_\mathbf{x} ds_\mathbf{y} = \tag{5.9}$$

$$= -\frac{1}{2} \int_\Gamma u_\Gamma(\mathbf{x}) v(\mathbf{x}) ds_\mathbf{x} + \int_\Gamma \int_\Gamma u_\Gamma(\mathbf{y}) \frac{\partial g(\mathbf{x}, \mathbf{y})}{\partial \nu} v(\mathbf{x}) ds_\mathbf{x} ds_\mathbf{y} \quad \text{for} \ \ \mathbf{x} \in \Gamma,$$

where $w(\mathbf{y})$ again represents the unknown Neumann data and $u_\Gamma = \psi$ on Γ. In the variational setting, we are to find w satisfying

$$\langle L_k w, v \rangle_\Gamma = \langle (-\frac{1}{2} I + M_k) \psi, v \rangle_\Gamma \quad \text{for all} \ \ v \in H^{-1/2}(\Gamma).$$

Now, approximating w by w_h,

$$w_h = \sum_{k=1}^M c_k \phi_k,$$

where $\phi_k \in S_h$, and taking the test functions $v \in S_h$ only will yield the Galerkin approximation

$$\langle L_k w_h, \phi_k \rangle_\Gamma = \langle (-\frac{1}{2} I + M_k) \psi, \phi_k \rangle_\Gamma \quad \text{for} \ \ k = 1, ..., N.$$

The actual form of the system depends on the choice of S_h.

5.4.1 Galerkin with Constant Basis Functions

Taking $\phi_k \in S_h^0$ and substituting into (5.9) gives

$$\sum_{k=1}^N c_k \int_\Gamma \int_\Gamma \phi_k(\mathbf{y}) g(\mathbf{x}, \mathbf{y}) \phi_j(\mathbf{x}) ds_\mathbf{x} ds_\mathbf{y} =$$

$$-\frac{1}{2} \int_\Gamma \psi(\mathbf{x}) \phi_j(\mathbf{x}) ds_\mathbf{x} + \int_\Gamma \int_\Gamma \psi(\mathbf{y}) \frac{\partial g(\mathbf{x}, \mathbf{y})}{\partial \nu} \phi_j(\mathbf{x}) ds_\mathbf{x} ds_\mathbf{y},$$

for $j = 1, ..., N$. The formula represents a system of N linear equations for the unknown coefficients c_k,

$$\mathbf{K}_h \mathbf{c} = \mathbf{f}.$$

Since $\phi_k = 1$ on $\mathbf{e}_k$ and zero everywhere else, for the matrix entries there is

$$\mathbf{K}_h(k, j) = \int_{\mathbf{e}_k} \int_{\mathbf{e}_k} g(\mathbf{x}, \mathbf{y}) ds_{\mathbf{x}} ds_{\mathbf{y}},$$

and for the right-hand side

$$f_k = -\frac{1}{2} \int_{\mathbf{e}_k} u_\Gamma(\mathbf{x}) ds_{\mathbf{x}} + \int_{\mathbf{e}_k} \int_\Gamma \psi(\mathbf{y}) \frac{\partial g(\mathbf{x}, \mathbf{y})}{\partial \nu} ds_{\mathbf{x}} ds_{\mathbf{y}}.$$

The matrix of the system is again full as in case of collocation, but for Galerkin method it will always be symmetric and positive definite. The operator $L_k : H^{-1/2}(\Gamma) \to H^{1/2}(\Gamma)$ is coercive and injective in case k^2 is not an eigenvalue of the interior Dirichlet problem (cf. section 3.3 and [24], [34]), the system arising from Galerkin discretization is uniquely solvable and the error estimate in the form of Cea's lemma is valid

$$||w - w_h||_{H^{-1/2}(\Gamma)} \le c \inf_{v \in S_h^0(\Gamma)} ||w - v||_{H^{-1/2}(\Gamma)}.$$

Substituting the approximation estimate for constant functions given in Theorem 5 for $\sigma = -1/2$ yields

$$||w - w_h||_{H^{-1/2}(\Gamma)} \le ch^{s+1/2} |w|_{H_{pw}^s(\Gamma)},$$

for $w \in H_{pw}^s(\Gamma)$ and $s \in [0, 1]$, subscript $._{pw}$ again stands for piece-wise, and more general estimate can also be obtained for $w \in H^s(\Gamma)$ and $s \in [0, 1]$ and $\sigma \in [-2, 0]$, namely

$$||w - w_h||_{H^\sigma(\Gamma)} \le ch^{s-\sigma} |w|_{H_{pw}^s(\Gamma)}.$$

For the procedure and details cf. [34].

These estimates are valid for the solution on the boundary, that is for the calculation of the unknown Neumann data. Denoting the approximate solution in the exterior obtained by solving the appropriate representation equation with w_h by u_h, for a point in the exterior there will be an error estimate

$$u(\mathbf{x}) - u_h(\mathbf{x}) = \int_\Gamma g(\mathbf{x}, \mathbf{y})(w(\mathbf{y}) - w_h(\mathbf{y})) ds_{\mathbf{y}}.$$

Using duality argument and the boundary error estimate, optimal order of convergence for $w \in H_{pw}^1(\Gamma)$ and $s = 1$ will be given as

$$|u(\mathbf{x}) - u_h(\mathbf{x})| \le ch^3 ||g(\mathbf{x}, .)||_{H^2(\Gamma)} |w|_{H_{pw}^1(\Gamma)}.$$

This results is again due to [34].

5.4.2 Galerkin with Linear Basis Functions

Taking $\phi_k \in S_h^1$, substituting into (5.9) and discretizing the boundary into N elements yields

$$\sum_{k=1}^{N} \sum_{m=1}^{N} \sum_{n=1}^{N} c_k \int_{\mathbf{e}_m} \int_{\mathbf{e}_n} \phi_k(\mathbf{y}) g(\mathbf{x}, \mathbf{y}) \phi_j(\mathbf{x}) ds_{\mathbf{x}} ds_{\mathbf{y}} = \quad (5.10)$$

$$-\frac{1}{2} \sum_{m=1}^{N} \int_{\mathbf{e}_i} \psi(\mathbf{x}) \phi_j(\mathbf{x}) ds_{\mathbf{x}} + \sum_{m=1}^{N} \int_{\mathbf{e}_m} \int_{\Gamma} \psi(\mathbf{y}) \frac{\partial g(\mathbf{x}, \mathbf{y})}{\partial \nu} \phi_j(\mathbf{x}) ds_{\mathbf{x}} ds_{\mathbf{y}},$$

for $j = 1, ..., N$. This represents a system of N linear equations for the unknown coefficients c_k,

$$\mathbf{K}_h \mathbf{c} = \mathbf{f}.$$

where the stiffness matrix terms are given by

$$
\begin{aligned}
\mathbf{K}_h(k, j) &= \int_{\mathbf{e}_k} \int_{\mathbf{e}_j} \varphi_1^{(1)}(\mathcal{M}(\xi)) g(\mathbf{x}, \mathbf{y}) \varphi_1^{(1)}(\mathcal{M}(\xi)) ds_{\mathbf{x}} ds_{\mathbf{y}} + \\
&+ \int_{\mathbf{e}_k} \int_{\mathbf{e}_{j+1}} \varphi_1^{(1)}(\mathcal{M}(\xi)) g(\mathbf{x}, \mathbf{y}) \varphi_2^{(1)}(\mathcal{M}(\xi)) ds_{\mathbf{x}} ds_{\mathbf{y}} + \\
&+ \int_{\mathbf{e}_{k+1}} \int_{\mathbf{e}_j} \varphi_2^{(1)}(\mathcal{M}(\xi)) g(\mathbf{x}, \mathbf{y}) \varphi_1^{(1)}(\mathcal{M}(\xi)) ds_{\mathbf{x}} ds_{\mathbf{y}} + \\
&+ \int_{\mathbf{e}_{k+1}} \int_{\mathbf{e}_{j+1}} \varphi_2^{(1)}(\mathcal{M}(\xi)) g(\mathbf{x}, \mathbf{y}) \varphi_2^{(1)}(\mathcal{M}(\xi)) ds_{\mathbf{x}} ds_{\mathbf{y}},
\end{aligned}
$$

and the right-hand side

$$
\begin{aligned}
f_j &= -\frac{1}{2} \int_{\mathbf{e}_j} \psi(\mathbf{x}) \varphi_1^{(1)}(\mathcal{M}(\xi)) ds_{\mathbf{x}} - \frac{1}{2} \int_{\mathbf{e}_{j+1}} \psi(\mathbf{x}) \varphi_2^{(1)}(\mathcal{M}(\xi)) ds_{\mathbf{x}} + \\
&+ \int_{\mathbf{e}_j} \int_{\Gamma} \psi(\mathbf{y}) \frac{\partial g(\mathbf{x}, \mathbf{y})}{\partial \nu} \varphi_1^{(1)}(\mathcal{M}(\xi)) ds_{\mathbf{x}} ds_{\mathbf{y}} + \int_{\mathbf{e}_{j+1}} \int_{\Gamma} \psi(\mathbf{y}) \frac{\partial g(\mathbf{x}, \mathbf{y})}{\partial \nu} \varphi_2^{(1)}(\mathcal{M}(\xi)) ds_{\mathbf{x}} ds_{\mathbf{y}}.
\end{aligned}
$$

5.4.3 Galerkin with Quadratic Basis Functions

Substitution of $\phi_k \in S_h^2$ into (5.10) leads to system of $2N$ linear equations for basis functions coefficients. The stiffness matrix entries are defined as

$$
\begin{aligned}
\mathbf{K}_h(k,j) \;=\; & \int_{\mathbf{e}_k}\int_{\mathbf{e}_j} \varphi_1^{(2)}(\mathcal{M}(\xi))g(\mathbf{x},\mathbf{y})\varphi_1^{(2)}(\mathcal{M}(\xi))ds_\mathbf{x}ds_\mathbf{y} \;+ \\
& + \int_{\mathbf{e}_k}\int_{\mathbf{e}_{j+1}} \varphi_1^{(2)}(\mathcal{M}(\xi))g(\mathbf{x},\mathbf{y})\varphi_2^{(2)}(\mathcal{M}(\xi))ds_\mathbf{x}ds_\mathbf{y} \;+ \\
& + \int_{\mathbf{e}_{k+1}}\int_{\mathbf{e}_j} \varphi_2^{(2)}(\mathcal{M}(\xi))g(\mathbf{x},\mathbf{y})\varphi_1^{(2)}(\mathcal{M}(\xi))ds_\mathbf{x}ds_\mathbf{y} \;+ \\
& + \int_{\mathbf{e}_{k+1}}\int_{\mathbf{e}_{j+1}} \varphi_2^{(2)}(\mathcal{M}(\xi))g(\mathbf{x},\mathbf{y})\varphi_2^{(2)}(\mathcal{M}(\mathbf{x}\xi))ds_\mathbf{x}ds_\mathbf{y},
\end{aligned}
$$

for k and j both odd,

$$
\begin{aligned}
\mathbf{K}_h(k,j) \;=\; & \int_{\mathbf{e}_k}\int_{\mathbf{e}_j} \varphi_1^{(2)}(\mathcal{M}(\xi))g(\mathbf{x},\mathbf{y})\varphi_3^{(2)}(\mathcal{M}(\xi))ds_\mathbf{x}ds_\mathbf{y} \;+ \\
& + \int_{\mathbf{e}_{k+1}}\int_{\mathbf{e}_j} \varphi_2^{(2)}(\mathcal{M}(\xi))g(\mathbf{x},\mathbf{y})\varphi_3^{(2)}(\mathcal{M}(\xi))ds_\mathbf{x}ds_\mathbf{y},
\end{aligned}
$$

for k odd and j even. For k and j both even there is

$$
\mathbf{K}_h(k,j) = \int_{\mathbf{e}_k}\int_{\mathbf{e}_j} \varphi_3^{(2)}(\mathcal{M}(\xi))g(\mathbf{x},\mathbf{y})\varphi_3^{(2)}(\mathcal{M}(\xi))ds_\mathbf{x}ds_\mathbf{y},
$$

and finally, for k even and j odd

$$
\begin{aligned}
\mathbf{K}_h(k,j) \;=\; & \int_{\mathbf{e}_k}\int_{\mathbf{e}_j} \varphi_3^{(2)}(\mathcal{M}(\xi))g(\mathbf{x},\mathbf{y})\varphi_1^{(2)}(\mathcal{M}(\xi))ds_\mathbf{x}ds_\mathbf{y} \;+ \\
& + \int_{\mathbf{e}_k}\int_{\mathbf{e}_{j+1}} \varphi_3^{(2)}(\mathcal{M}(\xi))g(\mathbf{x},\mathbf{y})\varphi_2^{(2)}(\mathcal{M}(\xi))ds_\mathbf{x}ds_\mathbf{y}.
\end{aligned}
$$

The right-hand side terms are given by the formula

$$
\begin{aligned}
f_k \;=\; & -\frac{1}{2}\int_{\mathbf{e}_j} \psi(\mathbf{x})\varphi_1^{(2)}(\mathcal{M}(\xi))ds_\mathbf{x} - \frac{1}{2}\int_{\mathbf{e}_{j+1}} \psi(\mathbf{x})\varphi_2^{(2)}(\mathcal{M}(\xi))ds_\mathbf{x} \;+ \\
& + \int_{\mathbf{e}_j}\int_\Gamma \psi(\mathbf{y})\frac{\partial g(\mathbf{x},\mathbf{y})}{\partial\nu}\varphi_1^{(2)}(\mathcal{M}(\xi))ds_\mathbf{x}ds_\mathbf{y} + \int_{\mathbf{e}_{j+1}}\int_\Gamma \psi(\mathbf{y})\frac{\partial g(\mathbf{x},\mathbf{y})}{\partial\nu}\varphi_2^{(2)}(\mathcal{M}(\xi))ds_\mathbf{x}ds_\mathbf{y},
\end{aligned}
$$

for k odd, and by

$$f_k = -\frac{1}{2}\int_{\mathbf{e}_j}\psi(\mathbf{x})\varphi_3^{(2)}(\mathcal{M}(\xi))ds_{\mathbf{x}} + \int_{\mathbf{e}_j}\int_\Gamma \psi(\mathbf{y})\frac{\partial g(\mathbf{x},\mathbf{y})}{\partial\nu}\varphi_3^{(2)}(\mathcal{M}(\xi))ds_{\mathbf{x}}ds_{\mathbf{y}},$$

for k even.

6

Test Problems and their Numerical Solutions

Both collocation and Galerkin variants of the BEM solver have been programmed. The solver is capable of finding solutions to exterior and interior problems as well, with either Dirichlet or Neumann boundary condition. Moreover, it can be easily modified to solve problems for the Laplace equation in integral form. Polynomial basis functions have been implemented in the form of constant, linear and quadratic elements. The exponential elements have also been included and tested with promising results, however, theory concerning their approximation properties is lacking so far.

In this chapter results are presented which can be compared to analytical solutions so that reliability of the solver can be checked. First, two problems for the Laplace equation are solved, then solutions for the Helmholtz exterior problems follow.

6.1   Laplace Equation as a Test Problem

The same types of interior and exterior problems may be formulated for the Laplace equation as for the Helmholtz equation. In fact, the Helmholtz equation may in certain sense be considered a special case of Poisson equation with specific right-hand side. Therefore, the theory concerning Boundary Element Method valid for the Helmholtz equation is in main part also applicable to the Laplace operator and in fact, the the Laplace problem is often studied first before advancing to acoustics modeled by the Helmholtz equation. From the practical point of view, the BEM solver for the Helmholtz problem may be easily changed into a solver for the Laplacian, and since the latter problem is much easier to solve and analyze and analytic solutions are available for many cases, it can be readily employed for basic testing of the solver.

The simplest problem for the Laplace equation in two dimensions is to find function $u(\mathbf{x}, \mathbf{y})$ satisfying

$$\Delta u(\mathbf{x}, \mathbf{y}) = 0 \ \text{ in } \ \Omega$$

with Dirichlet boundary condition

$$u(\mathbf{x}, \mathbf{y}) = g(\mathbf{x}, \mathbf{y}) \text{ on } \Gamma.$$

Assuming Γ at least piece-wise smooth, Green's second identity can be applied in the same way as in Chapter 3, where for the test function $v(\mathbf{y})$ the fundamental solution to the Laplace equation is substituted. In two dimensions this takes form

$$v = \frac{1}{2\pi} \ln\left(\frac{1}{|\mathbf{r}|}\right),$$

where $\mathbf{r} = |\mathbf{x} - \mathbf{y}|$, $\mathbf{y}$ being the point of application of concetrated source. Following the procedure described in the 3rd Chapter finally the boundary integral form of the Laplace equation is obtained as

$$\int_\Gamma \frac{\partial u_\Gamma(\mathbf{y})}{\partial \nu} \ln\left(\frac{1}{|\mathbf{r}|}\right) ds_\mathbf{y} = -\theta^i u_\Gamma(\mathbf{x}) + \int_\Gamma u_\Gamma(\mathbf{y}) \frac{\partial \ln\left(\frac{1}{|\mathbf{r}|}\right)}{\partial \nu} ds_\mathbf{y} \text{ for } \mathbf{x} \in \Gamma,$$

with θ^i being an internal angle at point $\mathbf{x}$.

6.1.1 Collocation Method for the Laplace Equation

Discretization of the boundary Γ into N linear elements leads to the expression

$$\sum_{j=1}^N \int_{\Gamma_j} \frac{\partial u_\Gamma(\mathbf{y})}{\partial \nu} \ln\left(\frac{1}{|\mathbf{r}|}\right) ds_\mathbf{y} = -\theta^i u_\Gamma(\mathbf{x}) + \sum_{j=1}^N \int_{\Gamma_j} u_\Gamma(\mathbf{y}) \frac{\partial \ln\left(\frac{1}{|\mathbf{r}|}\right)}{\partial \nu} ds_\mathbf{y} \text{ for } \mathbf{x} \in \Gamma,$$

where functions $u(\mathbf{y})$ and $\frac{\partial u(\mathbf{y})}{\partial \nu}$ will be replaced on each element by some polynomial interpolation functions φ_k, so that

$$u(\mathbf{y}) = \sum_{k=1}^M u_k \varphi_k,$$

where M is the number of nodes on each element. Now, since values of c_i and u_i, where index i denotes the global nodes, are known, after substitution the problem may be written in the matrix form

$$\mathbf{Ku} = \mathbf{b},$$

where

$$k_{ij} = \sum_{k=1}^{M} \frac{1}{2\pi} \int_{\Gamma_j} \varphi_k \ln\left(\frac{1}{|\mathbf{r}|}\right) ds_{\mathbf{y}},$$

and

$$b_i = c_i \cdot u_i + \sum_{j=1}^{N} \sum_{k=1}^{M} \frac{1}{2\pi} \int_{\Gamma_j} \varphi_k \frac{\partial \ln\left(\frac{1}{|\mathbf{r}|}\right)}{\partial \nu} ds_{\mathbf{y}}.$$

As soon as the nodal values on the boundary are calculated, the boundary integral form of the Laplace equation can be used to compute values of u in the interior of Ω.

6.1.2   Numerical Results for the Laplace Equation

Solutions to two test problems on simple geometry of unit circle are presented. Both of them compare well to the results found in the literature. First example is a Dirichlet problem with constant boundary condition $g = 1$ on Γ.
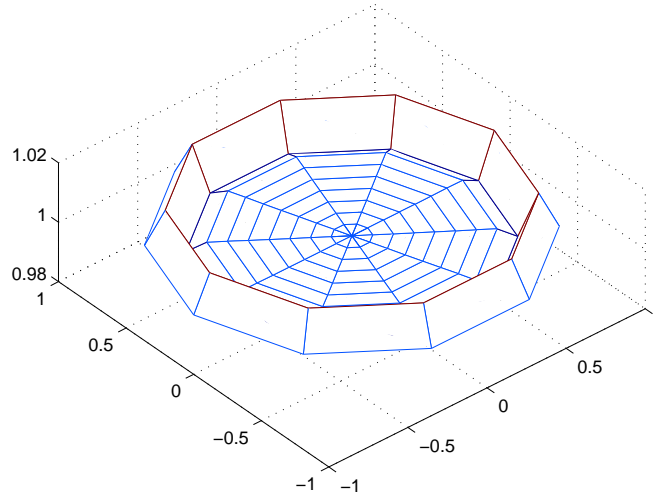
Figure 6.1: *Dirichlet problem with constant boundary condition $g = 1$ on Γ, 20 elements*

The second problem is defined in the following way: $g = 1$ on Γ_1, where Γ_1 is formed by the 'upper' half of the circle, and $g = 0$ on Γ_2, where Γ_2 is formed by the 'lower' half of the unit circle.
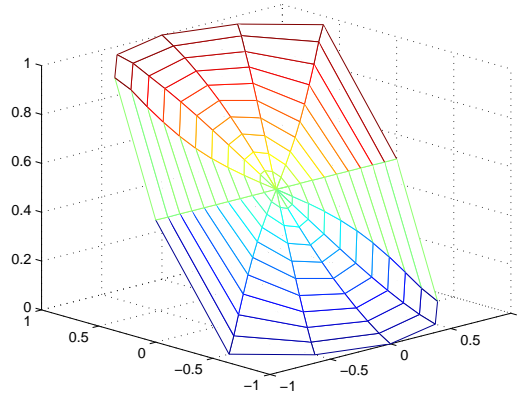
Figure 6.2: *Dirichlet problem with discontinuous boundary condition, 10 elements.*

The solution for second problem may be compared with the results for the same problem given in [11] by Brebbia at el. The tabulated interior values given by the authors compared to our solution follow (all solutions are calculated using collocation with constant elements):

x-coord	y-coord	analytical	Brebbia (24 elements)	our solution (20 elements)
0	0	0.500	0.500	0.500
0	0.5	0.795	0.799	0.798
0.25	0.43	0.773	0.776	0.776
0.43	0.25	0.687	0.689	0.690
0.5	0	0.500	0.500	0.500
0.43	-0.25	0.313	0.311	0.309
0.25	-0.43	0.227	0.224	0.223
0	-0.5	0.205	0.201	0.201

6.2 Analytical Solutions for the Helmholtz Equation

Some interior and exterior problems for Helmholtz equation on simple geometries may be solved analytically and used for comparison with results provided by our numerical solver. The solutions are achieved through separation of variables technique taking advantage of certain symmetries, cylindrical or spherical coordinates are often adopted. Since we are focusing on Helmholtz equation problems in two dimensions, the analytical solutions will be calculated for various boundary problems with circular scatterer using the cylindrical coordinates.

Let us consider the exterior problem of scattering from a circular body of radius a. That is, we want to find u which will be a solution to the problem as stated in section 2.3:

$$\Delta u^s(\mathbf{x}) + k^2 u^s(\mathbf{x}) = 0 \quad \text{in} \quad \Omega^\infty,$$

$$\frac{\partial u^s(\mathbf{x})}{\partial \nu} + a u^s(\mathbf{x}) = f(\mathbf{x}) \quad \text{on} \quad \Gamma, \tag{6.1}$$

$$\frac{\partial u^s(\mathbf{x})}{\partial \mathbf{r}} - i k u^s(\mathbf{x}) = o(\mathbf{r}^{-(n-1)/2}) \quad \text{for} \quad |\mathbf{x}| \to \infty.$$

Considering a model of scattering from infinitely-long cylinder in cylindrical system with r, ϕ, z coordinates, the two-dimensional problem with circular scatterer is obtained as a section through the cylinder in r, ϕ plane, thus neglecting z and only leaving the polar coordinates.

The Laplace operator in two dimensions in polar coordinates takes form

$$\Delta u(r, \phi) = \frac{1}{r} \frac{\partial}{\partial r} \left(r \frac{\partial u}{\partial r} \right) + \frac{1}{r^2} \frac{\partial^2 u}{\partial \phi^2}. \tag{6.2}$$

Separating the variables, the unknown function will be written as $u(r, \phi) = f(r)g(\phi)$ and substituting the separated unknown function into (6.2) and then into the first equation in (6.1) gives

$$\frac{1}{r} \frac{\partial}{\partial r} \left(r \frac{\partial (f(r)g(\phi))}{\partial r} \right) + \frac{1}{r^2} \frac{\partial^2 (f(r)g(\phi))}{\partial \phi^2} + k^2 f(r)g(\phi) = 0,$$

which after differentiation of $f(r)g(\phi)$ products yields

$$\frac{1}{r} \frac{d}{dr} \left(r \frac{df(r)}{dr} g(\phi) \right) + \frac{1}{r^2} f(r) \frac{d^2 g(\phi)}{d\phi^2} + k^2 f(r)g(\phi) = 0.$$

Rearranging the latter equation to separate the variables to left and right-hand sides we get

$$r \frac{d}{dr} \left(r \frac{df(r)}{dr} \right) \frac{1}{f(r)} + r^2 k^2 = -\frac{d^2 g(\phi)}{d\phi^2} \frac{1}{g(\phi)}.$$

Since expressions on the right-hand and left-hand side must be equal, we may consider both as equal to some constant which will be denoted as n^2, which splits the problem into two ordinary differential equations for functions $f(r)$ and $g(\phi)$,

$$r\frac{d}{dr}\left(r\frac{df(r)}{dr}\right) + (r^2k^2 - n^2)f(r) = 0, \tag{6.3}$$

and

$$\frac{d^2g(\phi)}{d\phi^2} + n^2g(\phi) = 0. \tag{6.4}$$

Equation (6.4) is the second-order equation with constant coefficients defined on a circular domain and therefore must satisfy the condition $g(0) = g(2\pi)$. This periodicity condition requires integer values of n, and in such case the fundamental solutions follow as

$$g_1(\phi) = \sin(n\phi) \quad \text{for} \quad n = 0, 1, 2...,$$

and

$$g_2(\phi) = \cos(n\phi) \quad \text{for} \quad n = 0, 1, 2....$$

For the equation (6.3), which is the Bessel's equation, the periodicity condition again only allows integer values of $n = 0, 1, 2...$. The fundamental solutions for the radial equation for given n are the Bessel's functions of the first and second kind $J_n(kr)$ and $Y_n(kr)$ introduced in section (3.1), also known as cylindrical harmonics. Another set of two linearly independent solutions is represented by functions

$$H_n^1(r) = J_n(kr) + iY_n(kr),$$

which is Hankel function of the first kind, and

$$H_n^2(r) = J_n(kr) - Y_n(kr),$$

which is the second kind Hankel function. From the asymptotics of the far-field pattern follows that the Hankel function of the second kind corresponds to the incoming wave and therefore will be eliminated by the Sommerfeld condition. Bearing this in mind and combining the fundamental solutions for h and g we obtain the general solution of Helmholtz equation in polar coordinates

$$u(r, \phi) = \sum_{n=0}^{\infty} H_n(kr)(A_n \cos(n\phi) + B_n \sin(n\phi)).$$

where $H_n(kr)$ now stands for the Hankel function of the first kind. By application of Euler formula this may be re-written as a series

$$
\begin{aligned}
u(r, \phi) &= \sum_{n=-\infty}^{\infty} u_n H_n(kr) e^{in\phi} = \qquad (6.5)\\
&= u_0 H_0(kr) + 2 \sum_{n=1}^{\infty} u_n H_n(kr) e^{in\phi},
\end{aligned}
$$

where the equality $H_{-n} = H_n$ for $n = 1, 2, ...$ has been used and coefficients u_n has been introduced to account for the change from $\sum_{n=0}^{\infty}$ to $\sum_{n=-\infty}^{\infty}$ (cf. [16]). Now, $\sum_{n=-\infty}^{\infty} u_n e^{in\phi}$ is apparently the Fourier series in which the coefficients u_n are defined by

$$
u_n = \frac{1}{2\pi} \int_0^{2\pi} u(\phi) e^{-in\phi} d\phi.
$$

To obtain the solution for given boundary condition coefficients u_n must be found. This is achieved by taking the expression (6.5) and the Fourier expansion of the boundary condition function f in polar coordinates, substituting into (6.1) and comparing the coefficients on both sides. (Note, that the Fourier expansion exists for every $f \in L_2(\Gamma)$.)

6.2.1 Analytical Solution for Dirichlet Problem with Constant Boundary Condition on Circle

Consider problem (6.1) on circular domain Ω of radius a. The simplest case of boundary value problem arises from Dirichlet condition with constant function $f(a, \phi) = 1$ on the boundary. Substituting (6.5) into the boundary condition we get the equality

$$
u(a, \phi) = \sum_{n=-\infty}^{\infty} u_n H_n(ka) e^{in\phi} = 1,
$$

since the Fourier expansion of the boundary condition is trivial in this case. Because of the orthogonality of the Fourier coefficients for individual n, we get

$$
u_0 H_0(ka) = 1,
$$

from where

$$
u_0 = \frac{1}{H_0(ka)},
$$

and

$$u_n = 0 \ \text{ for } \ n \neq 0.$$

For the outcoming wave then follows

$$u_s(r, \phi) = \frac{H_0(kr)}{H_0(ka)}.$$

6.2.2   Analytical Solution of Scattering of a Plane Wave on Sound-Soft Circle

More importantly, analytical solution for the problem of scattering of the incident plane wave on a circular object of radius a with sound-soft or sound-hard surface can also be found. For sound-soft boundary, the situation corresponds to problem with Dirichlet boundary condition, since the total field must satisfy

$$u_t(a, \phi) = u_i(a, \phi) + u_s(a, \phi),$$

and therefore

$$u_s(a, \phi) = -u_i(a, \phi).$$

The incident wave in polar coordinates takes form

$$u_i(r, \phi) = P_0 e^{ikr \ \cos(\phi)},$$

where P_0 is the amplitude, k the wave number and ϕ defines the direction of the wave. Expanding the incident wave into series yield (cf. [16])

$$P_0 e^{ikr \ \cos(\phi)} = P_0 J_0(kr) + 2P_0 \sum_{n=1}^{\infty} i^n J_n(kr) \cos(n\phi).$$

Substituting the series expansions into the boundary condition gives

$$u_0 H_0(ka) + 2 \sum_{n=1}^{\infty} u_n H_n(ka) e^{in\phi} = P_0 J_0(ka) + 2P_0 \sum_{n=1}^{\infty} i^n J_n(ka) \cos(n\phi),$$

from where again by the orthogonality the coefficients are expressed as

$$u_n = -P_0 i^n \frac{J_n(ka)}{H_n(ka)} \frac{\cos(n\phi)}{e^{in\phi}},$$

and for the scattered wave follows

$$u_s(r,\phi) = -\left(P_0 \frac{J_0(ka)H_0(kr)}{H_0(ka)} + 2P_0 \sum_{n=1}^{\infty} i^n \frac{J_n(ka)H_n(kr)}{H_n(ka)} \cos(n\phi)\right).$$

The total wave in the exterior of the sound-soft obstacle will then be given as

$$
\begin{aligned}
u_t(r,\phi) &= u_i(r,\phi) + u_s(r,\phi) = \\
&= P_0\left(J_0(kr) - \frac{J_0(ka)H_0(kr)}{H_0(ka)}\right) + 2P_0 \sum_{n=1}^{\infty} i^n \left(J_n(kr) - \frac{J_n(ka)H_n(kr)}{H_n(ka)}\right)\cos(n\phi).
\end{aligned}
$$

6.2.3 Analytical Solution of Scattering of a Plane Wave on Sound-Hard Circle

Similarly, scattering from the sound-hard boundary is represented by Neumann boundary condition

$$\frac{\partial u_s(a,\phi)}{\partial \nu} = -\frac{\partial u_i(a,\phi)}{\partial \nu}.$$

The derivative of the incident wave

$$\frac{\partial u_i(r,\phi)}{\partial \nu} = kP_0 J_0'(kr) + 2kP_0 \sum_{n=1}^{\infty} i^n J_n'(kr)\cos(n\phi),$$

is substituted into the boundary condition to give equality

$$ku_0 H_0'(ka) + 2k \sum_{n=1}^{\infty} u_n H_n'(ka)e^{in\phi} = kP_0 J_0'(ka) + 2kP_0 \sum_{n=1}^{\infty} i^n J_n'(ka)\cos(n\phi),$$

and the same reasoning as in the previous cases leads to

$$u_n = -P_0 i^n \frac{J_n'(ka)}{H_n'(ka)} \frac{\cos(n\phi)}{e^{in\phi}},$$

and therefore the scattered wave will be expressed as

$$u_s(r, \phi) = -(P_0 \frac{J_0'(ka)H_0(kr)}{H_0'(ka)} + 2P_0 \sum_{n=1}^{\infty} i^n \frac{J_n'(ka)H_n(kr)}{H_n'(ka)} \cos(n\phi)).$$

Finally, for the total wave in the exterior of the sound-hard obstacle we then have

$$
\begin{aligned}
u(r, \phi) &= u_i(r, \phi) + u_s(r, \phi) = \\
&= P_0 \left(J_0(kr) - \frac{J_0'(ka)H_0(kr)}{H_0'(ka)} \right) + 2P_0 \sum_{n=1}^{\infty} i^n \left(J_n(kr) - \frac{J_n'(ka)H_n(kr)}{H_n'(ka)} \right) \cos(n\phi).
\end{aligned}
$$

6.2.4 Convergence and Truncation

The series expressing solutions to sound-soft and sound-hard scattering are absolutely convergent, cf. [16]. Since we want to use them as analytic solutions for comparison with numerical results, the question of how many terms are to be used to obtain reasonable precision arises. The matter of truncation of the series is also discussed in [16], where empirical 'rule' is given to calculate

$$N \approx 2k$$

terms of the expansion (where k represents the wave number).

6.3 Numerical Solutions for the Helmholtz Equation

Numerical solutions for the cases of constant boundary condition and sound-soft scattering have been included. Naturally, the values in the exterior are of primary interest, but it is not possible to calculate 'continuous' L_2-norm of the error in the exterior. Therefore, a simple approach is used of calculating 'point-wise' norm for the limited number of exterior nodes in which the solution is evaluated. This is not a rigorous technique, but we believe it gives a good enough quantification. In the following the error is quantified by figures depicting the ratio of numerical and analytical solutions, which is basically the same, while it gives the information on the error distribution in addition.

6.3.1   Dirichlet Problem with Constant Boundary Condition
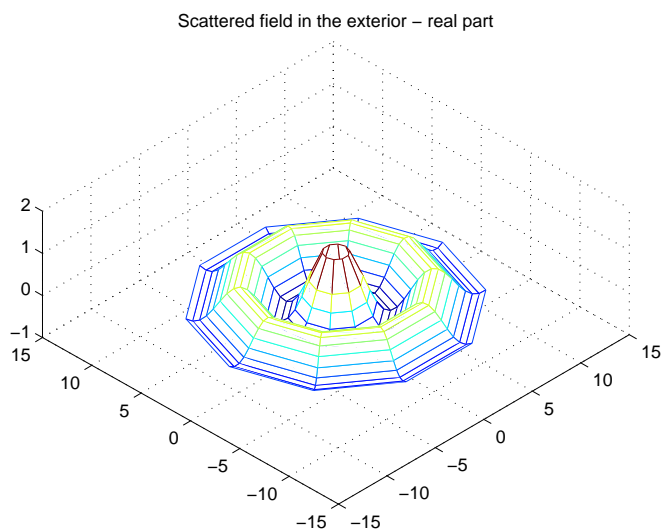
Figure 6.3: *Constant b. c., k = 1, analytical solution, real part.*
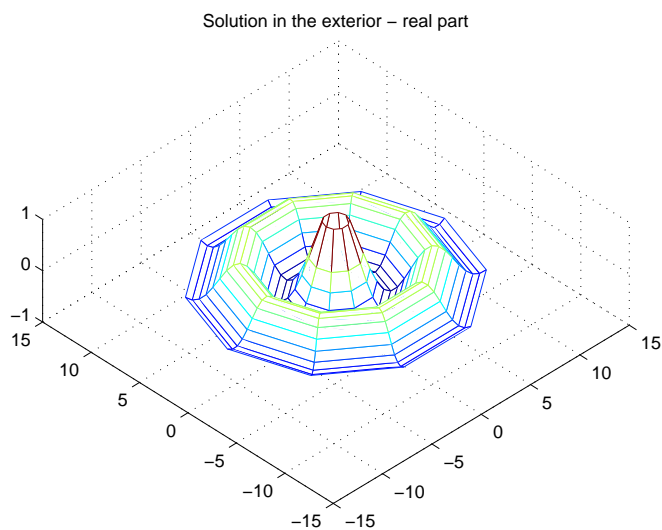
Figure 6.4: *Constant b. c., k = 1, collocation solution, real part, 10 constant elements.*
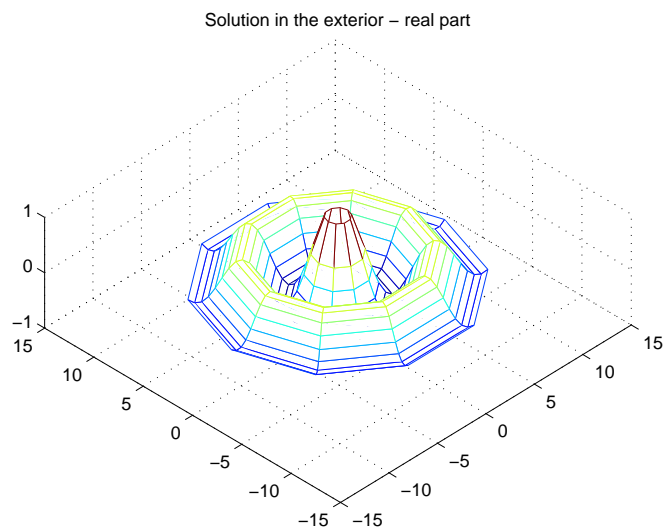
Figure 6.5: *Constant b. c., k = 1, Galerkin solution, real part, 10 constant elements.*
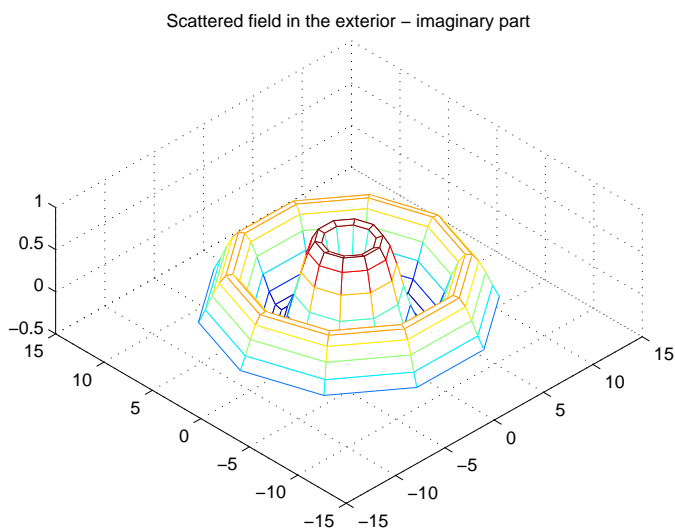
Figure 6.6: *Constant b. c., k = 1, analytical solution, imaginary part.*
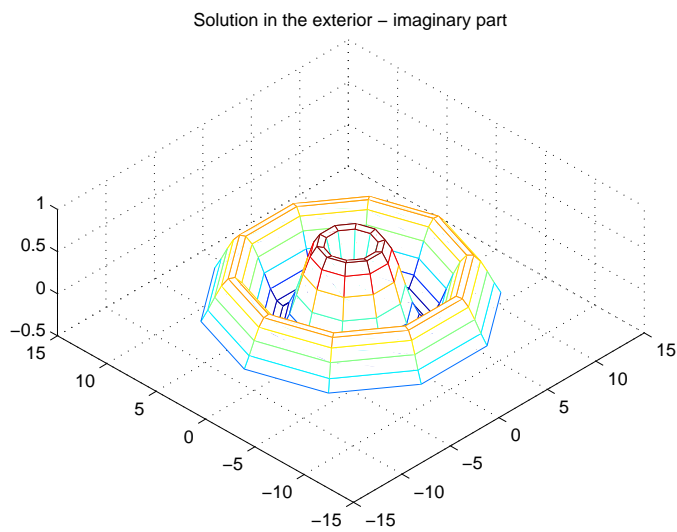
Figure 6.7: *Constant b. c., k = 1, collocation solution, imaginary part, 10 constant elements.*
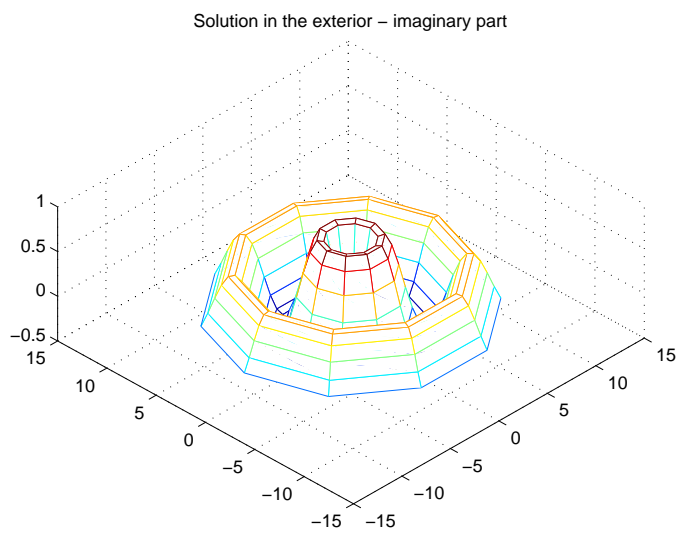
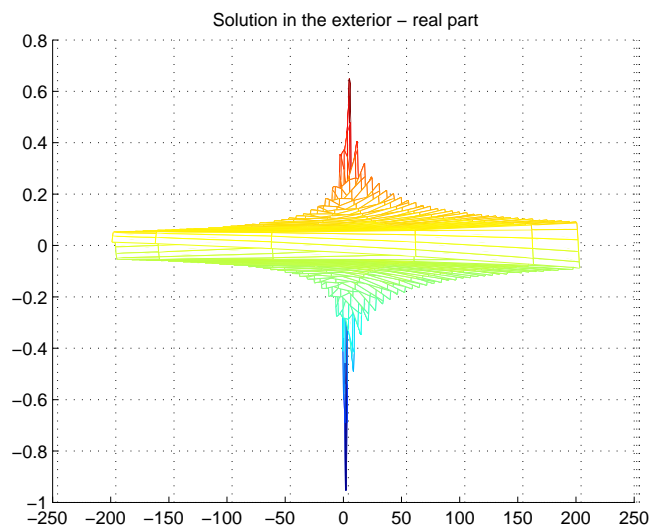Figure 6.8: *Constant b. c., k = 1, Galerkin solution, imaginary part, 10 constant elements.*
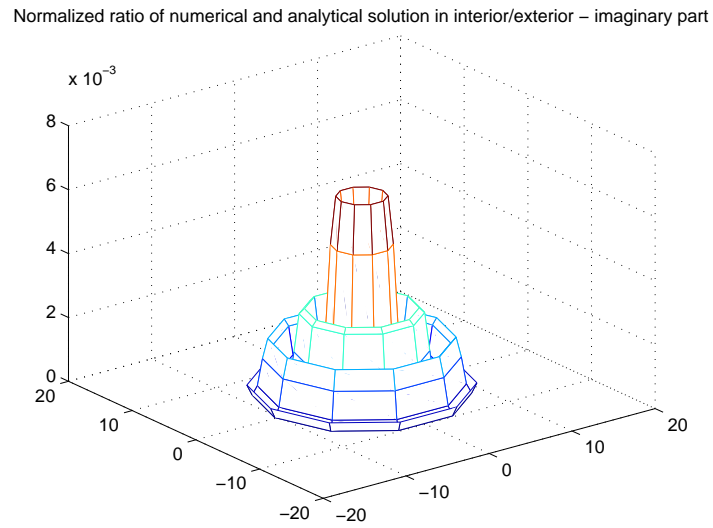
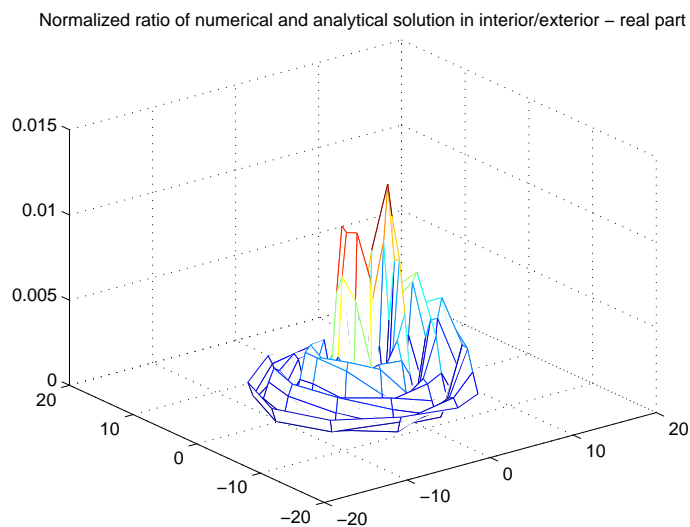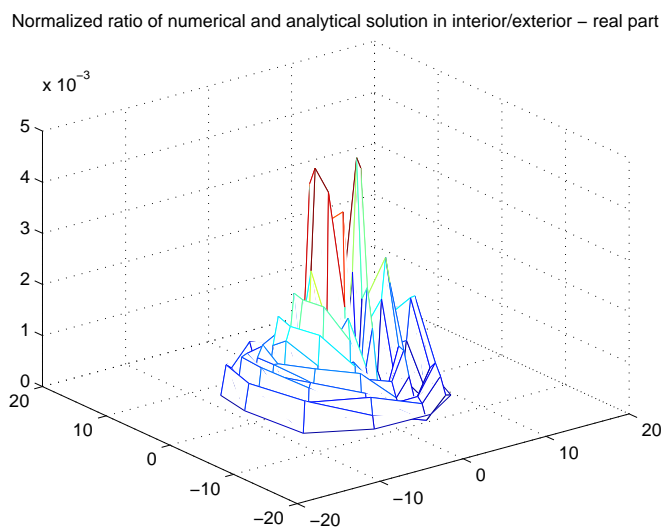Figure 6.9: *Constant b. c., k = 1, ratio analytical/collocation, real part, 10 constant elements.*
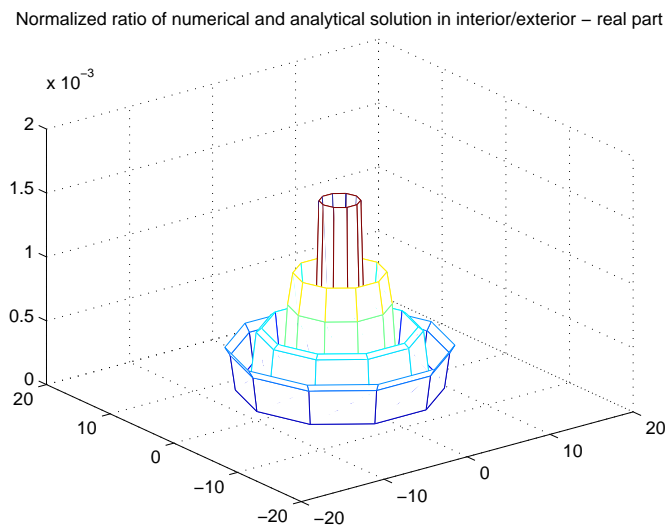
Figure 6.10: *Constant b. c., k = 1, ratio analytical/Galerkin, real part, 10 constant elements.*

Normalized ratio of numerical and analytical solution in interior/exterior – imaginary part
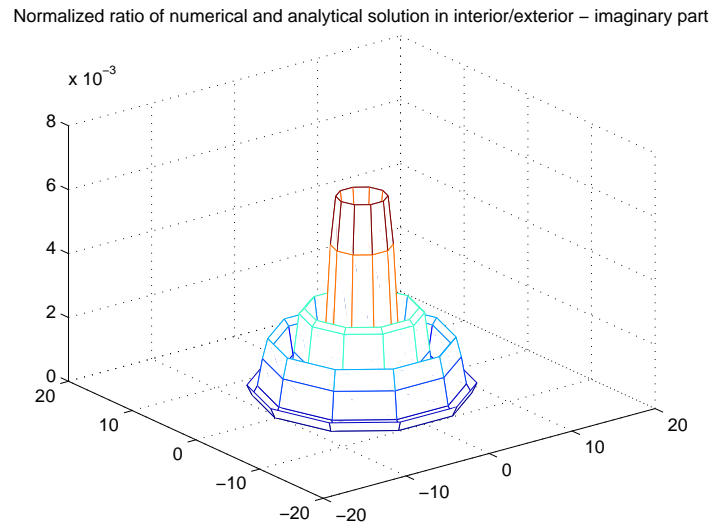
Figure 6.11: *Constant b. c., k = 1, ratio analytical/collocation, imaginary part, 10 constant elements.*

Normalized ratio of numerical and analytical solution in interior/exterior – imaginary part
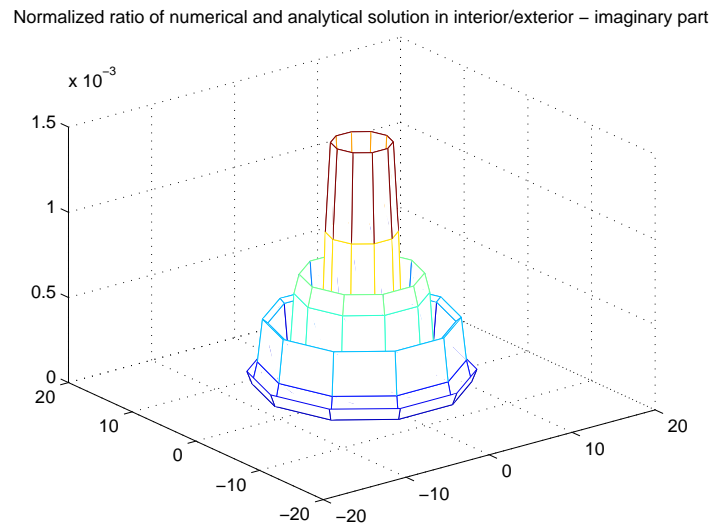
Figure 6.12: *Constant b. c., k = 1, ratio analytical/Galerkin, imaginary part, 10 constant elements.*
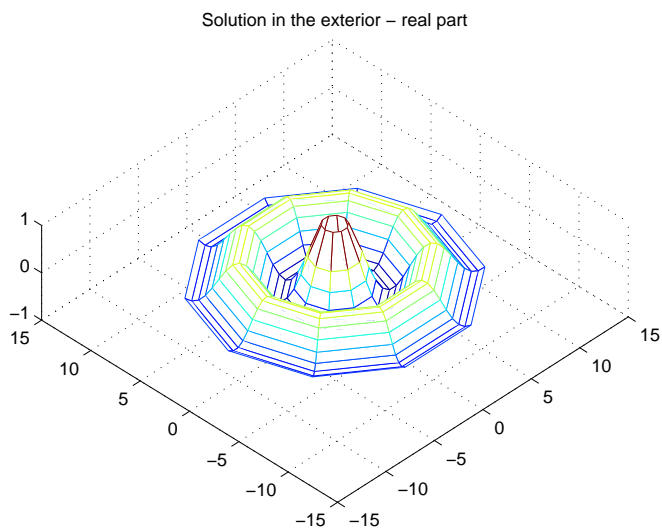
Figure 6.13: *Constant b. c., k = 1, collocation solution, real part, 40 linear elements.*
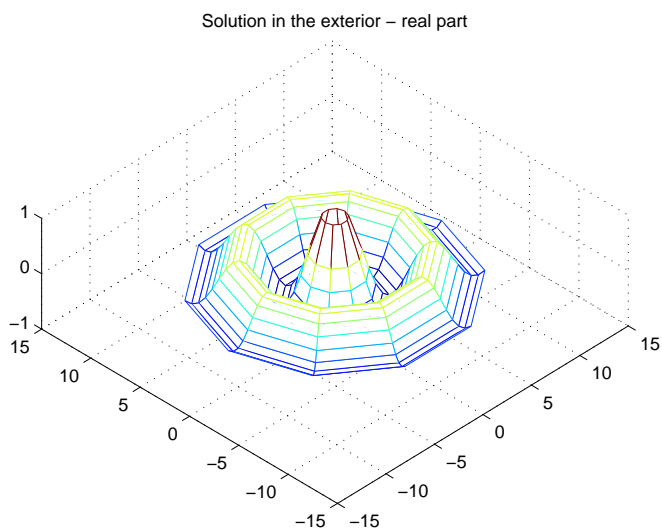
Figure 6.14: *Constant b. c., k = 1, Galerkin solution, real part, 40 linear elements.*
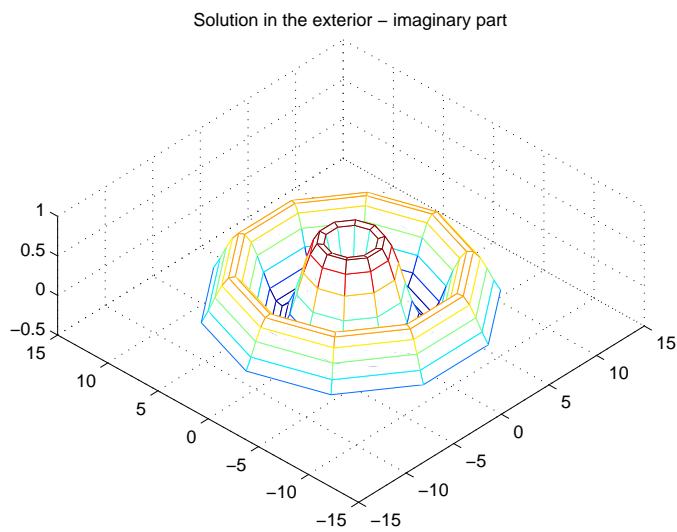
Figure 6.15: *Constant b. c., k = 1, collocation solution, imaginary part, 40 linear elements.*
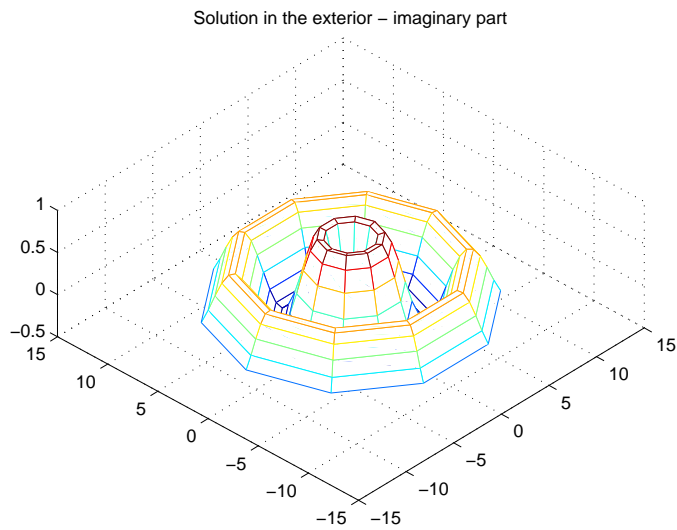
Figure 6.16: *Constant b. c., k = 1, Galerkin solution, imaginary part, 40 linear elements.*
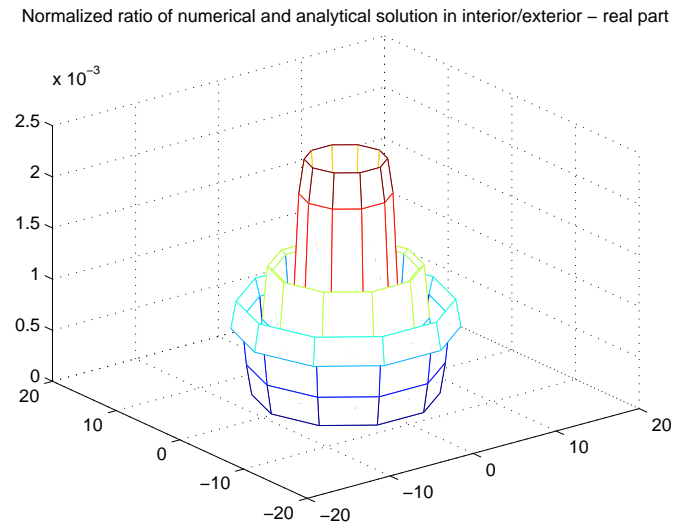
Figure 6.17: *Constant b. c., k = 1, ratio analytical/collocation, real part, 40 linear elements.*
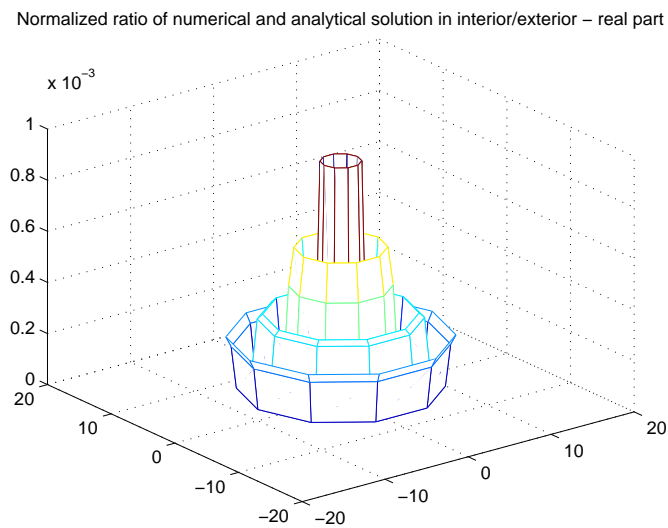
Figure 6.18: *Constant b. c., k = 1, ratio analytical/Galerkin, real part, 40 linear elements.*

Figure 6.19: *Constant b. c., k = 1, ratio analytical/collocation, imaginary part, 40 linear elements.*

Normalized ratio of numerical and analytical solution in interior/exterior – imaginary part

Normalized ratio of numerical and analytical solution in interior/exterior – imaginary part
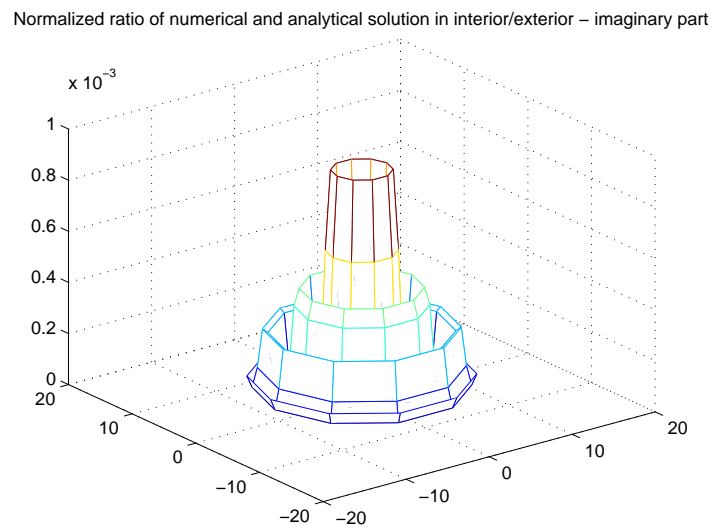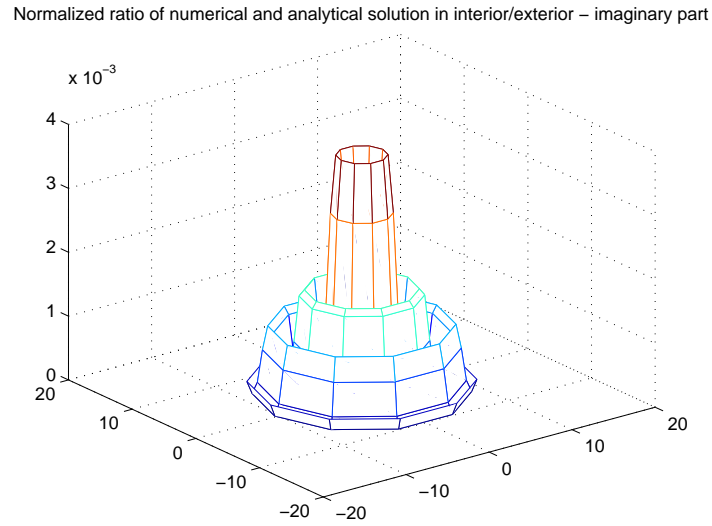
Figure 6.20: *Constant b. c., k = 1, ratio analytical/Galerkin, imaginary part, 40 linear elements.*

6.3.2 Dirichlet Problem with Plane Wave Boundary Condition
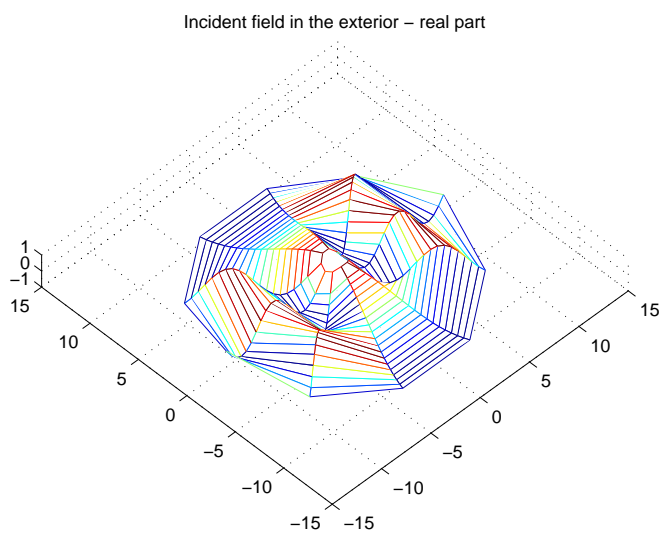
Figure 6.21: *Plane wave b. c., k = 1, incident field, real part.*
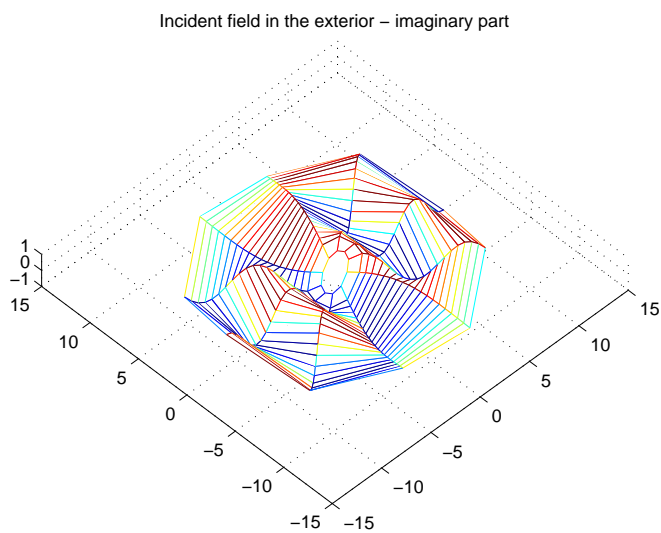
Figure 6.22: *Plane wave b. c., k = 1, incident field, imaginary part.*
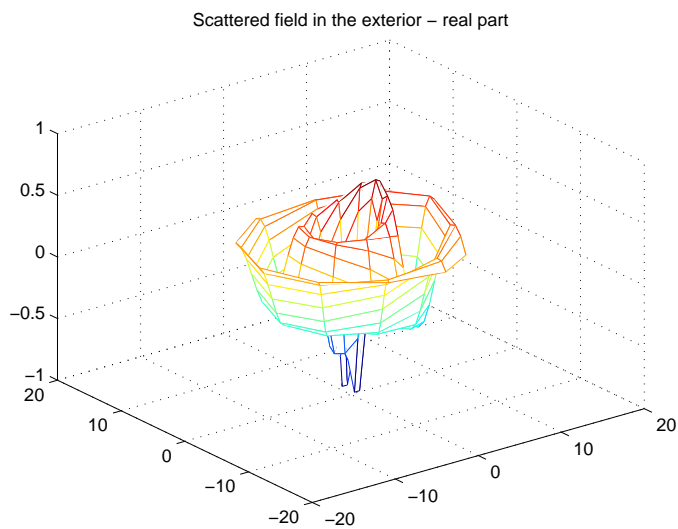
Figure 6.23: *Plane wave b. c., k = 1, scattered field analytical, real part.*
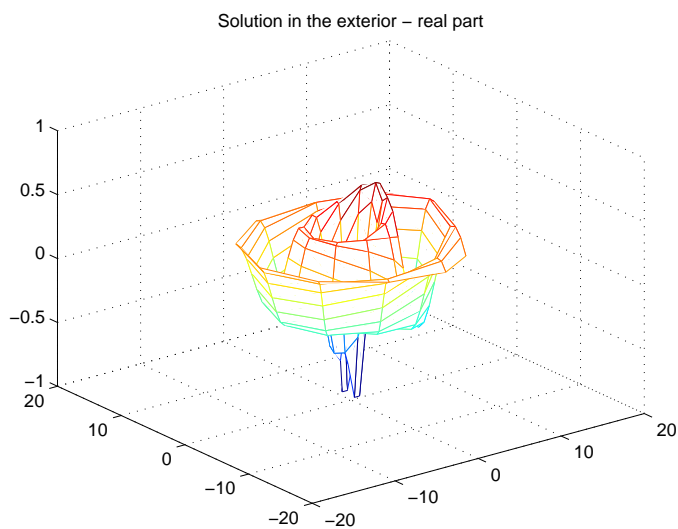
Figure 6.24: *Plane wave b. c., k = 1, scattered field collocation, real part, 10 constant elements.*

Solution in the exterior – real part
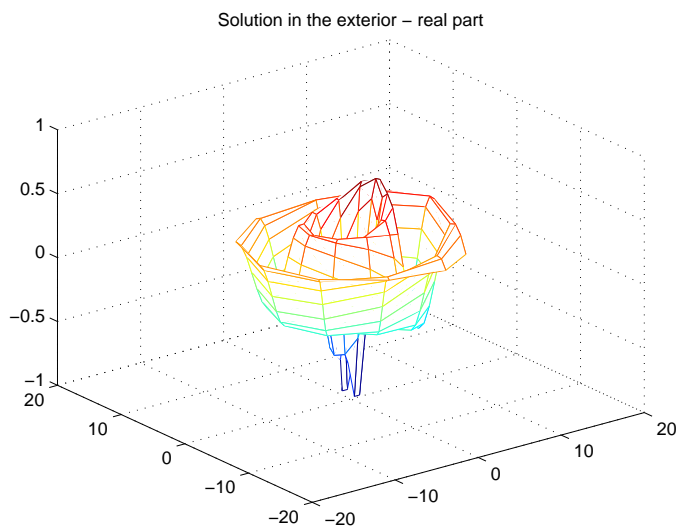
Figure 6.25: *Plane wave b. c., k = 1, scattered field Galerkin, real part, 10 constant elements.*

Scattered field in the exterior – imaginary part
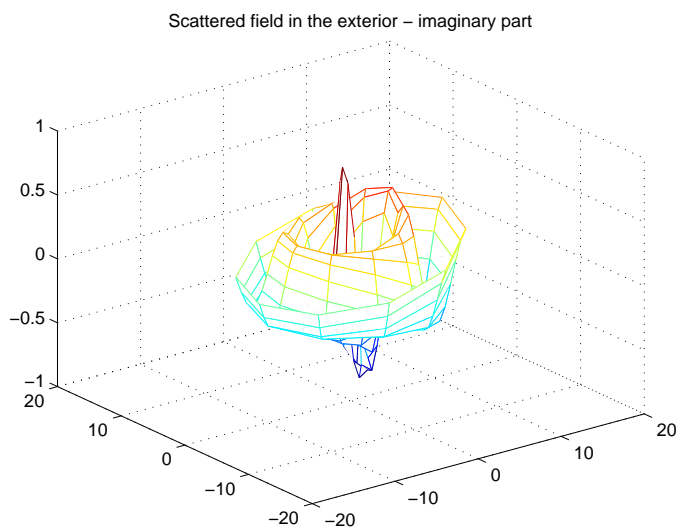
Figure 6.26: *Plane wave b. c., k = 1, scattered field analytical, imaginary part.*
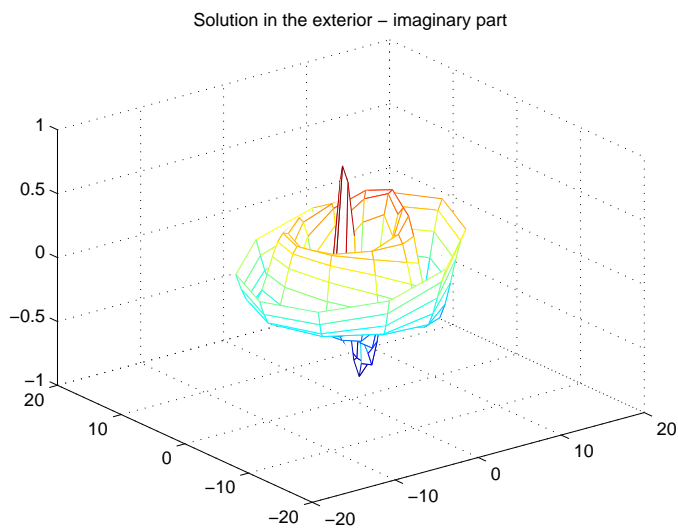
Figure 6.27: *Plane wave b. c., k = 1, scattered field collocation, imaginary part, 10 constant elements.*
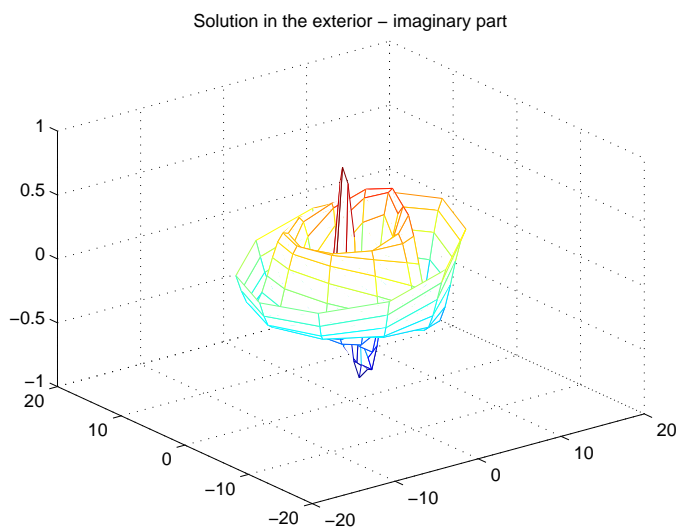
Figure 6.28: *Plane wave b. c., k = 1, scattered field Galerkin, imaginary part, 10 constant elements.*

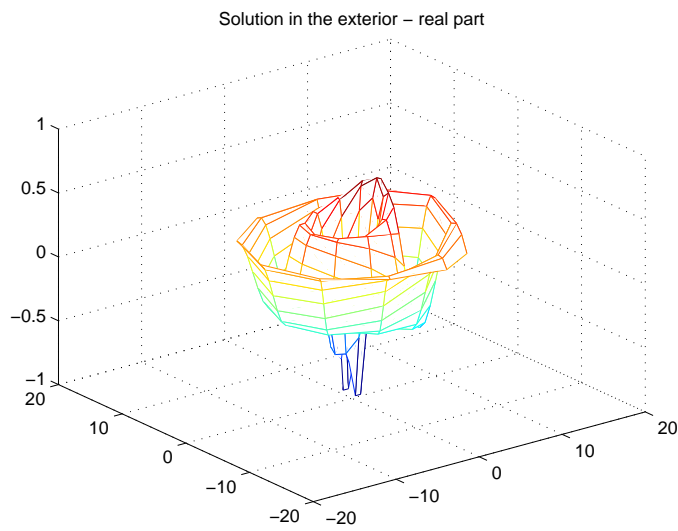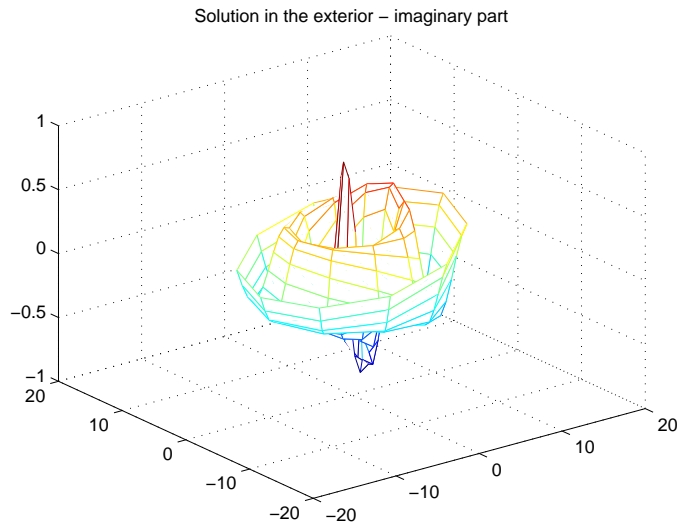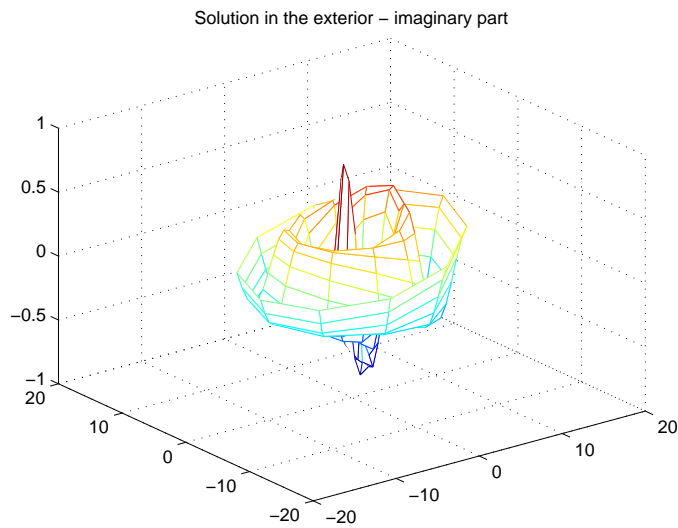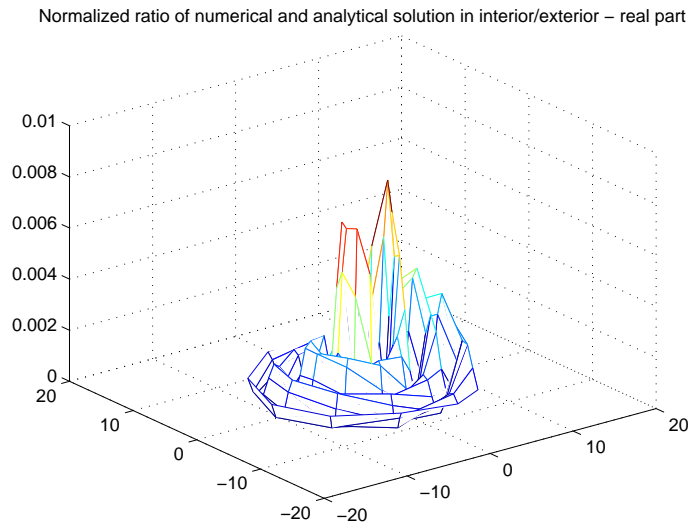Figure 6.29: *Plane wave b. c., k = 1, scattered field collocation, real part, 10 constant elements, broad view.*
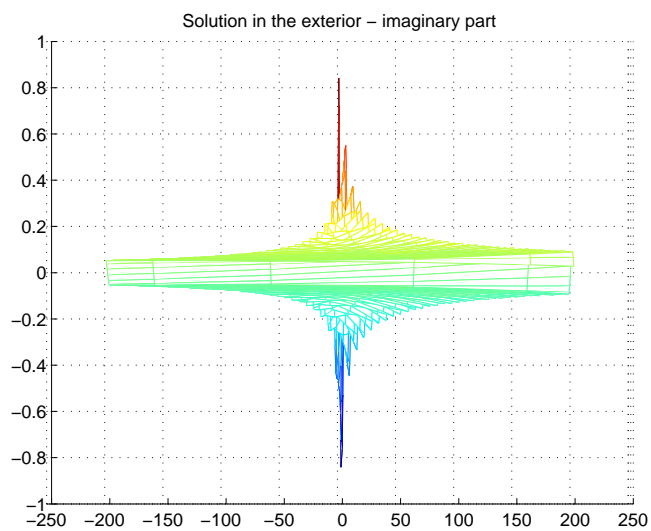
Figure 6.30: *Plane wave b. c., k = 1, scattered field Galerkin, imaginary part, 10 constant elements, broad view.*

Normalized ratio of numerical and analytical solution in interior/exterior – real part

Figure 6.31: *Plane wave b. c., k = 1, ratio analytical/collocation, real part, 10 constant elements.*

Normalized ratio of numerical and analytical solution in interior/exterior – real part

Figure 6.32: *Plane wave b. c., k = 1, ratio analytical/Galerkin, real part, 10 constant elements.*

Normalized ratio of numerical and analytical solution in interior/exterior – imaginary part
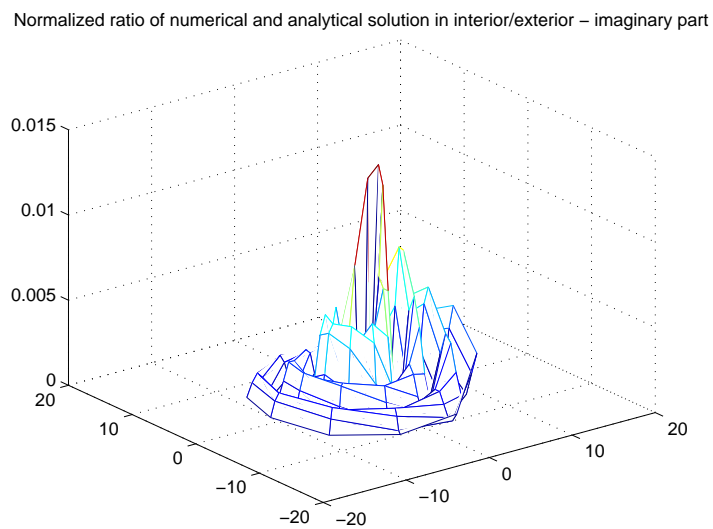
Figure 6.33: *Plane wave b. c., k = 1, ratio analytical/collocation, imaginary part, 10 constant elements.*

Normalized ratio of numerical and analytical solution in interior/exterior – imaginary part
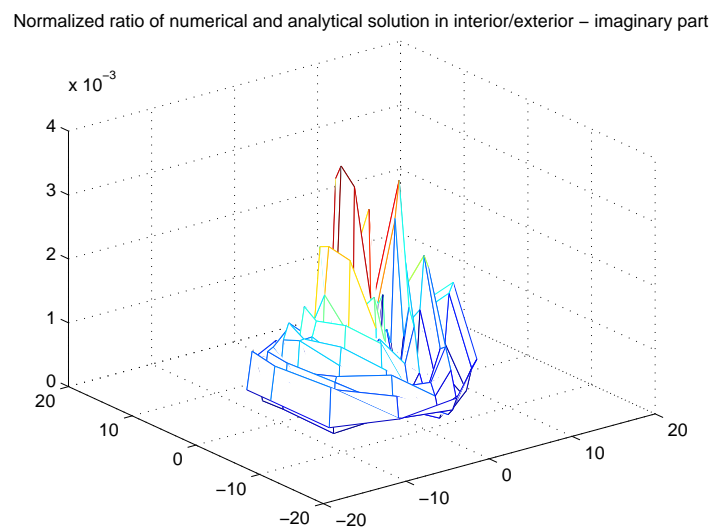
Figure 6.34: *Plane wave b. c., k = 1, ratio analytical/Galerkin, imaginary part, 10 constant elements.*

Total field in the exterior – real part
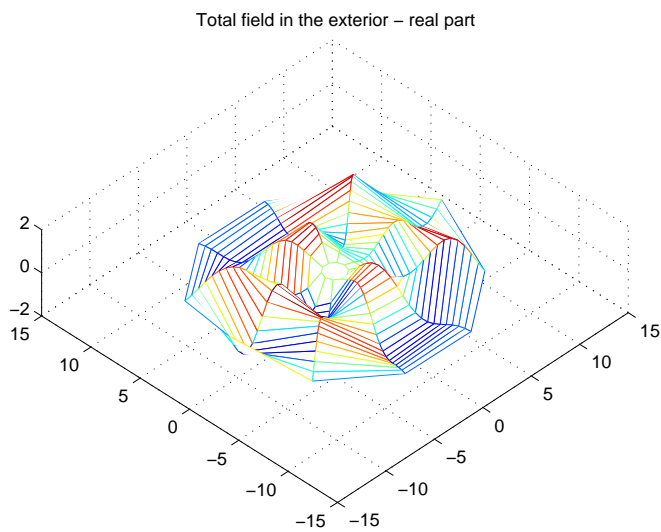
Figure 6.35: *Plane wave b. c., k = 1, total field, real part, 10 constant elements.*

Total field in the exterior – imaginary part
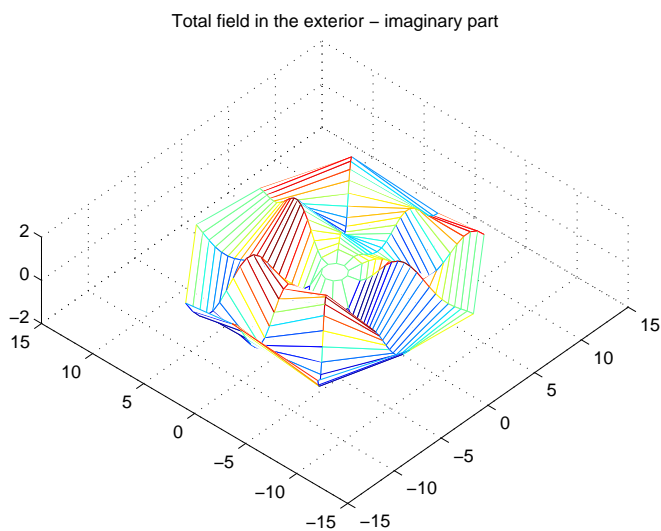
Figure 6.36: *Plane wave b. c., k = 1, total field, imaginary part, 10 constant elements.*
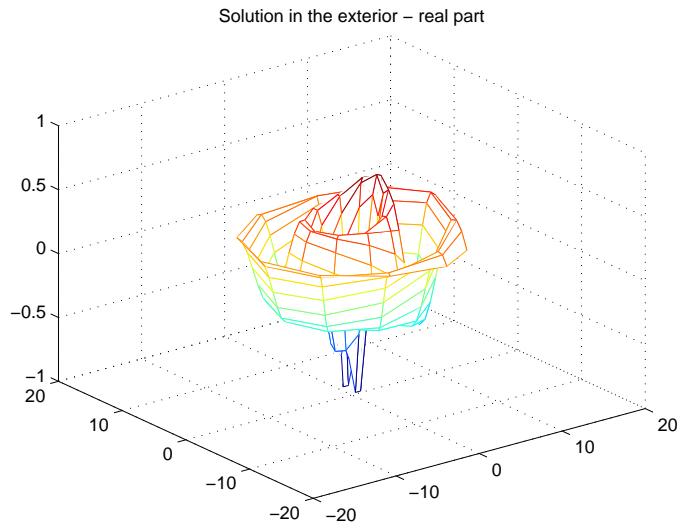
Figure 6.37: *Plane wave b. c., k = 1, scattered field collocation, real part, 10 quadratic elements.*

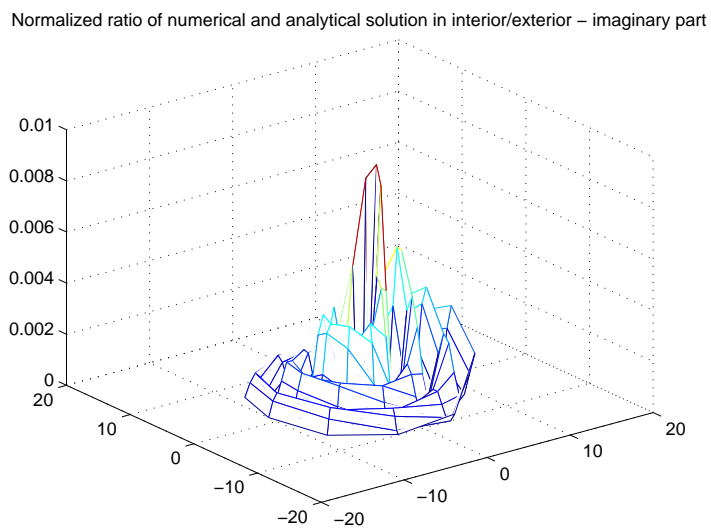Figure 6.38: *Plane wave b. c., k = 1, scattered field Galerkin, real part, 10 quadratic elements.*

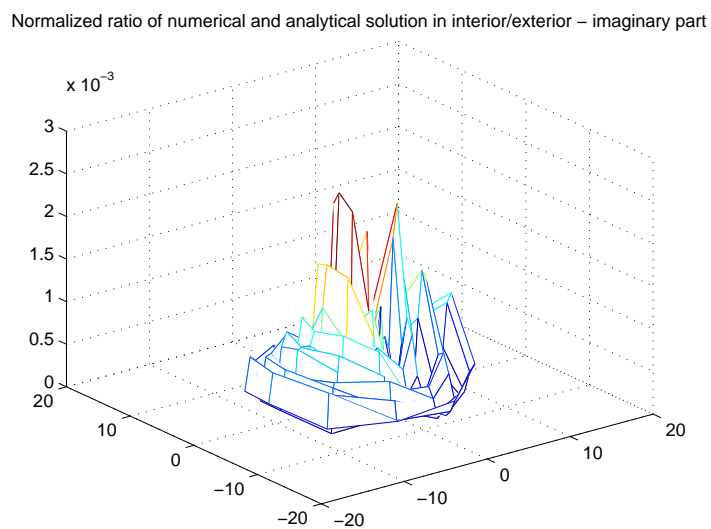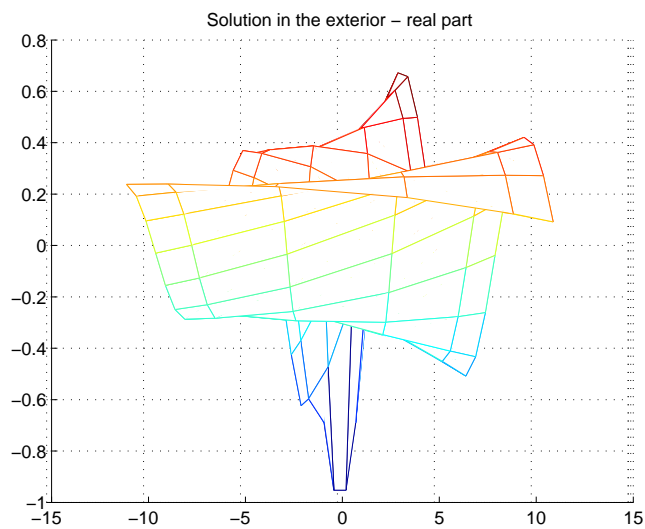Figure 6.39: *Plane wave b. c., k = 1, scattered field collocation, imaginary part, 10 quadratic elements.*

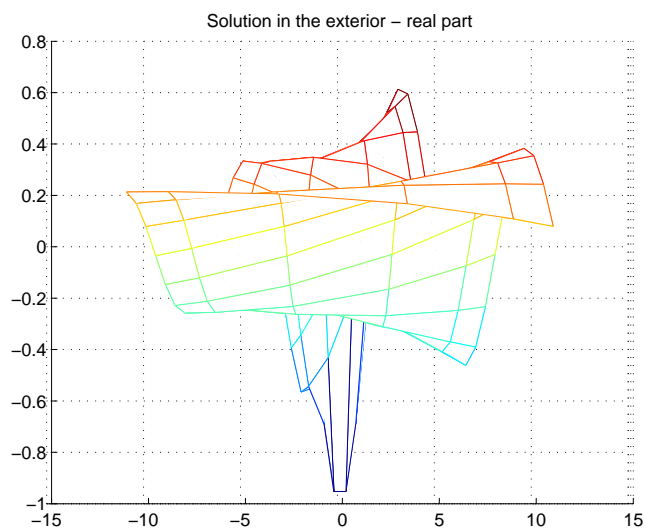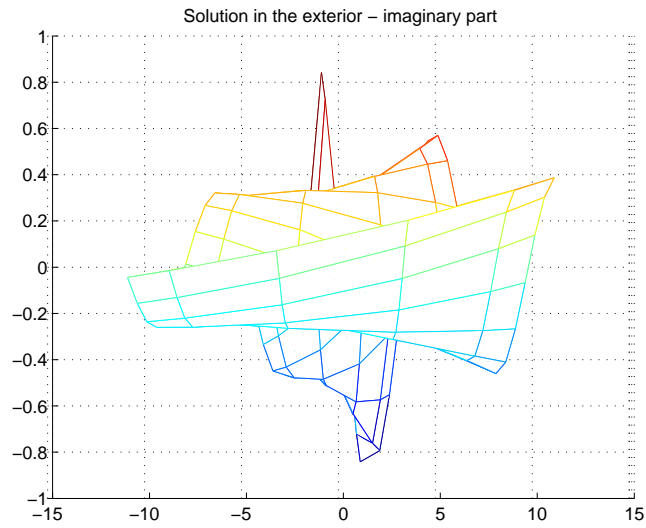
Figure 6.40: *Plane wave b. c., k = 1, scattered field Galerkin, imaginary part, 10 quadratic elements.*

Normalized ratio of numerical and analytical solution in interior/exterior – real part

Figure 6.41: *Plane wave b. c., k = 1, ratio analytical/collocation, real part, 10 quadratic elements.*

Normalized ratio of numerical and analytical solution in interior/exterior – real part
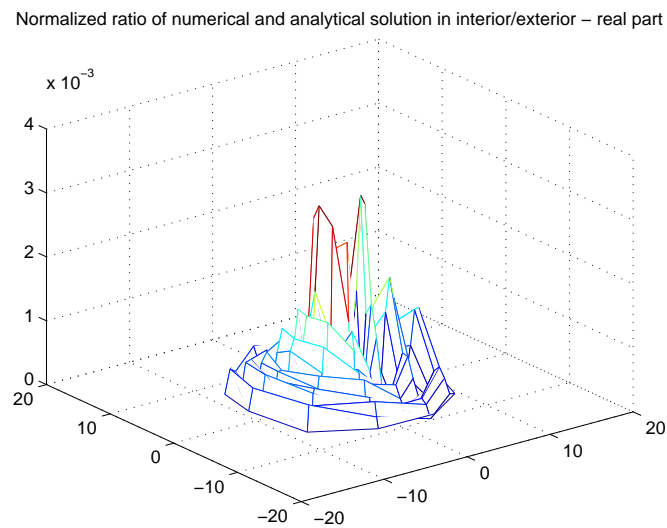
Figure 6.42: *Plane wave b. c., k = 1, ratio analytical/Galerkin, real part, 10 quadratic elements.*

Normalized ratio of numerical and analytical solution in interior/exterior – imaginary part

Figure 6.43: *Plane wave b. c., k = 1, ratio analytical/collocation, imaginary part, 10 quadratic elements.*

Normalized ratio of numerical and analytical solution in interior/exterior – imaginary part

Figure 6.44: *Plane wave b. c., k = 1, ratio analytical/Galerkin, imaginary part, 10 quadratic elements.*

Figure 6.45: *Plane wave b. c., k = 1, scattered field collocation, real part, 40 quadratic elements.*

Figure 6.46: *Plane wave b. c., k = 1, scattered field collocation, real part, 40 exponential elements.*

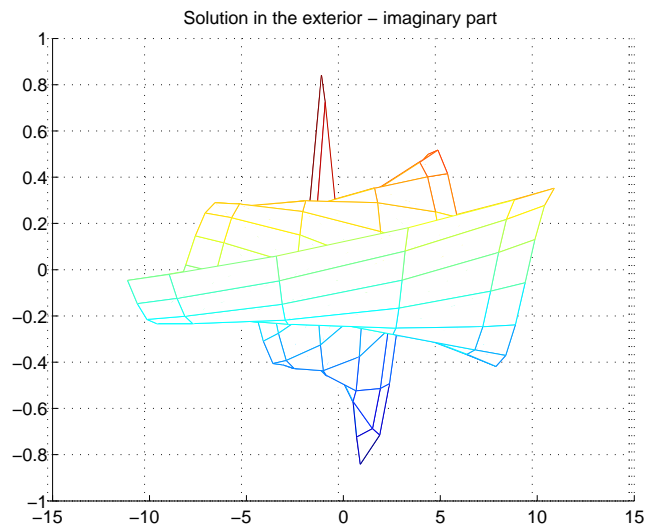Figure 6.47: *Plane wave b. c., k = 1, scattered field collocation, imaginary part, 40 quadratic elements.*

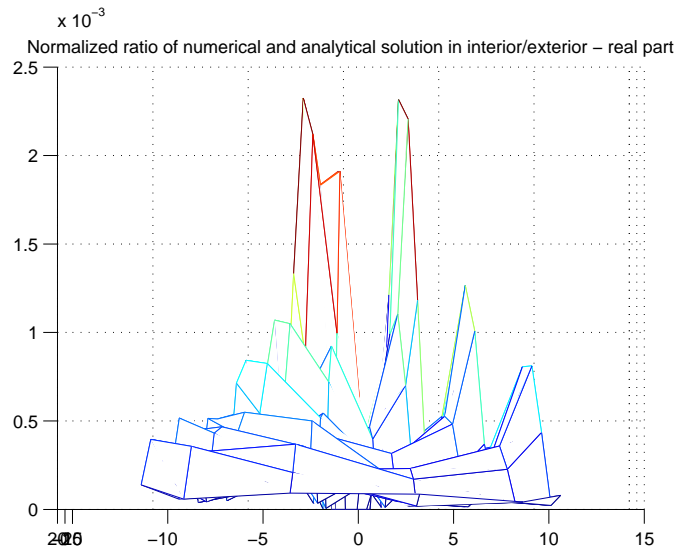Figure 6.48: *Plane wave b. c., k = 1, scattered field collocation, imaginary part, 40 exponential elements.*

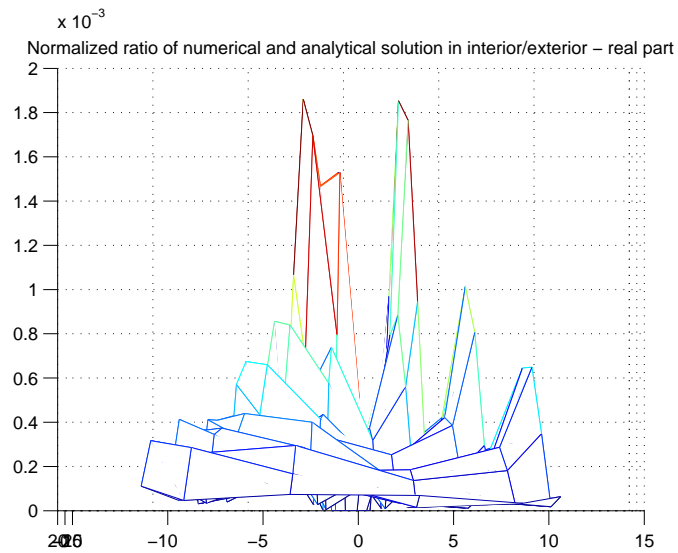Figure 6.49: *Plane wave b. c., k = 1, ratio analytical/collocation, real part, 40 quadratic elements.*

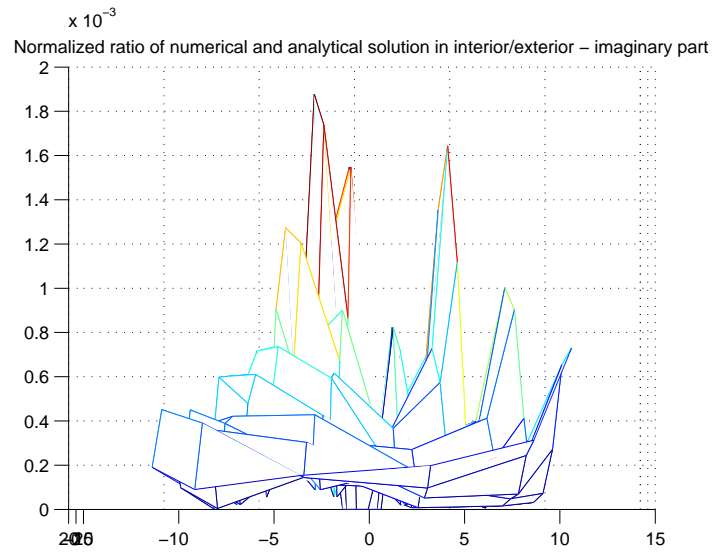Figure 6.50: *Plane wave b. c., k = 1, ratio analytical/collocation, real part, 40 exponential elements.*

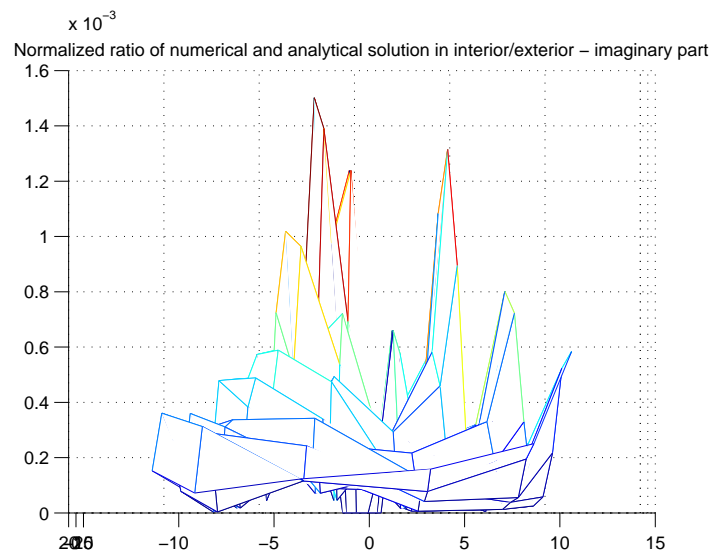Figure 6.51: *Plane wave b. c., k = 1, ratio analytical/collocation, imaginary part, 40 quadratic elements.*

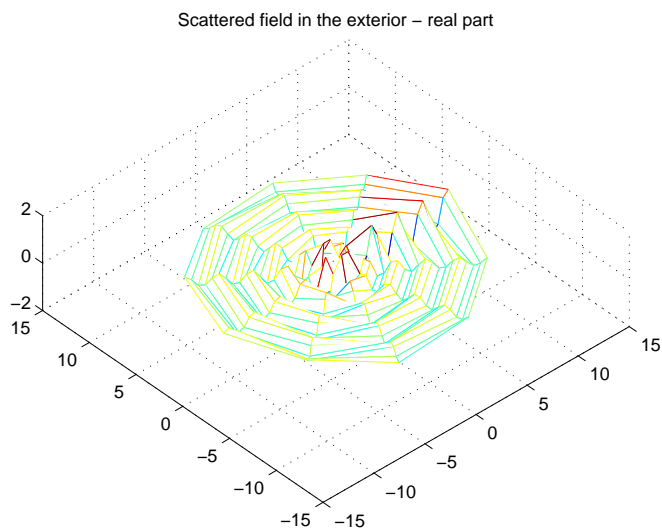Figure 6.52: *Plane wave b. c., k = 1, ratio analytical/collocation, imaginary part, 40 exponential elements.*

Scattered field in the exterior – real part

Figure 6.53: *Plane wave b. c., k = 10, scattered field analytical, real part.*

Scattered field in the exterior – imaginary part
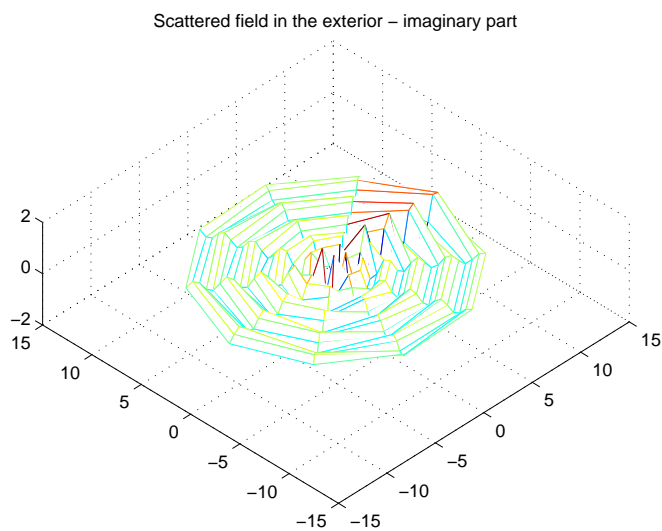
Figure 6.54: *Plane wave b. c., k = 10, scattered field analytical, imaginary part.*

Solution in the exterior – real part

Figure 6.55: *Plane wave b. c., k = 10, scattered field collocation, real part, 40 quadratic elements.*

Solution in the exterior – real part

Figure 6.56: *Plane wave b. c., k = 10, scattered field Galerkin, real part, 40 quadratic elements.*

Figure 6.57: *Plane wave b. c., k = 10, scattered field collocation, imaginary part, 40 quadratic elements.*

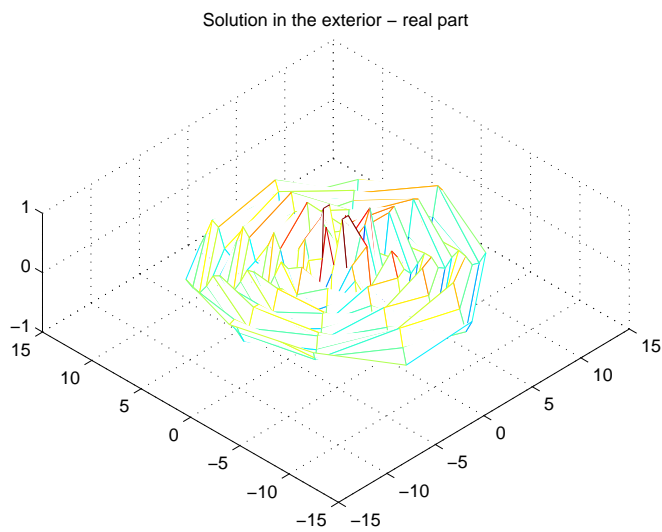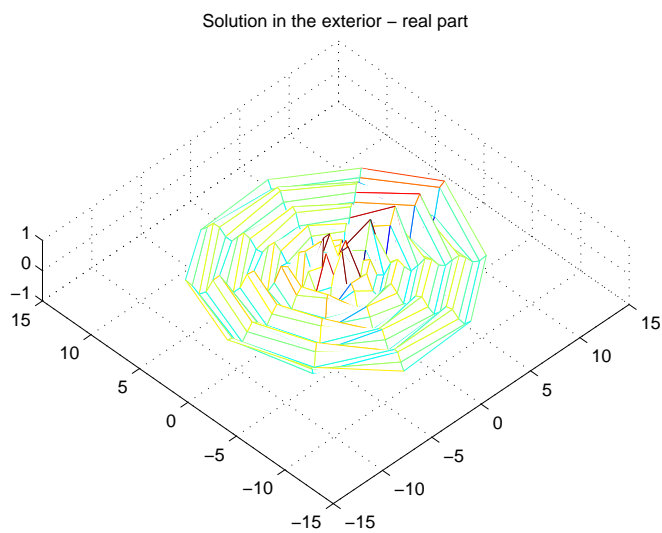Figure 6.58: *Plane wave b. c., k = 10, scattered field Galerkin, imaginary part, 40 quadratic elements.*

Figure 6.59: *Plane wave b. c., k = 10, ratio analytical/collocation, real part, 40 quadratic elements.*

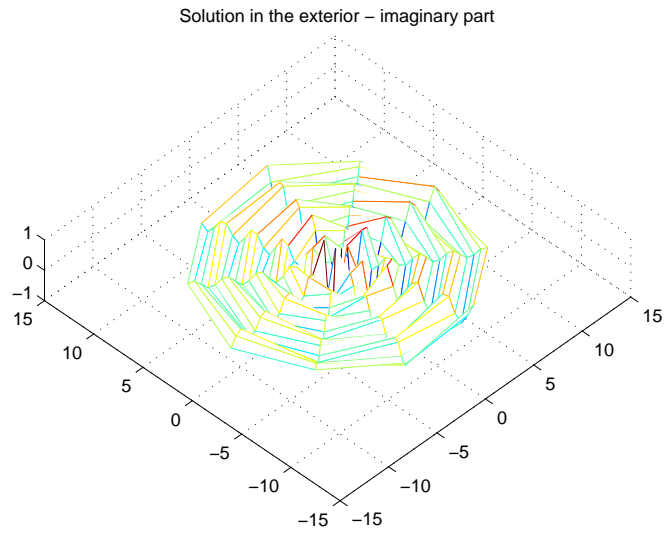Figure 6.60: *Plane wave b. c., k = 10, ratio analytical/Galerkin, real part, 40 quadratic elements.*

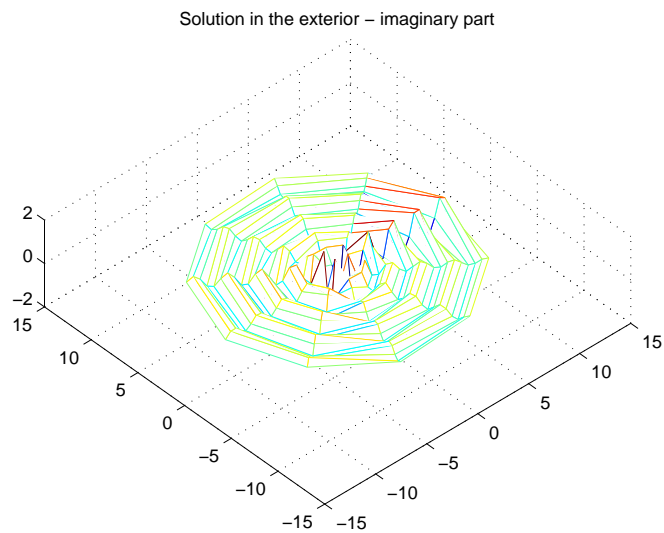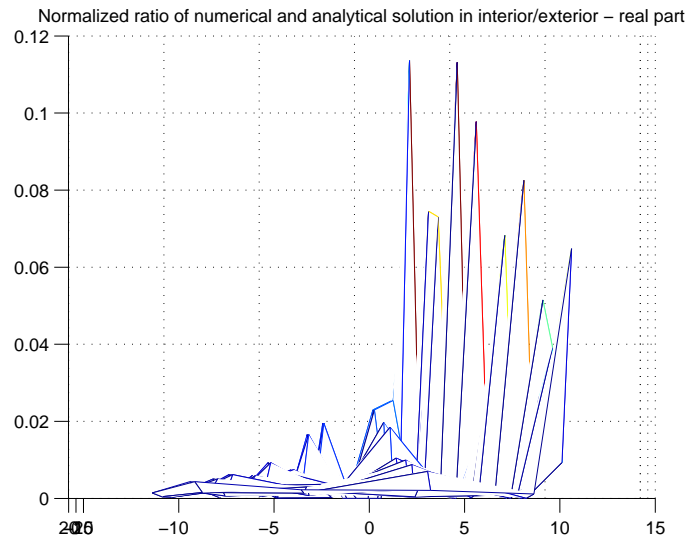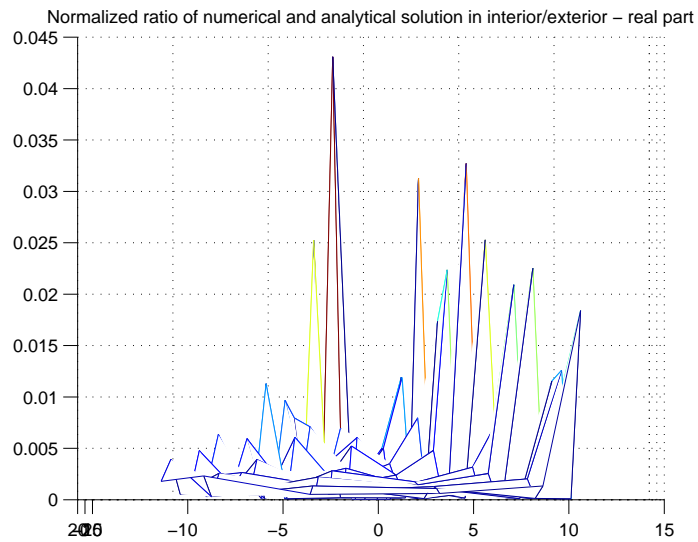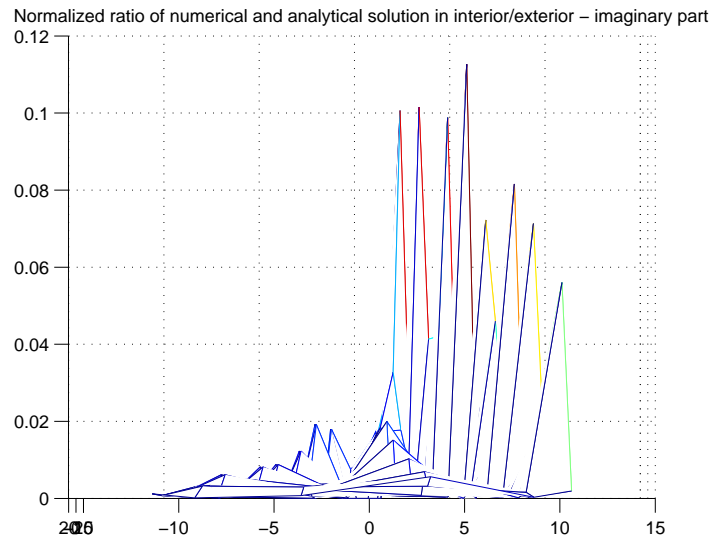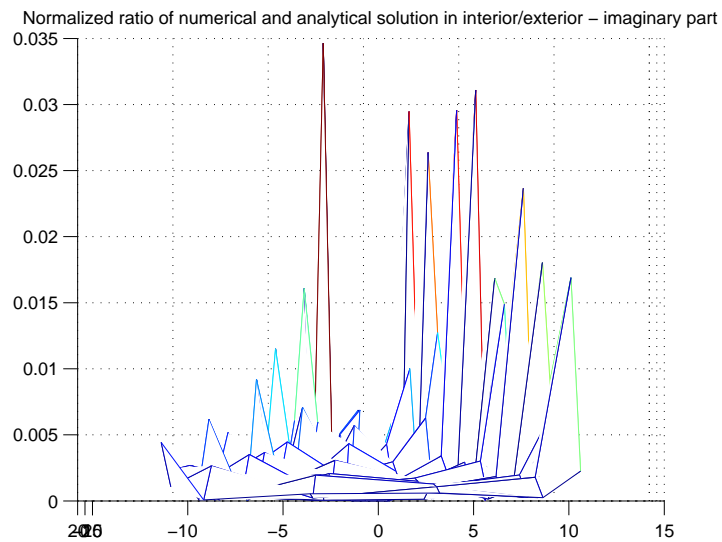Figure 6.61: *Plane wave b. c., k = 10, ratio analytical/collocation, imaginary part, 40 quadratic elements.*

Figure 6.62: *Plane wave b. c., k = 10, ratio analytical/Galerkin, imaginary part, 40 quadratic elements.*

7

Conclusions

The objective of the research resulting in this thesis has been programming of reliable and robust numerical solver for acoustic scattering problems based on Boundary Element Method. The choice of BEM has been made on grounds of its assumed advantage in case of exterior problems, since it essentially reduces the calculations from the domain to the boundary of the scatterer and subsequently pressure field can be evaluated at an arbitrary point of the exterior knowing the solution on the boudary, without having to form stiffness matrix for the whole domain. This approach requires reformulating the Helmholtz equation modeling the time-harmonic pressure field (described in the second chapter) into a boundary integral form. This can be done in several ways resulting in slightly different integral equations. Since these integral equations are the starting point for the BEM discretization, their properties must be well analyzed. This has been subject to research by many scholars and a number of books and papers concerning the theory of the Helmholtz integral equations are at hand. Nevertheless, since the whole procedure must be understood properly, derivation of the standard, so called 'direct', formulae is included in the third chapter. The derivation also underlines necessity of proper treatment of boundary corners. Basic properties of the boundary operators are also given in the same chapter and requirements on the data and boundary are discussed. The argument for choosing the direct formulation lays simply in our familiarity with Green's equations and weak solutions, since all the formulations appear to be virtually equivalent in terms of complexity and theoretical as well as numerical considerations.

The fourth chapter briefly summarizes attempts of improving the basic integral formulations in order to resolve the issue of non-uniqueness of solution arising under certain conditions. The Burton-Miller formulation appears to be the solution to this problem. Unfortunately, it suffers from presence of hypersingular term, very hard to treat numerically, which so far prevented it from becoming the standard formulation. It is a subject of ongoing research and one of the candidates for the next steps in our work.

Out of the three methods available for numerical discretization of the Helmholtz integral equation, that is Nyström, collocation and Galerkin, the latter two have been applied. Collocation appears to be the simplest approach and very well suited for engineering applications. Galerkin method is somewhat more difficult to code, but on the other hand it

supplies better results. Both collocation and Galerkin methods are introduced in the fifth chapter. They have been applied previously, but, as far as is known to us, not much has been published concerning the basic questions of convergence and error analysis. Some results in this respect are given in the book by Steinbach and Rjasanow. Their most important results are included in the fifth chapter for constant and linear elements. The quadratic elements have been analyzed by our team and the results are presented.

Also, the use of a new type of element, which we call exponential, has been proposed in some papers. Being defined by combination of polynomial basis function and an exponential part similar to the plane-wave boundary condition, it is assumed to produce better results for precisely the problems of sound-scattering. We have used this type of elements with both collocation and Galerkin and the results seem to be promising, unfortunately the theoretical analysis is not available so far.

The sixth chapter presents the solutions obtained by our solver. First, solution for the interior problem for the Laplace equation is given, since this equation may be considered a prototype for the Helmholtz equation and the solver may be easily converted. Because analytical solutions to the Laplace equation are much easier to find, it served as the first test of the solver reliability. Further, solutions to some problems for the Helmholtz equation where analytical solutions may be found are presented. The comparison of the results proves the general reliability of our software.

Summing up, new fields of acoustics and Boundary Element Method have been studied. A reliable numerical solver for exterior problems of sound-scattering has been created. Necessary theory has been researched and some results proved concerning the application of quadratic elements. It should be pointed out that the solver is also capable of solving interior problems and large proportion of the theory as well as the solver may be adapted to other practically important problems, e.g. electromagnetics.

There are several directions in which the work can be extended in the future. Firstly, the Burton-Miller formulation may be applied to obtain a robust solver not sensitive to the data. Also, problems with non-convex scatterers are of importance with appropriate modifications to the solver. A possible solution may be the use of exponential elements with a star of directions combined with an algorithm for adaptive choice of the directions as suggested in [23] in the case of Finite Element Method. Finally, the inverse problems may be studied, for which the present solver would form the basis.

The author considers the following to be the achievements of this work:

- BEM solver capable of finding numerical solutions for exterior and interior problems for the Helmholtz equation and applicable in engineering practice has been programmed

- the theory of integral equations and Boundary Element Method has been studied and partially extended, namely error analysis for quadratic elements has been done

- advanced type of basis functions has been used to create new type of element, which has been tested in calculations with promising results

- experience in a new field of research has been gained and the recent work forms a basis for further development

Appendix A

Kellogg Regular Surfaces

Definition 3 *A curve is regular if it is continuous, consists of a finite number of continuously differentiable arcs, has no double points and is of finite lengths.*

A regular surface element is a point set which for at least one cartesian coordinate system (x, y) can be represented in the form

$$z = F(x, y), \quad (x, y) \in H,$$

where F is continuously differentiable in H and H is a finite closed area of the $x - y$ plane which is bounded by a regular closed curve.

A regular surface is a point set which can be divided into a finite number of regular surface elements in the following way:

(a) *Two of the regular surface elements may have in common either a single point which is a vertex (the point at which two edges meet) for both, or a regular arc, which is an edge (continuously differentiable arc bounding a surface element or its part) for both, but no other points.*

(b) *Three or more regular surface elements may have, at most, vertices in common.*

(c) *Any two of the regular surface elements are the first and the last of a chain, such that each has an edge in common with the next.*

(d) *All of the regular surface elements having a vertex in common form a finite chain such that each has an edge terminating in that vertex in common with the next. The last may or may not have an edge in common with the first.*

A surface is closed if each of the edges of every regular surface element belongs to two surface elements.

A point is regular to a regular surface if there exists a decomposition of the surface into regular surface elements such that the point does not belong to an edge. It is regular to curve if the curve is continuously differentiable at that point.

A curve or surface is called smooth if all its interior points are regular points.

A regular region is a compact point set bounded by a finite number of closed regular surfaces such that no two of the surfaces have a point in common.

Bibliography

Abboud, T., Nedelec, J.C., Zhou, B.: Improvement of the integral equation method for high frequency scattering problems. ZAMM-Z. angew. Math. Mech. **76**, 331-332 (1996).

Abramowitz, M., Stegun, I.A.: *Handbook of mathematical functions with formulas, graphs, and mathematical tables*. Dover Publications, New York 1972.

Amini, S., Harris, P.J.: A comparison between various boundary integral formulations of the exterior acoustic problem. Comput. Methods Appl. Mech. Engrg. **84**(1), 59-75 (1990).

Arnold, D.N., Wendland, W.L.: On the asymptotic convergence of collocation methods. Math. Comp. **41**, 349-381 (1983).

De La Bourdonnaye, A.: High frequency methods for integral equations. ZAMM-Z. angew. Math. Mech. **76**, 263-266 (1996).

Brakhage, H., Werner, P.: *Ü*ber das Dirichletsche aussenraumproblem *fü*r die Helmholtzsche schwingungsgleichung. Archiv. der Math. **16** 325-329 (1965).

Brenner, S.C., Ridgway Scott, L.: *The mathematical theory of Finite Element Methods*. Springer-Verlag, New York 1996.

Burton, A.J.: *The solution of Helmholtz equation in exterior domains using integral equations*. NPL Report NAC 30 1973.

Burton, A.J., Miller, G.F.: The application of integral equation methods to the numerical solution of some exterior boundary valu problems. Proc. Roy. Soc. Lond. **A323** 201-210 (1971).

Cakoni, F., Colton, D.: *Qualitative methods in inverse scattering theory*. Springer Verlag, Berlin Heidelberg 2006.

Brebbia, C.A., Telles, J.C.F., Wrobel, L.C.: *Boundary Element Techniques*. Springer-Verlag, Berlin Heidelberg 1984.

ed. Ciskowski, R.D., Brebbia, C.A.: *Boundary element methods in acoustics*. Computational Mechanics Publications, Southampton Boston 1991.

Colton, D., Kress, R.: *Integral equation methods in scattering theory*. Wiley-Interscience Publication, New York 1983.

Colton, D., Kress, R.: *Inverse acoustic and electromagnetic scattering theory*. Springer-Verlag, Berlin Heidelberg 1998.

Erichsen, S., Sauter, S.A.: Efficient automatic quadrature in 3-d Galerkin BEM. Comput. Methods. Appl. Mech. Engrg. **157**, 215-224 (1998).

Ihlenburg, F.: *Finite element analysis of acoustic scattering*, Springer-Verlag, New York 1998.

Hall, W. S.: *The boundary element method*, Kluwer Academic Publishers, Dordrecht 1994.

Harari, I., Hughes, T.J.R.: A cost comparison of boundary element and finite element methods for problems of time-harmonic acoustics. Comput. Meth. Appl. Mech. Eng. **97**, 77-102 (1992).

Harari, I., Hughes, T.J.R.: Finite element methods for the Helmholtz equation in an exterior domain: model problems. Comput. Meth. Appl. Mech. Eng. **87**, 59-96 (1991).

Jeans, R., Mathews, I.C.: A comparison of numerical collocation and variational procedures to the hypersingular acoustic integral operator. Comput. Meth. Appl. Mech. Eng. **101**, 5-26 (1992).

Karafiat, A.: Adaptive integration techniques for almost singular functions in the Boundary Element Method. Comput. Math. Appl. **32**(5), 11-30 (1996).

Kirkup, S.: *The boundary element method in acoustics.* Integrated Sound Soufware, Heptonstall 1998.

Mayer, P., Mandel, J.: The finite ray element method for the Helmholtz equation of scattering: first numerical experiments. UCD/CCM Report 111, 1997. `http://www-math.cudenver.edu/ccm/reports/`

McLean, W.: *Strongly elliptic systems and boundary integral equations.* Cambridge University Press, New York 2000.

Lukáš, D.: A Shape Optimization Method for Nonlinear Axisymmetric Magnetostatics Using A Shape Optimization Method for Nonlinear Axisymmetric Magnetostatics Using a Coupling of Finite and Boundary Elements, J. Sci. Comput. (2009).

Moses, P.: Collocation method for Laplace equation, In: *Interaction and Feedbacks.* Ústav termomechaniky AV ČR, Praha, 85-88 (2005).

Moses, P., Novotný, J., Burda, P.: Collocation method for exterior scattering problem, In: *Proceedings of the XVI-th summer school Software and Algorithms of Numerical Mathematics.* Západočeská Univerzita v Plzni, Plzeň, 180-184 (2006).

Moses, P.: Fast solver with exponential basis functions for Helmholtz integral equation, ICCFD4, Gent 2006, to appear in the proceedings by Springer.

Moses, P.: Řešení úlohy rozptylu metodou hraničních prvku, In: *Proceedings of SNA07.* Institute of Geonics AS CR Ostrava, Ostrava, 79 (2007).

Moses, P.: Numerical solution of Helmholtz equation by boundary elements method, Matematický Workshop 2007, Brno. To appear in Proceedings.

Sadowská, M., Bouchala, J., Dostál, Z.: Theoretically supported scalable BETI method for variational inequalities, Computing **82**(1), 53-75 (2008).

Schenck, H.A.: Improved integral formulation four acoustic radiation problems. J. Acoust. Soc. Amer. **44**, 41-58 (1968).

Skelton, E.A., James, J.H.: *Theoretical acoustics of underwater structures.* Imperial College Press, London 1998.

Steinbach, O., Rjasanow, S.: *The fast solution of boundary integral equations*, Springer-Verlag, New York 2007.

Terai, T.: On calculation of sound fields around three dimensional objects by integral equation methods. J. Sound. Vib. **69**(1), 71-100 (1980).

Vaněk, P., Mandel, J., Brezina, M.: Solving a two-dimensional Helmholtz problem using algebraic multigrid. UCD/CCM Report 110, 1997. `http://www-math.cudenver.edu/ccm/reports/`